ABSTRACT

Title of Dissertation:	MAPPING LANGUAGE FUNCTION AND PREDICTING CORTICAL STIMULATION RESULTS WITH INTRACRANIAL ELECTROENCEPHALOGRAPHY
	Yujing Wang Doctor of Philosophy 2018
Dissertation directed by:	Professor Nathan E. Crone, Department of Bioengineering

To avoid post-operative language impairments after surgery for drug-resistant epilepsy, clinicians rely primarily on electrocortical stimulation mapping (ESM), but this can trigger afterdischarges, clinical seizures, or cause uncomfortable sensations. Moreover, ESM can be time-consuming and the results are usually all-or-none, complicating their interpretation. These practical limitations have long motivated spatial-temporal analysis of passive intracranial electroencephalographic (iEEG) recordings as an alternative or complementary technique that can map cortical function at all sites simultaneously, resulting in significant time savings without adverse side-effects. However, there has not yet been widespread clinical adoption of passive iEEG for pre-operative language mapping, largely because of a failure to realize the potential advantages of iEEG over ESM and other methods for language mapping.

The overall goals of this dissertation were to improve and validate passive iEEG as a method for mapping human language function prior to surgical resection for epilepsy and other brain disorders. This was accomplished through three separate aims. First, a spatial-temporal functional mapping (STFM) system was developed and tested for online passive iEEG mapping, providing immediate mapping feedback to both clinicians and researchers. The system output was compared to ESM and to canonical regions of interest in the human language network. In the second aim, the STFM system was used to study the fine temporal dynamics by which Broca's area is activated and interacts with other areas of language network during a sentence completion task. This study showed that Broca's area plays a pivotal role in the coordination of language networks responsible for lexical selection. Finally, the third aim sought to reconcile inconsistencies between the results of STFM and ESM. Agreement between these methods has not been as good for language mapping as it has been for motor mapping, which may be due to propagation of ESM effects to cortical areas connected to the site of stimulation. We used cortico-cortical evoked potentials to estimate the effective connectivity of stimulation sites to other sites in the language network. We found that this method improved the accuracy of STFM in predicting ESM results and helped explain similarities and differences between STFM and ESM language maps.

MAPPING LANGUAGE FUNCTION AND PREDICTING CORTICAL
STIMULATION RESULTS WITH INTRACRANIAL
ELECTROENCEPHALOGRAPHY

by

Yujing Wang

Dissertation submitted to the Faculty of the Graduate School of the
University of Maryland, College Park, in partial fulfillment
of the requirements for the degree of
Doctor of Philosophy
2018

Advisory Committee:
 Professor Nathan E. Crone, Co-Chair
 Professor Yu Chen, Co-Chair
 Professor Yang Tao
 Professor Rao Gullapalli
 Professor Jonathan Simon, Dean's Representative

Dedication

This thesis is dedicated to my grandfather Binggong Zhang, who had made it possible for three generations of our family to pursue their education and thus, their dreams. Thank you for everything that you have done for us and for me. May you rest in peace.

Acknowledgements

First and foremost, I would like to offer my sincerest gratitude to my advisor, Dr. Nathan Crone, for his consistent encouragement, invaluable advice and unconditional support throughout my Ph.D. Also, to my thesis committee members, Drs. Yu Chen, Yang Tao, Rao Gullapalli and Jonathan Simon, thank you all for providing invaluable feedback throughout the development of this dissertation.

This work would not have been possible without the support from members – past and present – of the Cognitive Neurophysiology Laboratory at Hopkins. I thank Drs. Anna Korzeniewska, Heather Benz and Matthew Fifer for their help in developing my ideas into decent research directions during the early years of my graduate study. Special thanks to Dr. Griffin Milsap, Dr. Kyle Rupp, Maxwell Collard, Tessy Thomas, Dr. Kiyohide Usami, Daniel Candrea, Christopher Coogan and Alyssandra Valenzuela for their inspirations during countless discussions throughout all the years and making the lab an enjoyable place to work in. I would also like to thank my fellow students and colleagues at University of Maryland College Park as well as Johns Hopkins University for the support and friendship that helped making the journey a lot more fun.

I'd like to thank Dr. Williams S. Anderson, Dr. Joon Kang and other clinicians in the Epilepsy Monitoring Unit, for guiding me how to work with patients and providing the

important bridge between neuroscience research and clinical applications. I would appreciate all patients I've worked with, who have willingly shared their precious time and cooperated perfectly despite their unfortunate experience of life. The researches under this dissertation were supported by the National Institute of Neurological Disorders and Stroke (NINDS) grant NS40596 (to N.E.C.) and NS91139 (to N.E.C.).

Last but not least, I would like to thank my family for their support. I'd love to thank my beloved parents for their unconditional love, gracious generosity and strong support when their daughter is pursuing her Ph.D. degree 8,000 miles away. I'd love to thank my best friend, the love of my life, my amazing husband, Renjun Zhu. I would never have made it without you standing by my side, 24/7/365 for more than ten years. I'd love to thank our son Chenhao Zhu, for always cheering for Mama no matter what, and for sleeping through the night. I love you to the moon and back.

I offer my regards and blessings to all of those who supported me in any respect during the completion of the dissertation.

Table of Contents

List of Tables

List of Figures

Chapter 1 Introduction

1.1 The Human Brain

The human brain – a jelly-like, 3-pound mass of tissue – is the most complex organ in the human body, and the most sophisticated machine imaginable in the universe. It is composed of more than 100 billion nerve cells, each of which forms as many as 10,000 connections with other neurons. With the capacity to create a network of connections that far surpasses any social network and stores more information than a supercomputer, the brain allows us to perform all kinds of functions that makes us human, ranging from sensory-motor actions to emotion, memory and language. In 2007, the World Health Organization estimated that neurological disorders affect up to one billion people worldwide (1). In fact, neurological diseases make up 11% of the world's disease burden, not including mental health and addiction disorders.

1.2 Functional Mapping

To avoid post-operative language and motor impairments after surgery for drug-resistant epilepsy or other brain disorders, mapping the relationship between cortical activity and behavioral activity is an invaluable tool in planning these surgical resections (2–4). Prior to the resection, clinicians localize the site of seizure origination and "eloquent cortex", or cortical sites that are deemed necessary for the performance

of motor, sensory, language, and other activities that are relevant to the patient's quality of life. Identification of the site of seizure origination is performed by neurologists reading intracranial electroencephalographic (iEEG) (5), electrical signals recorded from penetrating electrodes (stereo electroencephalographic, or SEEG) (6) and electrodes placed subdurally (7) or epidurally (8) over the surface of the brain (electrocorticography, or ECoG). Identification of eloquent cortex is typically performed using electrocortical stimulation mapping (ESM) (9–11), in which current is delivered through the iEEG electrodes, and the resulting disruption of related task performance or initiation of movement and sensation is documented.

The major advantage of this ESM is that it allows clinicians to simulate the neurological consequences of lesioning tissue before it is permanently resected (9). However, there are important practical limitations on its clinical application. ESM is by nature time-consuming, due to the need to individually stimulate sites of interest, and sometimes causes pain, discomfort, after-discharges, or even seizures (12, 13). Additionally, there have been reports of short-term and persistent language deficits following resections guided by ESM (4). An alternative approach to cortical mapping based solely on cortical recordings could complement or even replace ESM. Such functional mapping has been demonstrated using fMRI (14) and the iEEG signal (15). One feature of the iEEG, the high gamma (60-200Hz) power, is particularly promising, as it has been shown to reflect local population firing rates (16, 17). However, the sensitivity and

specificity of these functional mapping approaches in identifying language related eloquent cortex, as compared to ESM, are too low to rely upon them alone. An ability to map the propagation of information through the cortex during language processing such as lexical retrieval, phonological code retrieval, syllabification, and articulation would improve clinicians' understanding of the most relevant cortical sites for these tasks in individual patients.

1.3 Intracranial EEG

Soon after Berger's first recordings of electrical activity from the human brain – the 'elektrenkephalogramm' (EEG) in 1929 (18), Jasper and Carmichael performed the first human iEEG recordings from cortical areas and the cerebellum during surgery for epilepsy and tumor resection (19). Due to its invasive nature, iEEG has been restricted to be mainly used in clinical circumstances such as epilepsy foci resective surgery. Under these circumstances, invasive recordings are either made from the surface of the cerebral hemisphere using impenetrable electrode grids or strips, or from depth electrodes that are advanced into the medial temporal lobe in most cases.

After Crone et al.'s first report of task-related high-gamma activation in human ECoG recordings in 1998 (20), recent studies have emphasized the utility of increases in signal energy in a broad range of high-gamma frequencies (~60-200Hz) as a general electrophysiological index of cortical processing during a variety of tasks (16, 21, 22).

Activity in this frequency range is highly correlated with blood oxygen level-dependent (BOLD) responses (23, 24). Moreover, ECoG can provide excellent temporal resolution needed to probe the dynamics of cognition whereas BOLD signals have a significant delay and smears activity over long periods. ECoG high-gamma responses also have close correlations with average firing rates in cortical neuronal populations (25). In addition, high-gamma responses have exhibited functional properties that distinguish them from both phase-locked responses such as event-related potentials (ERP, phase-locked electrocorticogram activity, obtained by averaging data segments recorded after presentation of a stimulus), and event-related synchronization or desynchronization observed in other frequency bands such as alpha/beta bands (Figure 1.1).
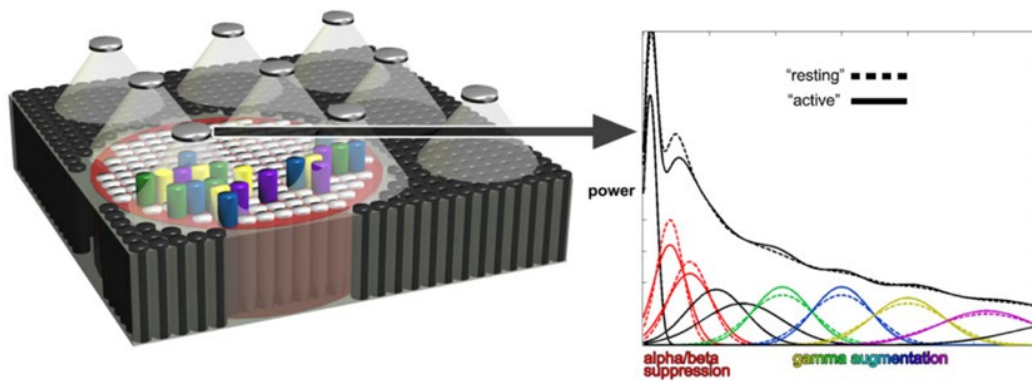
Figure 1.1. Conceptual schematic of how ECoG broadband gamma activity increases could result from modulation of band-limited gamma oscillations.

Area of cerebral cortex is recorded by array of ECoG electrodes on the left. The power spectrum for one ECoG site recorded under resting vs. active conditions is schematized on the right (arrow). The field of view of each recording site (inverted cones) includes many neuronal assemblies/cortical columns (colored cylinders) with different functional response sensitivities (larger size and smaller number for illustration). Neuronal assemblies activated by a task (colored cylinders) are synchronized and generate membrane potential oscillations at different band-limited gamma frequencies that depend on the resonant properties of each assembly. Membrane potential oscillations with different center frequencies (colored bands on right corresponding to cylinders to left) collectively contribute to signals recorded by ECoG electrodes and their summation gives a broadband shape to gamma responses in the power spectrum. Note that many more assemblies and bands than can be represented here would be needed to produce the shape of commonly observed spectral responses. Also, different sets of neural assemblies and bands may be involved during different trials of the same task, depending on stimulus properties and a variety of initial conditions. Assemblies not immediately engaged in task-related cortical processing are represented by black (and white) cylinders. Task-related power suppression in alpha/ beta frequencies (red circular area on left and red bands on right) occurs in a wider area and theoretically reflects thalamocortical gating mechanisms that permit or facilitate cortical processing in assemblies with similar but distinct response sensitivities. Figure adapted from (17) with permission.

Previous reports suggested that during limb movements, the spectral pattern of iEEG recordings exhibited event-related desynchronization (ERD) in the alpha band and event-related synchronization (ERS) in the gamma band. The distribution of gamma ERS is more localized than the alpha ERD, hence the power change in the gamma band

5

is more useful for brain function mapping. For example, high-gamma features have been employed to localize the sensorimotor areas of hand, tongue, foot, and the areas for language processing (26).

While traditional functional mapping methods mentioned above all have limits on their accuracy, efficiency, and reliability to some extent, cortical functional mapping using passive iEEG recordings from the same implanted electrodes has been of increasing interest for clinicians over past ten years. This approach has a variety of important potential advantages, including the ability to simultaneously and rapidly evaluate brain function at all electrode sites without artificially perturbing the brain as in ESM. In addition, iEEG high-gamma responses provide a graded measure of local population activity, which can be used to estimate the degree to which individual recording sites contribute to overall activity in cortical networks responsible for normal brain function. Also, since ECoG functional mapping is a passive process, there is no risk of after-discharges or seizure induction, providing a safer approach to functional mapping.

Although the application of neuroimaging technology like fMRI and PET-CT enhances the accuracy of localization and provides the references for functional mapping, the complexity of dynamical functional organization of cortical networks has not been well defined. It has been shown that using iEEG functional mapping, functional activation of cortex is associated with power increase in high-gamma frequencies. It has been

found that high-gamma power is highly correlated with the average firing rate recorded by the single-unit electrodes and is more sensitive to the changes of neuronal synchrony than firing rate. Cortical mapping can be completed after spectral analysis of high-gamma power recorded while patients perform certain tasks. Although the generating mechanisms for high-gamma activity are hotly debated, it appears to have great practical value as an electrophysiological index of overall activity in local neuronal populations.

1.4 Language

One of the most prominent human abilities is language, a complex system involving many components, including sensory-motor functions and memory systems. Although language is not fully understood, scientists have learned a great deal about this brain function from studies of patients who have lost speech and language abilities as a result of a stroke. Genetic analyses of developmental disorders of speech and language, as well as brain imaging studies of normal people, also have added to our knowledge.

It has long been known that damage to different regions within the left hemisphere produces different kinds of language impairments, or aphasias. Damage to the left frontal lobe can produce nonfluent aphasia, such as Broca's aphasia, a syndrome in which speech production abilities are impaired. Speech output is slow and halting, requires effort, and often lacks complexity in word or sentence structure. Although

speaking is impaired, nonfluent aphasics still comprehend heard speech, although structurally complex sentences may be poorly understood.

Damage to the left temporal lobe can produce fluent aphasia, such as Wernicke's aphasia, in which comprehension of heard speech is impaired. Speech output, although of normal fluency and speed, is often riddled with errors in sound and word selection and tends to be unintelligible gibberish.

Damage to the superior temporal gyri in both hemispheres can produce word deafness, a profound inability to comprehend auditory speech on any level. Whereas Wernicke's aphasics can often comprehend bits and pieces of a spoken utterance, as well as isolated words, patients with word deafness are functional deaf for speech, lacking the ability to comprehend even single words, despite being able to hear sound and even identify the emotional quality of speech or the gender of the speaker.

1.5 Neural activity propagation in language systems

Speech preparation and articulation requires a coordinated cascade of information propagation through a number of cortical areas. Figure 1.2 shows a simplified schematic of hypothesized cortical propagation preceding and during speech production. (27)
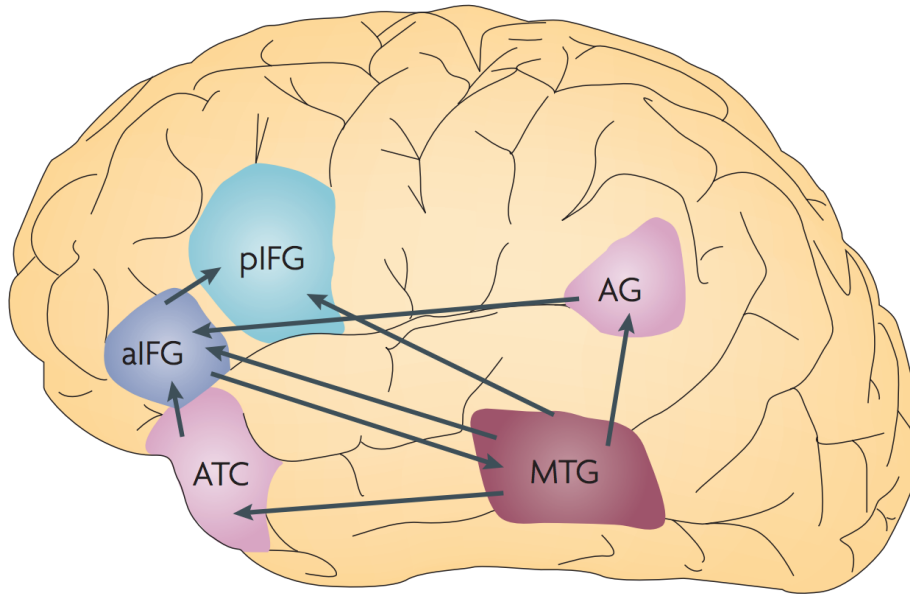
Figure 1.2. A functional neuroanatomic model for semantic processing of words in context.

Lexical representations are stored and activated in the middle temporal gyrus (MTG) and in the nearby superior temporal sulcus and inferior temporal cortex, and are accessed by other parts of the semantic network. The anterior temporal cortex (ATC) and angular gyrus (AG) are involved in integrating incoming information into current contextual and syntactic representations. The anterior inferior frontal gyrus (aIFG) mediates controlled retrieval of lexical representations based on top-down information, and the posterior IFG (pIFG) mediates selection between highly activated candidate representations. Figure adapted from (27) with permission.

Following early visual processing of the stimulus, fusiform gyrus is involved in object or word identification (28). This information is passed to middle temporal gyrus, which is active during lexical retrieval (29), or the identification of the word to be spoken.

Posterior superior temporal gyrus (Wernicke's area) transforms the lexical concept to phonological code (30), following which Broca's area participates in syllabification and additional articulatory preparation (31). Cortical processing converges in inferior primary motor cortex, which is responsible for articulation of the vocal tract (32). Finally, somatosensory feedback from primary somatosensory cortex in parietal cortex and auditory feed- back from the superior temporal gyrus and other auditory areas monitor articulation through interactions with primary motor cortex (33, 34).

Processing information propagated through widespread cortical areas during movement and speech is likely to be informative for mapping how cortical activity leads to movement and speech, and decoding movement and speech parameters from cortical signals.

1.6 Overview of thesis

The overall goals of the research done under this dissertation were to improve and validate passive iEEG as a method for mapping human language function prior to surgical resection for epilepsy and other brain disorders. This was accomplished through three separate aims.

In **Chapter 2**, a system was developed and tested for online passive iEEG mapping at the bedside, providing immediate feedback to both clinicians and researchers on

mapping results. To test the accuracy and utility of this system, spatial-temporal functional maps (STFM) of brain activation were obtained during a picture naming and a word repetition task. The system output was compared to ESM and to canonical regions of interest in the human cortical language network.

In **Chapter 3**, the online STFM system was used to study the fine temporal dynamics by which Broca's area is activated and interacts with other areas in the human language network during a sentence completion task. This study showed that Broca's area plays a pivotal role in the coordination of language networks responsible for lexical selection. This study demonstrated a key advantage of passive iEEG language mapping, namely its ability to detail the timing of neural activation and network interactions during complex cognitive tasks.

Finally, **Chapter 4** sought to reconcile inconsistencies between the results of STFM and ESM. Agreement between these methods has not been as good for language mapping as it has been for motor mapping. We hypothesized some of these discrepancies may be due to propagation of ESM effects to cortical areas connected to the site of stimulation. To test this hypothesis, we used cortico-cortical evoked potentials to estimate the effective connectivity of stimulation sites to other sites in the language network. We found that this method improved the accuracy of STFM in

predicting ESM results and helped explain similarities and differences between STFM and ESM language maps.

Chapter 5 summarizes the overall conclusions from Chapters 2-4, discusses the impact of the results, and proposes future directions for additional investigation.

This dissertation has exerted its most profound and lasting impact by improving the clinical utility of iEEG for both extraoperative and intraoperative functional mapping prior to respective surgery, as well as gaining deeper insights into the cortical network dynamics of spoken word production and how they are affected by ESM.

Chapter 2 Spatial-temporal functional mapping of language at the bedside with electrocorticography

2.1 Abstract

Objective: To investigate the feasibility and clinical utility of using passive electrocorticography (ECoG) for online spatial-temporal functional mapping (STFM) of language cortex in patients being monitored for epilepsy surgery.

Methods: We developed and tested an online system that exploits ECoG's temporal resolution to display the evolution of statistically significant High Gamma (HG, 70-110 Hz) responses across all recording sites activated by a discrete cognitive task. We illustrate how this spatial-temporal evolution can be used to study the function of individual recording sites engaged during different language tasks, and how this approach can be particularly useful for mapping eloquent cortex.

Results: Using electrocortical stimulation mapping (ESM) as the clinical gold standard for localizing language cortex, the average sensitivity and specificity of online STFM across seven patients were 69.9% and 83.5%, respectively. Moreover, relative to regions of interest where discrete cortical lesions have most reliably caused language impairments in the literature, the sensitivity of STFM was significantly greater than

that of ESM, while its specificity was also greater than that of ESM, though not significantly so.

Conclusions: This study supports the feasibility and clinical utility of online STFM for mapping human language function, particularly under clinical circumstances in which time is limited and comprehensive ESM is impractical.

2.2 Introduction

Functional human brain mapping is commonly performed during or prior to invasive brain surgery for the treatment of drug-refractory epilepsy (35, 36) and brain tumors (4). The current gold standard, electrocortical stimulation mapping (ESM), is time-consuming (37, 38) and often induces afterdischarges or seizures (12, 37, 39). Additionally, it is difficult to rule out distant effects through diaschisis or action potentials evoked by stimulation (39–41). These limitations have long motivated the investigation of passive electrocorticographic (ECoG) recordings as a tool for rapidly and safely mapping cortical function prior to resective surgery (13, 42, 43).

Here we introduce and test the feasibility and clinical utility of an online trial-based system for spatial-temporal functional mapping (STFM) of language cortex. High Gamma (HG, ~60 to 200 Hz) power changes have been demonstrated to be a robust and reliable index of task-related activation of cortical populations of neurons with high

14

spatial and temporal specificity (16, 17). The STFM system builds upon previous passive ECoG mapping software (44–47) by providing a trial-based framework for online display and statistical validation of HG dynamics.

In seven patients, estimates of the system's sensitivity and specificity for language mapping, relative to the benchmark of ESM, were the same or better than previous reports (47–50). Moreover, we found that relative to predefined language cortex boundaries, the sensitivity and specificity of STFM were greater than that of ESM, though the increase in specificity was not statistically significant.

2.3 Methods

Patient and Clinical Settings. Seven English-speaking patients (Table 2.1) with intractable epilepsy underwent placement of subdural electrodes in the dominant hemisphere to localize their ictal onset zone and to identify language and motor areas using ESM. The implanted electrodes consisted of arrays of macroelectrodes (2.3mm exposed diameter, 1cm spacing, Adtech, Racine, WI or PMT Crop, Chanhassen, MN). In five of seven patients, the macroelectrodes were supplemented by 4 x 4 arrays of microelectrodes (75micron diameter, 0.9mm spacing, PMT Corp, Chanhassen, MN). In all patients, the anatomical placement of electrodes was dictated solely by clinical considerations for recording seizures and/or mapping cortical function.

Pat ient	Ag e	Gen der	Hande dness	Hemisphere dominance for language (Wada (51))	Hemisph eric Coverage	Seizure onset zone
1	23	F	Right	Left	Left	Anterior temporal
2	13	F	Right	Left	Left	Amygdala
3	55	M	Right	Left	Left	Anterior temporal
4	22	M	Right	N/A	Left	Occipital
5	62	M	Right	N/A	Left	Anterior temporal
6	25	M	Right	N/A	Left	Frontal
7	55	F	Right	Left	Left	Anterior temporal

Table 2.1. Patient Demographic and Clinical Information

Standard Protocol Approvals, Registrations, and Patient Consents. Patients were admitted to the Johns Hopkins Epilepsy Monitoring Unit after electrode implantation for a period of 6-14 days. All patients gave informed consent to participate in research testing under a protocol approved by the Institutional Review Board of the Johns Hopkins Medical Institutions.

Experimental Testing and Event Markers. In this study, the online STFM system performed functional mapping during two distinct behavioral tasks. During visual object naming, patients were shown a picture on a monitor directly in front of them during each trial, and were instructed to speak the name of the object in the picture. The stimulus onset was determined by a thresholded output from a photodiode mounted on the monitor presenting the stimuli. During auditory word repetition, patients were

played an audio recording of a spoken word through insert earphones designed to attenuate external background noise during each trial, and were instructed to verbally repeat the cued word. The stimulus onset was determined by trigger pulses synchronized with the onset of the auditory stimuli in a separate channel. Inter-trial intervals (time from the start of a trial to the start of the next trial) ranged 6.5 to 8.2 seconds for visual object naming and 7.9 to 8.0 seconds for auditory word repetition. Patients completed a range of 55-251 trials for visual object naming and 96-116 trials for auditory word repetition, as governed by time constraints on patient testing and the set of stimuli used. Trials affected by artifacts or interruptions could be removed using the 'Remove Trial' button on the system graphical user interface shown in Figure 2.3.

Electrode Localization. Electrode locations were identified in a high-resolution post-operative brain CT, and then transformed onto a high-resolution pre-operative brain MRI by volumetrically co-registering the pre- and post-operative scans in Bioimage Suite (52). One or more viewpoint snapshots were then aggregated into a single image to visualize functional activations relative to individual anatomy.

Data Acquisition and Analysis. Recordings of all standard ECoG macroelectrodes were referenced to a single intracranial macroelectrode to minimize extracranial sources of artifact. ECoG microelectrodes were referenced to a single microelectrode on the opposite side of the same insert, facing the dura mater. Raw ECoG signals were

17

recorded with a 128-channel NeuroPort System (BlackRock Microsystems; Salt Lake City, UT) which amplified and sampled the data at 30 kHz with an analog third-order Butterworth anti-aliasing filter. The recordings for Patient 1 were sampled at 30 kHz, but for all other patients, the anti-aliased 30 kHz recording was downsampled to a lower rate (1 kHz, Patient 5; 2 kHz, Patient 2; 10 kHz, Patients 3, 4, 6, 7). This data was streamed using the built-in real-time streaming functionality of the NeuroPort system. The streaming data was immediately decimated to 1 kHz online in all patients prior to any subsequent analysis using a lowpass Chebyshev Type I IIR filter of order 8. Online STFM was performed with custom MATLAB (MathWorks, Inc.; Natick, MA) software, on a workstation with eight 3.40 GHz processing cores, 1.5 TB of hard drive disk space, and 32 GB of RAM (Dell, Inc., Round Rock, TX).

Channels with excessive amounts of noise were identified by a clinical neurophysiologist and excluded from analysis prior to online ECoG mapping. The remaining channels were re-referenced using a common average reference (CAR) to remove spatial bias in the raw ECoG amplitudes. Separate CAR blocks were used for: (1) all the macroelectrodes in each patient, and (2) each microelectrode array (in Patients 1, 3, 4, 5 and 6).

Spectral Feature Extraction. The CAR-referenced ECoG signal was analyzed for the duration of the task in 512 ms epochs of data with 256 ms overlap (Patient 1) or 128

ms epochs of data with 112 ms overlap (other patients). The Fast Fourier transform (FFT) was computed on each window, and the resulting coefficients were then multiplied by a modified flat-top Gaussian window with cutoff between 67-115Hz (Patient 1) or 72-110 Hz (other patients) to minimize noise at 60 Hz and 120 Hz. The bandpass-filtered spectrum was converted to high gamma amplitude by zeroing the negative frequency components, doubling the positive frequency components, computing the inverse FFT, and taking the magnitude of the result (i.e. the Hilbert transform) (53, 54). The right column of Figure 2.1 shows the spectral feature extraction process in block diagram form. The resulting high-gamma amplitude was then log transformed to approximate a normal distribution and decimated to a temporal resolution of 16 ms using a moving average filter. Figure 2.2 shows the signal at several key points in this process.
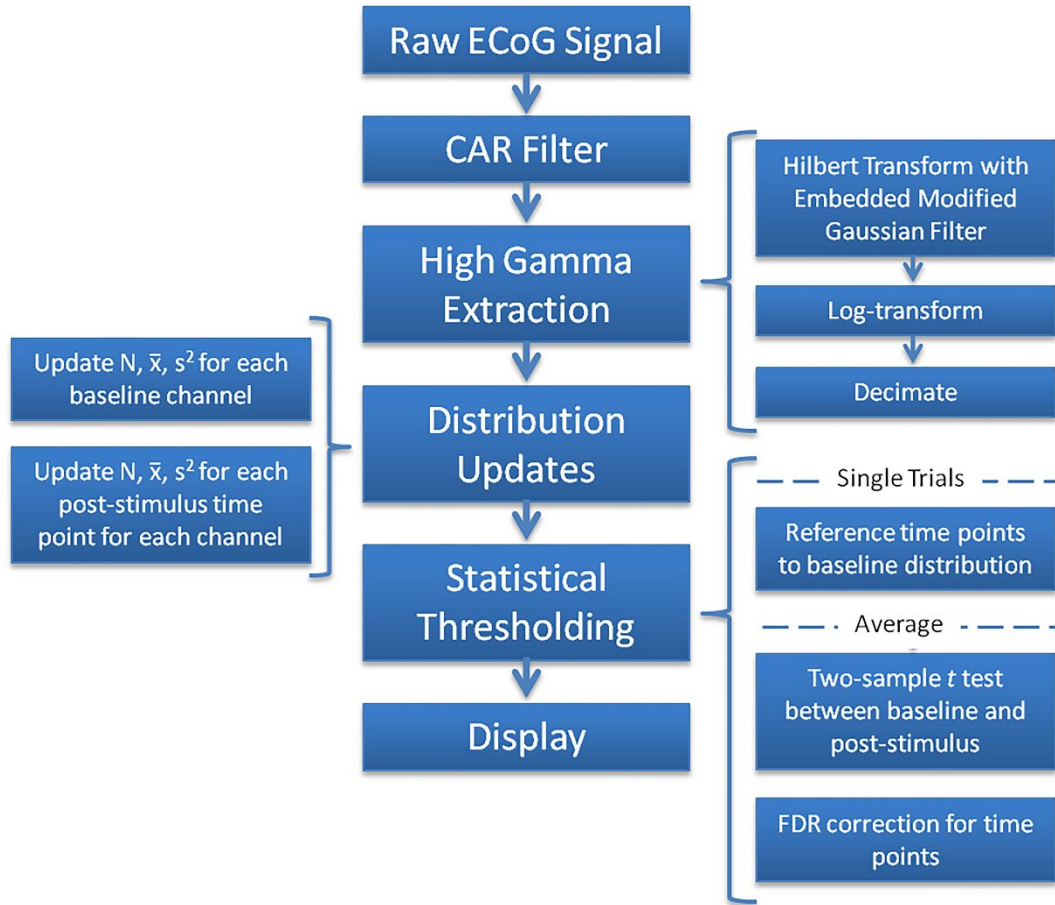
Figure 2.1. Online STFM Signal Processing Algorithm.

A visual schematic is presented to describe the online signal processing and statistical methods used. A more detailed description of each step can be found in *Methods*. N, $\bar{x}$, and s^2 represent sample size, mean, and variance, respectively.
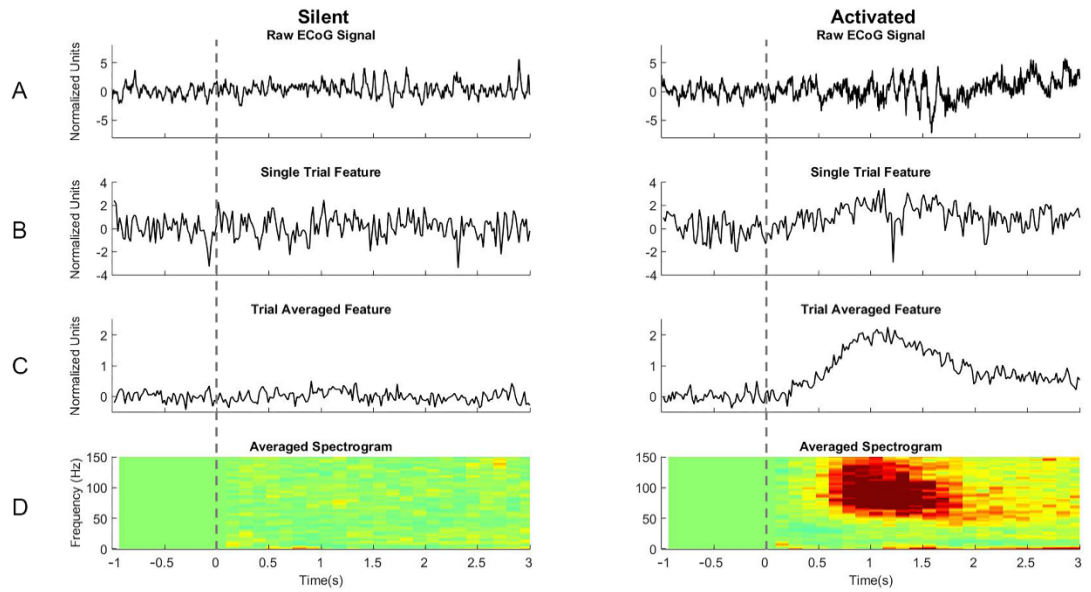
Figure 2.2. Feature extraction algorithm illustration from auditory word repetition in Patient 1.

The 'Silent' column plots are from a macroelectrode (LFT33 in Figure 2.6B) that had no significant task-related high gamma response. The 'Activated' column plots are from a microelectrode (PMIC13 in Fig 2.6B) with a significant task-related high gamma response. In (A)-(C), the units have been normalized so that the baseline period has zero mean and unit standard deviation. (A) Raw ECoG signals from the same single trial are shown after re-referencing to the common average reference (CAR). (B) The high gamma amplitude feature is shown after it was extracted from the same single trial shown in (A) using the steps described in Figure 2.1 under the 'Single trials' section of 'Statistical Thresholding'. (C) Post-stimulus high gamma amplitude averaged across all 96 trials of auditory word repetition is shown for both electrodes, using the steps described in Figure 2.4 under the 'Average' section of 'Statistical Thresholding'. (D) The average post-stimulus spectrogram is shown, calculated by averaging the FFT coefficients time-locked to the stimulus

21

marker in 512 ms bins with 256 ms overlap. Time zero is the stimulus onset of each trial. This spectrogram is not shown to the system user online, but is included here only for comparison with the feature output.

Statistical Analysis. The time series of log-transformed high-gamma amplitude estimates, extracted as described above, was segmented separately into baseline and task-activated distributions. The baseline distribution for each channel was drawn from 64 samples of the analytic amplitude, corresponding to 1024 ms prior to stimulus onset (i.e., 16 ms resolution *x* 64 points = 1024 ms). A separate task-activated distribution was estimated for each channel and time point after stimulus onset (i.e., 3072 ms in this study, with 16 ms resolution, for 192 total time points per channel). The baseline and task-activated amplitude distributions were approximated as Gaussian, parameterized by the sample size, mean, and variance, and were updated after each trial according to the following equations:

$$n_{new} = n_{old} + \Delta n \tag{2.1}$$

$$\bar{x}_{new} = \frac{\sum\limits_{i=n_{old}+1}^{n_{new}} x_i + \bar{x}_{old} n_{old}}{n_{new}} \tag{2.2}$$

$$s^2{}_{new} = \sum_{i=n_{old}+1}^{n_{new}} x_i^2 + \left(\frac{n_{old}-1}{n_{old}} s_{old}^2 + \bar{x}_{old}^2 \right) \frac{n_{old}}{n_{new}-1} - \bar{x}_{new}^2 \frac{n_{new}}{n_{new}-1} \tag{2.3}$$

22

where n_{old} and n_{new} are the previous and current sample size, $\bar{x}_{old}$ and $\bar{x}_{new}$ are previous and current sample mean, and s^2_{old} and s^2_{new} are the previous and current sample standard deviations after update.

For trial-averaged activation maps, a two-way t-test was performed between the accumulated amplitude distribution from all baseline time points in each channel, and the accumulated amplitude distribution from each time point after stimulus onset in that same channel. The threshold for significance was determined using the false discovery rate (FDR) correction (55), where the two-sided significance threshold of $\alpha < 0.05$ was adjusted for m positively correlated tests, where m was the number of time points after stimulus onset. Each statistically significant difference from the baseline distribution was also tagged as an increase or a decrease in high gamma amplitude. Single trial results were computed similarly, but with a simple two-sided z-test with a threshold of $\alpha < 0.05$ uncorrected for multiple comparisons. Note that although we avoided testing during or soon after seizures, we did not attempt to remove trials with interictal spikes due to the lack of integration with a spike detector. It is possible that interictal spikes with energy in high gamma frequencies could alter the results of STFM, and this could potentially affect parametric statistics more than nonparametric statistics.

Visualization. Raster plots (Figure 2.4) display the magnitude of event-related changes in the HG amplitude at each time point after stimulus onset, as compared to the

baseline. These rasters display either trial-averaged amplitude changes (Figure 2.4, rows represent electrodes) or single-trial amplitude changes (Figure 2.6, rows represent trials). The magnitudes are thresholded for significance ($p < 0.05$) using False Discovery Rate (FDR) correction in the channel raster and are uncorrected in the trial raster.

To facilitate clinical interpretation of time-varying cortical activity displayed by STFM, a brain map was displayed alongside the channel raster to show the locations and relative magnitudes of activations either integrated over the entire post-stimulus interval or at any user-selectable time point in the channel raster. In Figures 2.4 and 2.5, early and late task stages have been modified offline, with the early stage beginning at stimulus onset and the late stage beginning at the mean speech onset and ending at the mean speech offset. The end of the early stage was chosen to maximize exclusion of sites that were prominently activated during the late stage. The magnitude of the HG response at a particular electrode and time is represented by the size and color of disks overlaid on ECoG electrode locations in a two dimensional snapshot of the three dimensional brain reconstruction.

ECoG Maps vs. Electrical Stimulation Maps. To investigate the degree of correspondence between STFM and ESM, the sensitivity and specificity of STFM was computed using ESM as the gold standard. In this analysis, sensitivity was calculated

as the proportion of ESM+ sites correctly identified as STFM+; specificity was the proportion of ESM- sites correctly identified as STFM- :

$$Sensitivity = \frac{STFM_+ / ESM_+}{STFM_+ / ESM_+ + STFM_- / ESM_+} \qquad (2.4)$$

$$Specificity = \frac{STFM_- / ESM_-}{STFM_+ / ESM_- + STFM_- / ESM_-} \qquad (2.5)$$

A site was marked STFM+ if it exhibited significant task-related HG amplitude increase. A site was marked ESM+ if stimulation at this site inhibited language and/or inhibited or elicited movements or sensations in face, tongue, or mouth. At sites categorized as ESM+ by bipolar stimulation (stimulation between two adjacent electrodes), either electrode being STFM+ resulted in both electrodes being labeled as STFM+/ESM+. Only one of these electrodes was counted towards the sensitivity since stimulation could have interfered with neural processing at either or both sites. In contrast, when pairs of electrodes were ESM- during bipolar stimulation, each electrode was marked independently as either STFM+ or STFM-. STFM of visual object naming was compared with ESM of picture naming. STFM of auditory word repetition was compared with ESM of comprehension and spontaneous speech, since auditory word repetition is not part of the standard battery of language tests used for ESM.

25

Region of Interest Analysis. For each patient, we performed an anatomical region of interest (ROI) analysis to compare both ESM and STFM results to regions where cortical lesions most consistently impair language function in literature. Task-relevant ROIs for auditory word repetition included Broca's area, sensorimotor cortex, and Wernicke's area, whereas the task-relevant ROIs for visual object naming included those from auditory word repetition in addition to the middle third of basal temporal-occipital cortex (yellow shaded areas in Figures 2.4 and 2.5). The middle-third was adopted as a convenient and inclusive boundary for inclusion of higher order visual cortex responsible for visual object processing (56, 57). For this analysis, Wernicke's area was defined as the posterior half of the superior temporal gyrus, supramarginal gyrus, and angular gyrus (blue shaded areas). Broca's area included pars triangularis and pars opercularis of the left inferior frontal gyrus (green shaded areas). Relevant sensorimotor cortex (red shaded areas) included pre- and postcentral gyri inferior to hand knob of central sulcus (red highlighted sulci).

Each stimulation site (i.e. monopolar or bipolar) was classified as ESM+ (positive) or ESM- (negative), and was considered either ROI+ when at least one of the stimulating electrodes was inside the ROIs, or ROI- otherwise. Each monopolar stimulation site was considered STFM+ when the site exhibited a significant task-related HG amplitude increase; bipolar stimulation sites were counted only once and were considered STFM+ when at least one of the two electrodes was activated.

Using the classification of inside or outside language ROIs as a rough diagnostic standard, we calculated the sensitivities and specificities of STFM and ESM for all stimulation sites across all patients. Sensitivity was calculated as the proportion of stimulation sites in task-relevant ROIs correctly classified as positive; specificity was calculated as the proportion of stimulation sites outside task-relevant ROIs correctly classified as negative:

$$Sensitivity(STFM) = \frac{STFM_+ / ROI_+}{STFM_+ / ROI_+ + STFM_- / ROI_+} \tag{2.6}$$

$$Sensitivity(ESM) = \frac{ESM_+ / ROI_+}{ESM_+ / ROI_+ + ESM_- / ROI_+} \tag{2.7}$$

$$Specificity(STFM) = \frac{STFM_- / ROI_-}{STFM_+ / ROI_- + STFM_- / ROI_-} \tag{2.8}$$

$$Specificity(ESM) = \frac{ESM_- / ROI_-}{ESM_+ / ROI_- + ESM_- / ROI_-} \tag{2.9}$$

McNemar's χ^2 test (58) was performed to assess the statistical discordance of the sensitivities and specificities of STFM and ESM relative to language ROIs.

2.4 Results

STFM Can Be Performed Online

In all patients, our STFM system successfully produced spatial-temporal functional maps of language function that could be reviewed online. Trial-based signal analyses, statistical testing, and STFM visualization were updated between trials. Figure 2.3 shows an unmodified screenshot of the online STFM system. Modified screenshots of online STFM during both tasks in Patient 1 are shown in Figure 2.4. In each illustration, a screenshot of the channel raster of ECoG activation has been modified to: a) highlight temporally clustered responses evident during online STFM, and b) compare online STFM to the results from ESM. ROIs are also highlighted as described in the Methods. Simplified brain maps for Patients 2-7 are shown in Figure 2.5, with online STFM and ESM results from visual object naming and auditory word repetition respectively.
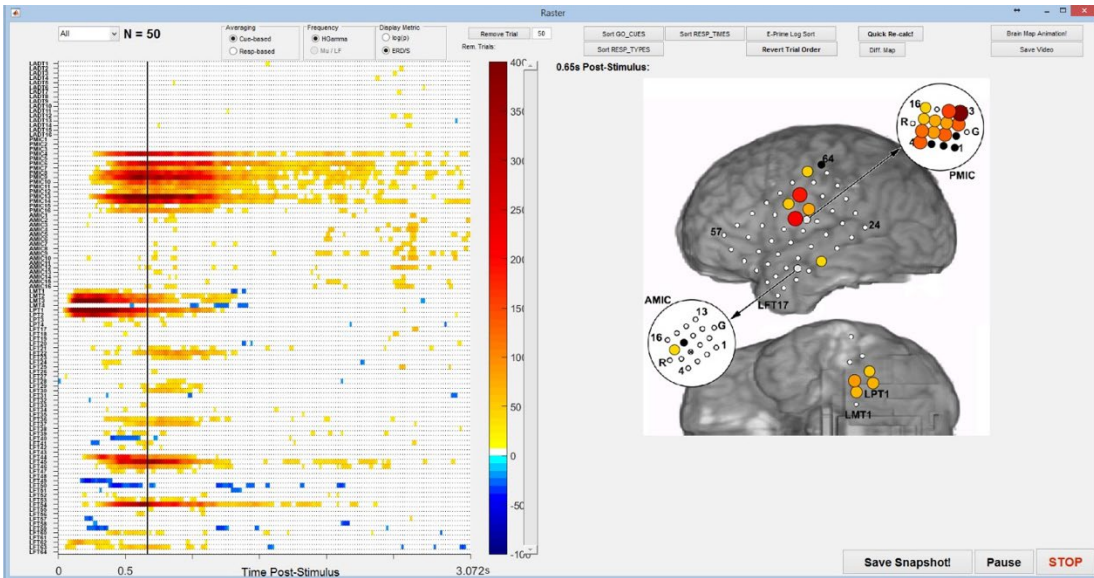
Figure 2.3. Unmodified screenshot of online STFM system, during visual object naming task of Patient 1.

System screenshot with brain map corresponding to selected point in time (0.65s post-stimulus shown in screenshot). See Figure 2.4 for detailed description.

Visual Object Naming

Auditory Word Repetition
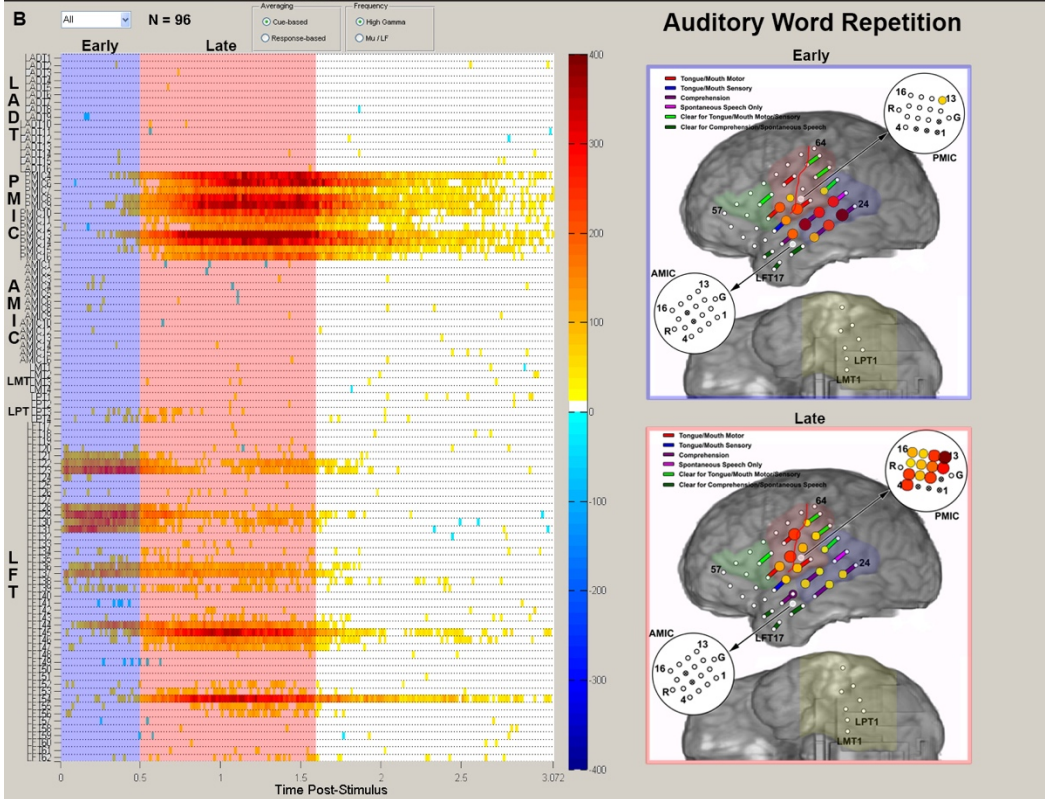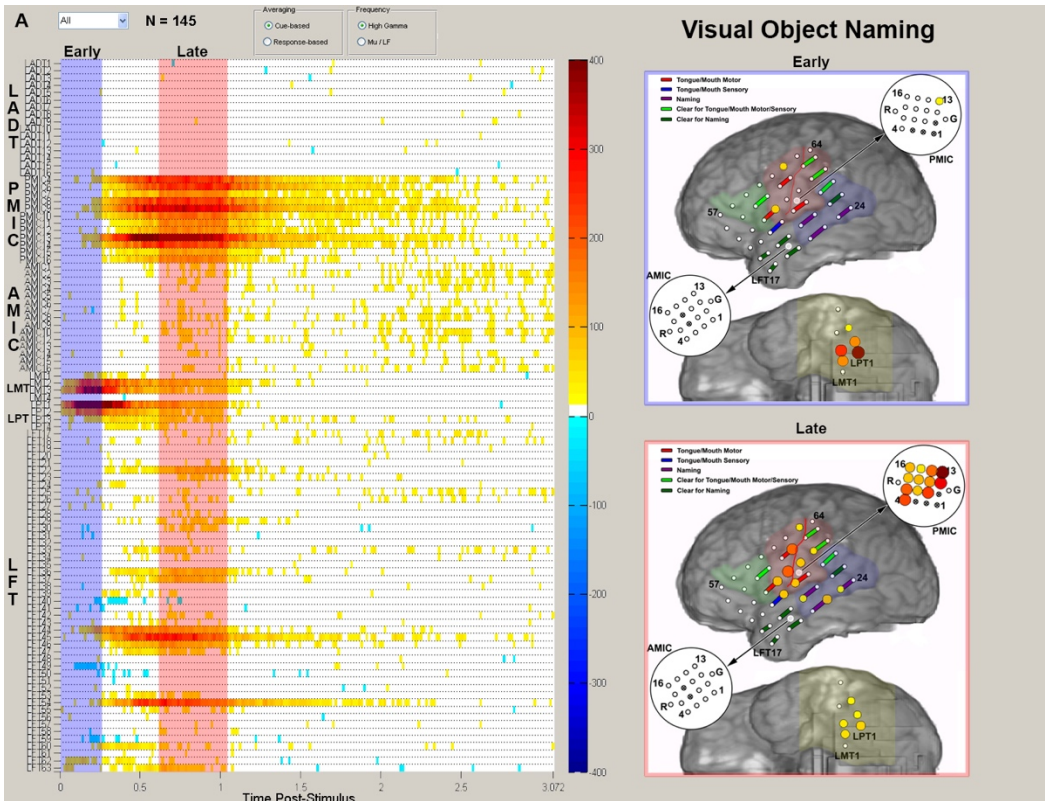
Figure 2.4. STFM of visual object naming (A) and auditory word repetition (B) in Patient 1.

STFM results are shown as a raster of HG responses on the left, and as brain maps of HG response magnitude (represented by disc size and color) on the right. ESM maps (colored bars between electrodes) are also shown. Color-shaded areas denote anatomical boundaries of classical language areas used as regions of interest (ROI) in ROI sensitivity/specificity analysis. Each raster plot displays the spatial-temporal distribution of significant increases (red spectrum) or decreases (blue spectrum) in HG energy relative to pre-cue baseline in 16 ms windows. Each row corresponds to a different electrode as displayed on the right brain maps. All times are relative to cue onset (t=0s). To highlight the spatial pattern of cortical activation at early (visual/auditory perception) and late (response production) stages, HG responses are integrated across an early and late temporal window (early stage highlighted in blue and late stage in red on raster plot), and shown in separate brain maps (early stage in the top brain and late stage in the bottom brain). Microelectrode arrays AMIC and PMIC are enlarged for better visualization of HG responses. The early and late stages can be modified by the user offline, based on the spatial-temporal evolution observed in the raster, to visualize the spatial distribution of activation during different observed task stages. In this illustration, the early sections were chosen to map perceptual processing stages and the late sections were chosen to map response production.

A

Visual Object Naming

Early	Late	Early	Late

B

Auditory Word Repetition

Early	Late	Early	Late

Figure 2.5. Visual object naming task (A) and Auditory word repetition task (B) results for Patients 2-7 (P2-P7).

ESM and Online STFM results are overlaid on brain maps with highlighted ROIs. As in Figure 2.4, online results are separated into early stage (visual perception, left brain) and late stage (response production, right brain), where HG responses were computed by integrating across an early or late temporal interval. Microelectrode arrays are enlarged for better visualization.

Spatial-temporal Functional Maps Are Task-specific

In all patients, online STFM revealed the temporal evolution of activation across all ECoG recording sites. As expected, the different components of each patient's cortical language networks were activated with different temporal envelopes, resulting in complex, cascading spatial-temporal patterns of activation. When functional maps for different language tasks were compared, their differences reflected the contrasting processing demands of the tasks. The STFM system highlighted cortical regions associated with visual processing (basal temporal-occipital cortex) during object visual naming (Figures 2.4A and 2.5A), speech processing (Wernicke's area) during auditory word repetition (Figures 2.4B and 2.5B), and speech planning and preparation (Broca's areas and sensorimotor cortex) during both tasks (Figures 2.4 and 2.5).

Micro-ECoG vs. Macro-ECoG Responses: Similarities and Differences

33

The overall response patterns within micro-ECoG arrays were consistent with those of macroelectrodes, and both were consistent with task-related processing demands. However, HG responses within micro-ECoG arrays were often more robust than those within macroelectrodes. This was most evident in single-trial responses, in which statistically significant responses occurred more consistently across time windows and across trials (Figure 2.6). This could have been due to greater temporal and functional homogeneity in population responses within micro-ECoG arrays than those within macroelectrodes. Micro-ECoG arrays sampled cortical activity from a surface area (2.7-mm2) only slightly larger than that of individual macroelectrodes (2.3-mm diameter). One might expect that task-related cortical activation at this scale would be highly correlated among adjacent microelectrodes, resulting in highly uniform spatial-temporal patterns of activation. However, in many instances we observed a surprising degree of heterogeneity in the temporal and spatial patterns of activation at different microelectrodes within individual micro-ECoG arrays.
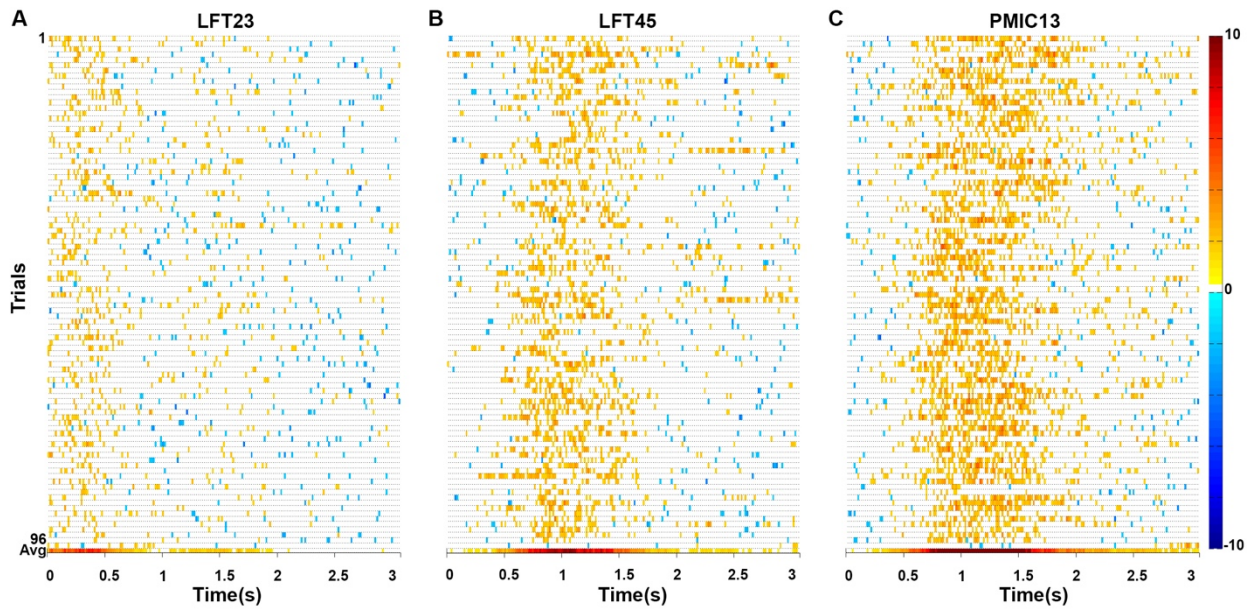
Figure 2.6. Single trial responses from online STFM results for Patient 1, auditory word repetition task.

The single trial activations are shown for the auditory word repetition task in three separate electrodes:(A) LFT23, a macroelectrode in the early responding, putative stimulus perception cluster, (B) LFT45, a macroelectrode in the late responding, putative verbal response cluster, and (C) PMIC13, a microelectrode from the late responding cluster. The colors shown are scaled according to the negative log of the p-value, computed as a series of t-tests with the channel baseline distributions at the time of the trial. Significance thresholds have not been FDR corrected for multiple comparisons, as the single trial responses are primarily intended as an indicator of neural response consistency across trials. Each trial raster has a row at the bottom with the FDR-corrected estimate of trial-averaged activation (identically displayed on the channel raster, Figure 2.4).

35

STFM results for both visual object naming and auditory word repetition tasks for each patient were first computed by using ESM results as the gold standard (Table 2.2). The average sensitivity across tasks and patients was 69.9%, and the average specificity was 83.5%. Table 2.3 shows STFM vs. ESM test results for both ROI+ and ROI-stimulation sites across all patients.

	Comparison of STFM vs. ESM			
Patient Number	**Visual Object Naming**		**Auditory Word Repetition**	
	Sensitivity (%)	**Specificity (%)**	**Sensitivity (%)**	**Specificity (%)**
1	100.0	94.4	100.0	78.6
2	33.3	69.2	100.0	78.6
3	75.0	62.5	100.0	77.8
4	85.7	65.0	28.6	92.9
5	100.0	90.0	100.0	100.0
6	0.0	90.3	50.0	90.3
7	50.0	92.3	55.6	86.7
Average	63.4	80.5	76.3	86.4

Table 2.2. Sensitivity and specificity values for STFM during visual object naming and auditory word repetition tasks, with ESM as the gold standard.

STFM vs. ESM test results among ROI+/ROI- stimulation sites						
	ROI+ stimulation sites			ROI- stimulation sites		
	STFM+	STFM-	Row total	STFM+	STFM-	Row total
ESM+	37	9	46	10	17	27
ESM-	26	24	50	7	89	96
Column total	63	33	96	17	106	123

Table 2.3. STFM vs. ESM test results among ROI+ and ROI- stimulation sites, across all patients

The sensitivity and specificity of both ESM and STFM using anatomical ROIs as a gold standard were calculated across patients, using Equations 2.6-2.8 and values from Table 2.3. The average sensitivity across tasks and patients was 65.6% for STFM vs. 47.9% for ESM; the overall average specificity was 86.2% for STFM vs. 78.0% for ESM. The sensitivity of STFM was significantly greater than that of ESM ($p = 0.0068$, McNemar's test), while the specificity of STFM appeared to be greater than that of ESM, but this difference was not statistically significant ($p = 0.066$, McNemar's test).

2.5 Discussion

Results from seven patients demonstrated that our online STFM system is fast and robust enough to compute cortical maps of language function for online review, using ECoG HG responses that correspond well to ESM results.

The time-consuming and taxing nature of ESM motivates the development of a passive functional mapping alternative. We believe that online STFM based on event-related changes in ECoG signals provides important opportunities for clinicians. The clinical utility of STFM currently lies in both augmenting the findings from ESM and identifying the areas of potential functional significance as a guide to further exploration by ESM. STFM has the advantage of being performed at all recording sites simultaneously. Additionally, it can provide a graded measure of cortical activation that allows clinicians to estimate the relative contribution of different cortical sites to task performance.

With a larger body of evidence, it may be possible to someday make clinical decisions from passive functional mapping alone. Mapping language cortex presents challenges, however, since multiple sites over large-scale cortical networks are involved. Although some studies have indicated poor sensitivity and specificity of ECoG mapping in relation to ESM (e.g. specificity of 78% and sensitivity of 38% during visual object naming (13)), recent reports have suggested that in some instances it can be more predictive of post-operative language impairments than ESM (21, 42, 59). More work will be required to correlate surgical outcomes with the location of resected and preserved sites identified by ESM and STFM.

Compared to existing ECoG functional mapping systems, our STFM system offers several key advantages. First, our trial-based system constructs a baseline distribution from the pre-cue phases of individual trials, rather than a pre-session block of baseline activity, as employed by previous studies (15, 44) . In our opinion, the pre-cue baseline provides the best control for active periods because it controls for variations in the arousal and attentiveness of the patient that are not directly related to testing. Trial-based analyses also provide greater cognitive control during both the baseline and the active period than do block-based designs. In a block design, it is difficult to ensure that a patient is continuously performing a task during a long active period without contaminating this period with unintended cognitive events or brief rest periods. Behavioral responses can also be used to trigger the STFM system, but variable response latencies and artifacts in speech onset detection can be challenging, particularly when implemented online.

Previous studies of ECoG mapping using the HG frequency band have shown comparable, if slightly lower, sensitivities and specificities relative to ESM (Table 2.4) (47–50). These studies have all assumed ESM as the gold standard for identifying eloquent cortex and predicting post-resection deficits. The ideal gold standard for functional mapping is post-operative outcome following resection of a cortical site. However, this is difficult to achieve in clinical practice because resections always include more than one site and because reorganization of function inevitably takes

place following resection such that deficits appearing immediately after surgery often resolve. To demonstrate superiority over ESM, ECoG would have to make better predictions of these deficits, as well as more persistent deficits, preferably in a prospective cohort of patients.

ECoG vs. ESM in previous studies					
Author	Year	Frequency Band (Hz)	Task	Sensitivity (%)	Specificity (%)
Wu et al.(50)	2010	75-100	Language	71.0	59.9
Cheung et al.(47)	2012	61-260	Motor/Speech	70.8	78.1
Ruescher et al.(49)	2013	60-400	Speech	18.9	96.7
Bauer et al. (48)	2013	69-95	Language	20.3	85.0
This paper	2015	70-110	Language	69.9	83.5

Table 2.4. Comparison of sensitivity/specificity calculation for different studies

Concerns about the accuracy of ESM can be traced back to its inception in clinical practice (60, 61). It has long been recognized that cortical stimulation can affect function at a distance (39), and that ESM does not always predict post-operative language outcomes (21, 42, 62). This concern is perhaps best illustrated in somatosensory and motor cortices where the effects of lesions are more predictable. Although stimulation of post-central gyrus often elicits motor responses, resection of this gyrus causes sensory impairments and apraxia, but not weakness per se (61, 63). Conversely, stimulation of pre-central gyrus can elicit somatic sensations. Indeed, clinical investigators have elicited movements with stimulation 1.5-4.7 cm anterior and

2 to 3.4 cm posterior to the central sulcus, but resection of most of this territory can be performed with little or no motor impairment (61, 63). Indirect evidence for distant effects of ESM can also be found in studies where direct cortical stimulation has elicited both evoked responses (64) and HG responses (65) in distant cortical regions that have putative functional connectivity with the stimulation site. Because HG responses reflect population firing rates (25, 66), the latter study suggests that ESM can affect neuronal firing in distant populations, though the effect on cortical function is unknown.

Because of the potential limitations of ESM for functional localization, we believe it is important to evaluate the accuracy of both ECoG and ESM with respect to an independent measure of cortical function. This can be drawn from the rich literature on the effects of discrete brain lesions (67, 68), as well as on regions typically activated on fMRI during experimental language tasks, albeit at far lower temporal resolution (67, 69, 70). Using this approach, we found that the sensitivity of STFM was significantly greater than that of ESM, while the specificity of STFM was greater than that of ESM, though not significantly so. In light of these findings, we believe that both ESM and passive ECoG mapping offer approximations of the patient's true functional anatomy and that more studies are needed to understand their comparative utilities in clinical practice.

We have demonstrated a system that is able to compute spatial-temporal functional maps online, allowing for immediate access to ECoG mapping results at the patient's bedside. Our approach is generalizable to a variety of clinical and experimental applications. For example, this system could easily be adapted to the time-pressured circumstances of an awake craniotomy. We believe that this information can help clinicians better understand the contributions that tested sites make to task performance and help avoid cortical areas critical to eloquent function during surgical planning.

Chapter 3 Neural dynamics of Broca's area during lexical selection: an intracranial EEG study

3.1 Abstract

Speaking in sentences requires the selection of words from among multiple competing candidates for a contextually determined lexical representation. Although previous studies have shown that this process depends on Broca's area, the spatial-temporal dynamics by which it is recruited and interacts with other key areas during lexical selection have yet to be elucidated. Using direct intracranial cortical recordings with a combination of high temporal and spatial resolution, we investigated the spatial-temporal dynamics of neural activity (indexed by 70-150Hz high gamma frequency band activation) in six patients while they performed a sentence completion task in which the difficulty of lexical selection (indexed by sentence cloze probability) was systematically varied. Across all six patients, neural activity in Broca's area appeared to accumulate throughout stimulus presentation, and decreased before the onset of response articulation. More importantly, neural activity in Broca's area was significantly higher during completion of sentences with greater demands on lexical selection. Further, analyses of effective connectivity found that more demanding sentences elicited larger neural interactions within Broca's area as well as between

Broca's area and areas in posterior temporal lobe storing lexical representations. Our findings provide a detailed picture of the fine temporal dynamics by which Broca's area coordinates lexical selection during speech.

3.2 Introduction

Broca's area has been associated with speech and articulation ever since the 19th century (71, 72). According to the classical Wernicke-Lichtheim-Geschwind model of the neurobiology of language (73–75), Broca's area was believed to be critically involved in speech production. However, the exact role that it plays in this process is still being debated.

In recent neurobiological models of human language, Broca's area has been linked with a number of different processes. In one viewpoint, Indefrey and Levelt (31, 76) hypothesized that Broca's area was engaged at the level of phonological processing and was particularly associated with the process of syllabification. In contrast, in the dual-stream model of speech processing proposed by Hickok and Poeppel (77, 78), Broca's area is involved in phonetic encoding and implementing mechanisms of retrieving or generating articulatory codes. Hagoort's memory, unification and control (MUC) model (79, 80) further linked Broca's area and adjacent cortex to the integration of linguistic meaning with world knowledge. This so-called unification component refers to contextual integration of representations during sentence comprehension and

production. Finally, a functional neuroanatomic model for semantic processing by Lau et al. (27) hypothesized that the posterior inferior frontal gyrus mediates selection between highly activated candidate lexical representations in the posterior middle temporal gyrus and neighboring areas, where lexical representations are stored and activated. These models predict the recruitment of Broca's area during different stages of speech production: phonological processing, phonetic encoding, representation integration, and lexical selection.

In order to better understand the role that Broca's area plays in speech production, a sufficiently detailed picture of the spatial-temporal dynamics of neural activity in Broca's area and interactions between it and other cortical language areas is required. Previous lesion, neuroimaging and non-invasive electrophysiological studies have probed the role of Broca's area using paradigms ranging from single word generation to full sentence comprehension. For example, one lesion study (81) found that patients with left focal frontal lesions made more errors generating verbs for items with competing responses. Another fMRI study (82) showed larger activation over posterior left inferior frontal cortex (LIFC) when reading sentences with lexical-syntactic ambiguities, providing evidence that Broca's area contributes to syntactic unification. However, these studies lacked precise measurements of the spatial-temporal dynamics of neural activity. Specifically, while functional magnetic resonance imaging (fMRI) offers sub-millimeter spatial resolution in localizing specific cortical areas, it does not

have enough temporal resolution to study the temporal dynamics of overt speech production (83).

In contrast, direct intracranial cortical recordings such as electrocorticography (ECoG) and stereoelectroencephalography (SEEG) offer a unique opportunity to overcome these limitations by acquiring neural signals with a combination of good temporal and spatial resolution, especially important for language tasks involving overt speech production. Recent studies have emphasized the utility of increases in signal energy in a broad range of high gamma frequencies (~ 60–200 Hz) as an index of cortical activation during a variety of tasks (20, 84–88). Activity in this frequency range is highly correlated with blood oxygen level-dependent (BOLD) responses (89, 90) and with average firing rates in cortical neuronal populations (91, 92). Several such studies have studied Broca's area cortical activity in various language tasks. An SEEG study (93) showed evidence for lexical, grammatical, and phonological processing in Broca's area. A recent ECoG study (94) reported evidence that Broca's area coordinates large-scale cortical networks for spoken word production, prior to articulation. Consistent with converging evidence from cognitive psychology and noninvasive neuroimaging, ECoG recordings reveal a temporal cascade of sub-network activation in the language cortex during speech production (95), capturing the fine temporal dynamics by which different cortical sites are activated and potentially yielding more insight into the functional role of Broca's area.

The goal of the present study was to test whether Broca's area is activated during the performance of a sentence completion task, and if so whether it is involved more under conditions that require selection of semantic knowledge among competing alternatives. The sentences used varied in their cloze probability, which is the probability that a specific word will be selected to end a sentence, based on previous performance by normal subjects (96–98). Our hypothesis was that the process of lexical selection during the task would require the integration of contextually determined representations that accumulate during sentence comprehension. With high cloze probability sentences, this integration process is highly determined and easily converges on few lexical targets, whereas with low cloze probability sentences, more targets are possible, making integration and selection more difficult. We would expect more neural activation over Broca's area in low cloze probability conditions than in high cloze probability ones.

In a series of six patients, we found that neural activity over Broca's area during sentence completion appeared to accumulate throughout stimulus presentation, and to decrease right around the onset of response articulation. More importantly, Broca's area activation was significantly higher during completion of sentences that required higher demands for lexical selection, in the interval between blank onset and response onset. In addition, effective connectivity analysis demonstrated larger neural interactions within Broca's area as well as between Broca's area and the posterior temporal cortex for more demanding sentences. In all, our findings appear to be

consistent with a chief prediction of a neuroanatomic model of semantic processing in which Broca's area plays a key role in the selection of unique lexical items from multiple competing representations during sentence completion.

3.3 Methods

Patient information. Six English speaking patients (Table 3.1) with intractable epilepsy underwent placement of subdural electrodes in the left (dominant) hemisphere to localize their ictal onset zone and to identify language and motor areas using electrocortical stimulation mapping. The implanted electrodes consisted of arrays (grids and/or strips) of standard electrodes (2.3mm exposed diameter, 1cm center-to-center spacing, Adtech, Racine, WI or PMT Crop, Chanhassen, MN) as well as high-density electrodes (2mm exposed diameter, 5mm center-to-center spacing, PMT Crop, Chanhassen, MN). In all patients, the anatomical placement of electrodes was dictated solely by clinical considerations for recording seizures or mapping cortical function.

Patient	Age	Gender	Handedness	Hemisphere Dominance	Hemispheric Coverage	Seizure Onset Zone
1	32	Male	Right	Left	Left	Left superior parietal lobule
2	49	Male	Right	Left	Left	Left fronto-central head regions
3	49	Male	Right	Left	Left	Left fronto-central head regions
4	26	Female	Both	Left	Left	Left frontal lobe

| 5 | 25 | Male | Right | Left | Left | Ventral left precentral gyrus and left inferior premotor area |
| 6 | 36 | Female | Right | Left | Left | Left inferior temporal gyrus |

Table 3.1. Patient Demographic and Clinical Information

Standard protocol approvals, registrations, and patient consents. Patients were admitted to the Johns Hopkins Epilepsy Monitoring Unit after electrode implantation for a period of 6-14 days. All patients gave informed consent to participate in research testing under a protocol approved by the institutional review board of the Johns Hopkins Medical Institutions.

Experimental Paradigm. During the sentence completion task, the patients were instructed to covertly read a sentence word by word (e.g. 'He mailed the letter without a'), and to complete the sentence with one overtly spoken word ('STAMP') upon seeing the blank ('_____.', shown in Figure 3.1). We chose 200 sentences (Appendix 1) from the Bloom and Fischler 1980 library (97). The sentences varied in their cloze probability, which is the probability that a specific word is selected to end a sentence, based on previous performance by normal subjects. The sentences were chosen so that their cloze probabilities were evenly distributed in the following 8 bins: [0.2, 0.3), [0.3, 0.4), [0.4, 0.5), [0.5, 0.6), [0.6, 0.7), [0.7, 0.8), [0.8, 0.9), [0.9, 1]. Sentences in each bin of cloze probability were matched for sentence length (6-9 words). The sentences were

divided into one training block and four testing blocks. The training block contained 8 sentences, each having a different cloze probability from the 8 bins described above. The four testing blocks contained 48 sentences in each block, with 6 sentences from each of the 8 bins described above. Two different presentation rates were used: Patients 1-4 viewed each word for 500ms (slow-timing), and Patients 5 and 6 viewed each word for 400ms (fast-timing). The presentation speed was determined before the experiment and was based on the patient's preferences. After the last word in the sentence, a blank with a period was presented for 3 seconds, upon which the patient was instructed to speak out the one word answer, and to say "pass" if not able to retrieve an answer. A fixation cross was then presented for 1.5-2 seconds jittered, just before the next trial.

The experiment was carried out using BCI2000 (99), running on a Windows PC computer with an extended LCD monitor presented in front of the patient during the task. We detected the onset of the first word as well as the offset of the last word for each sentence by recording the thresholded digital output of a photodiode mounted on the monitor presenting the stimuli. In each trial, the photodiode detected an increase in luminance that occurred when a small white square appeared at the bottom left corner of the screen during presentation onset of the visual stimulus. The white square then disappeared upon blank onset, creating a decrease in the analogue input. The verbal responses of the patient were recorded by a microphone, and were analyzed post-hoc for response accuracy as well as latency. The photodiode and microphone analog inputs

were fed into the neural recording system and synced with the ECoG channel recordings to get precise timing for analysis. Both of the analog input channels were recorded at a sampling rate of both 1 kHz and 30 kHz.

Response Time Analysis. The recorded verbal responses were manually transcribed and the response latencies manually marked in each trial for every patient. The response times (RTs) were measured by visual inspection of the waveforms using the Praat software for speech analysis (100). We calculated RTs from blank onset (i.e. offset of the last presented word) to verbal response onset (illustrated in Figure 3.1) for each trial on every patient. Incorrect trials were excluded from further analysis. We then grouped sentences with cloze probability (CP) higher than or equal to 0.6 as well as those with CP lower than 0.6, and calculated median RTs respectively. Numbers of sentences with CP$\geq$ 0.6 and sentences with CP<0.6 are equal (96 sentences in each category).

Electrode Localization. Electrode locations were identified in a high-resolution post-operative brain CT; electrode locations were then transformed onto a high-resolution pre-operative brain MRI by volumetrically co-registering the pre- and post-operative scans in Bioimage Suite (101). Pre-surgical volumetric MRI as well as electrode locations for individual patients were then normalized onto a Montreal Neurological Institute (MNI) brain atlas to show cross patient results. For details on the MNI electrode registration, see (102).

51

Data Acquisition and Analysis. Recordings of all standard and high-density electrodes were referenced to a single electrode to minimize extracranial sources of artifact. Raw ECoG signals were recorded with a 256-channel recording system (NeuroPort, BlackRock Microsystems, Salt Lake City, UT; or Nihon Kohden America, Irvine, CA, USA), amplified and sampled the data at up to 30 kHz of sampling rate with an analog third-order Butterworth anti-aliasing filter. The anti-aliased 30 kHz recording was decimated to 1 kHz in all patients prior to any subsequent analysis. Channels with excessive amounts of noise were identified by a clinical neurophysiologist and excluded from analysis. The remaining channels were re-referenced using a common average reference (CAR) filter to remove spatial bias in the raw ECoG amplitudes. Separate CAR blocks were used for all the standard electrodes and all the high-density electrodes in each patient.

High Gamma Activity Analysis. The CAR-filtered ECoG signal was analyzed for the duration of the task in 128 ms epochs of data with 112 ms overlap. The Fast Fourier transform (FFT) was computed on each window, and the resulting coefficients were then multiplied by a modified flat-top Gaussian window with cutoff between 70-150 Hz, with notch filters applied to 60 Hz and 120 Hz for line noise elimination. The bandpass-filtered spectrum was converted to high gamma amplitude by zeroing the negative frequency components, doubling the positive frequency components, computing the inverse FFT, and taking the magnitude of the result (i.e. the Hilbert

transform) (103, 104). The resulting high gamma amplitude was then log transformed to approximate a normal distribution and decimated to a temporal resolution of 16 ms using a moving average filter. More details of spectral feature extraction methods can be found in (105).

The red vs. blue curves in Figures 3.2, 3.3 and 3.4 illustrate cortical activation, aligned with onset of the blank, during trials with low vs. high CP sentences, respectively, with the shaded areas indicating the 95% confidence interval. The cyan highlighted areas show the statistical significance between the two groups, based on the results of an FDR corrected two-sample single-tail t-test ($p < 0.05$). Red and blue triangles show median RT in low vs. high CP sentences, respectively.

Event-related Causality (ERC) Analysis. ERC corresponds to significant differences in smoothed short-time direct directed transfer function (SdDTF) between baseline and post-stimulus periods and estimates the intensity, directionality, spectral characteristics and time course of statistically significant event-related changes in causal interactions or activity flows between recording sites. A detailed description of the method may be found in (106, 107). In this study, up to a total of 8-21 electrodes were selected for inclusion by order of the magnitude of task-related activation, to ensure there was sufficient data to fit model parameters. We calculated the SdDTF with a 0.15s overlapping window, with an 87% overlap to smooth the connectivity estimates. ERC

values were then obtained using statistical testing (penalized thin-plate spline) (108) to compare the estimates of connectivity during post-stimulus intervals to baseline connectivity estimates. The 1 second preceding the onset of the first word in each trial was used as a baseline. A 95% joint confidence interval was constructed for the differences between the estimates of connectivity during trials and the baseline estimate of connectivity. Only positive values of ERC were considered for this analysis because decreases in connectivity, as compared to baseline, are less likely to be related to task performance. For each patient, we performed an anatomical region of interest analysis to observe neural propagation from one brain region of interest to another. Broca's area included pars triangularis and pars opercularis (Brodmann Area BA44 and BA45, respectively) of the left posterior inferior frontal gyrus (IFG). Posterior temporal cortex (pTC) was defined here as the posterior half of the superior temporal gyrus and middle temporal gyrus.

Statistical Analysis. Behavioral differences between high vs. low CP sentences were tested with an analysis of variance (ANOVA) on the RT for each condition. The statistical significance of differences between the neural activation as well as the ERC flows of sentences with low vs. high CP were calculated using FDR corrected two-sample single-tail t-test (p<0.05).

3.4 Results

We recorded from a total of 737 left (dominant) hemisphere electrodes in six patients undergoing invasive monitoring for seizure localization (Table 3.1). All patients performed a sentence completion task in which they were instructed to covertly read a sentence word by word, and to complete the sentence with one overtly spoken word (Figure 3.1).
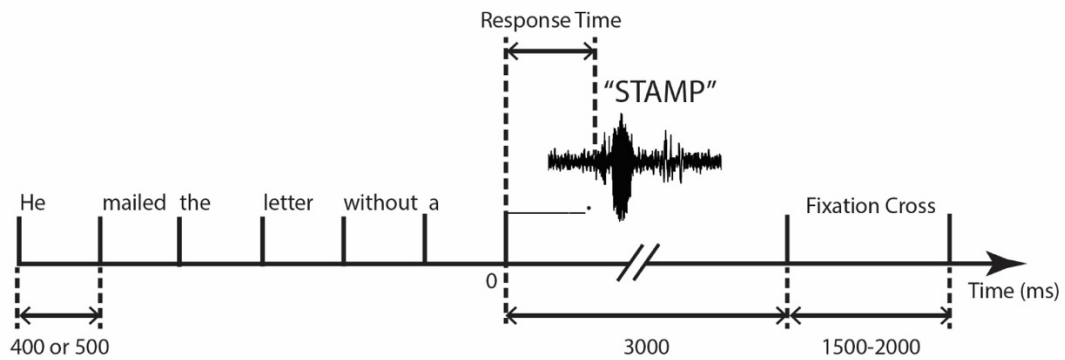
Figure 3.1. Experimental Setup.

Patients were instructed to read a sentence word by word, and to complete the sentence with one overtly spoken word upon seeing a blank. Each word was displayed on the screen for a duration of either 400 or 500ms, depending on the patient's preference. The blank was displayed for 3 seconds, and a fixation cross was then displayed for a duration ranging from 1.5-2 seconds. Reaction times were calculated from blank onset to verbal response onset.

55

Behavioral Analysis. The median reaction time (RT) across all patients was 1.31 ± 0.02s (standard error of the mean, SEM). The median RT for high cloze probability sentences (CP ≥ 0.6) was 1.22 ± 0.03s, and was 1.41 ± 0.03s for low CP sentences (CP < 0.6). An analysis of variance (ANOVA) confirmed that responses were significantly faster ($F_{(2,1209)}=12.05$, $p = 0.0005$) for sentences with high CP than in those with low CP.

Cortical Activation Analysis. We then analyzed high gamma power (70-150Hz): an index of cortical population firing rates near a recording site (109). During the sentence completion task, cortical activation over Broca's area accumulated throughout stimulus presentation, and decreased not too long after response articulation. More importantly, cortical activation over Broca's area appeared to be significantly higher for sentences with low CP than for sentences with high CP. We found no comparable significant differences outside Broca's area.

Figures 3.2 and 3.3 show the cortical activation results mentioned above for Patient 1 as an individual example. Cortical activation of LFPG12 over pars opercularis (Figure 3.2B) was significantly higher for low CP sentences. In contrast, we did not observe a significant difference for LFPG128 over posterior superior temporal gyrus (Figure 3.2C). We further investigated all 17 electrodes within Broca's area for this subject, 13 of which showed consistently significant differences for low vs. high CP sentences

(Figure 3.3A, electrodes in green). The cyan highlighted area in Figure 3.3B marks the averaged interval where the differences were statistically significant, ranging from 0.83 to 1.34s after blank onset for Patient 1.
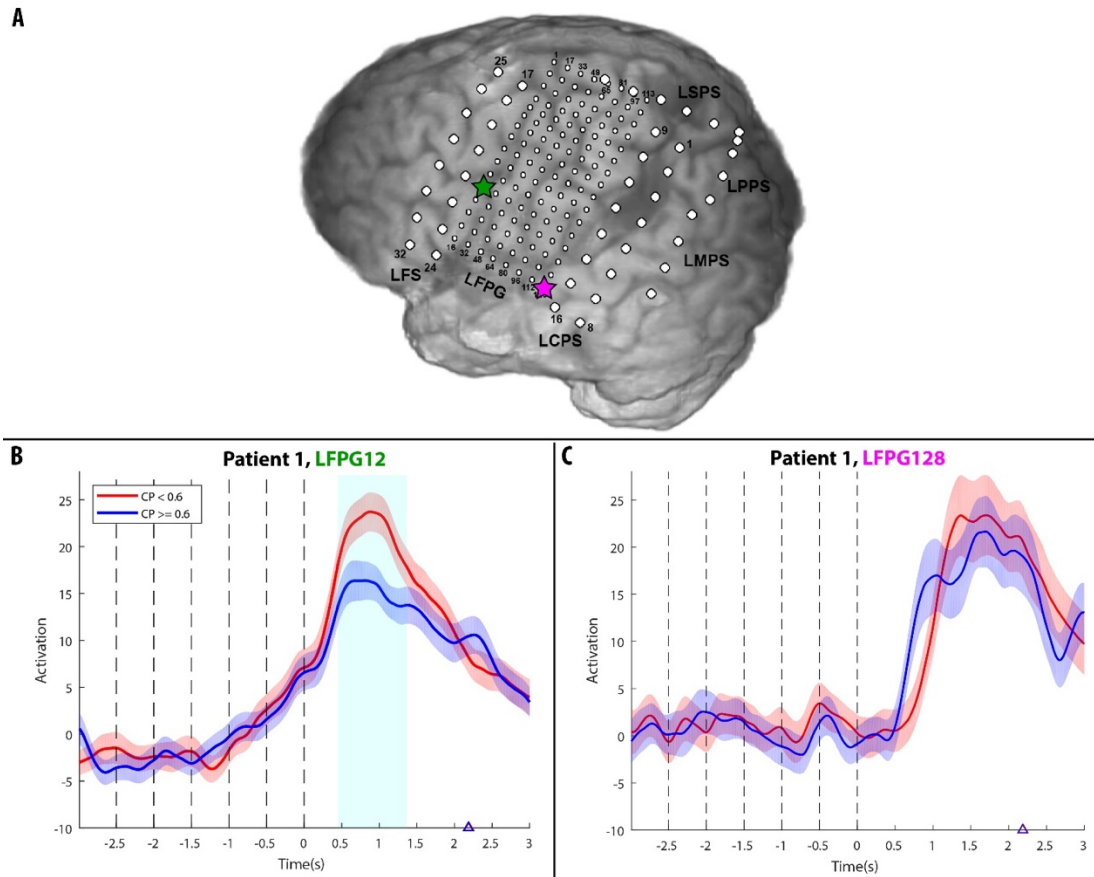
Figure 3.2. Cortical activation of electrodes LFPG12 and LFPG128 in Patient 1.

(A) Brain map for Patient 1. White discs with black strokes represent implanted electrodes. Green and magenta starred electrodes represent LFPG12 and LFPG128, respectively. (B) Cortical activation of LFPG12 over the pars opercularis, with significant differences (cyan highlighted area)

in low (red) vs. high (blue) CP sentences; (C) Cortical activation of LFPG128 over the posterior superior temporal gyrus, with no such differences in low vs. high CP sentences. Cortical activation was aligned with blank onset (Time = 0) in both panels B and C.
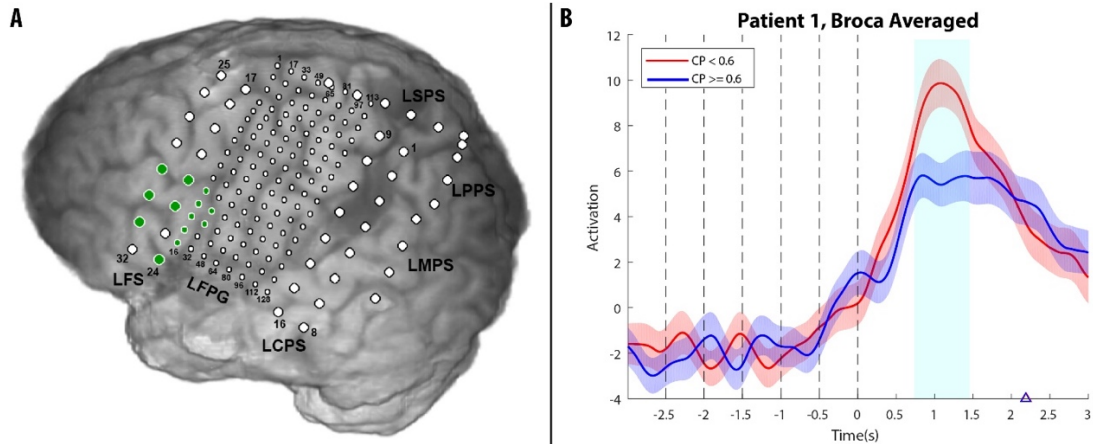
Figure 3.3. Averaged cortical activation across electrodes showing differences in low vs. high CP sentences for Patient 1.

(A) Brain map for Patient 1. White discs with black strokes represent implanted electrodes. Electrodes in green represent the ones showing differences in low vs. high CP sentences. (B) Averaged cortical activation of all green electrodes from panel A, with significant differences (cyan highlighted area) in low (red) vs. high (blue) CP sentences. Cortical activation was aligned with blank onset (Time = 0) in panel B.

The same analysis was further performed on five other patients, all showing similar accumulation patterns as well as significantly higher cortical activation over Broca's area in sentences with low vs. high CP. Altogether we found 45 electrodes over Broca's

area in six patients in which cortical activation showed differences over sentences with low vs. high CP. As illustrated in Figure 3.4, the average time interval of this effect was 0.52 – 1.99s after blank onset (Figure 3.4B, aligned with blank onset), and from 1.12s before to 0.4s after response onset (Figure 3.4C, aligned with response onset). These conclusions held for both blank and response onset alignments, indicating that the effect was significant regardless of data alignment. In contrast, cortical activation averaged across 4 patients with coverage of the posterior temporal cortex did not show a significant difference over sentences with low vs. high CP (Figure 3.5).
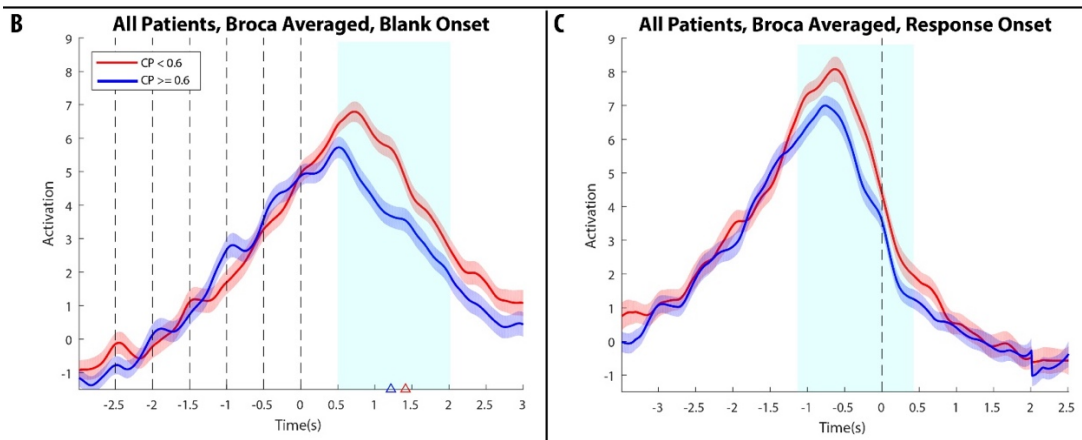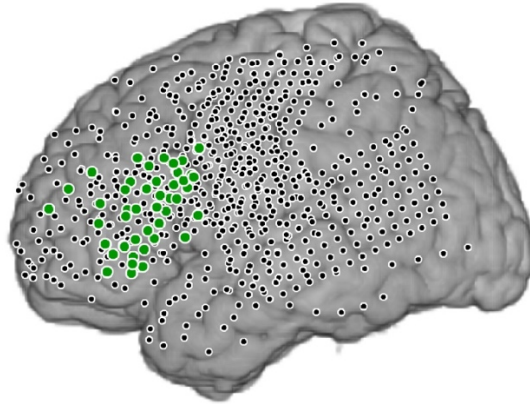
Figure 3.4. Averaged cortical activation across electrodes showing differences in low vs. high CP sentences across all patients.

(A) Standard brain map with normalized electrodes in all patients. Black discs with white strokes represent all implanted electrodes. Electrodes in green (shown here with larger diameters for illustration purpose) were used to generate the averaged neural activity plot in panels B and C. (B) Averaged cortical activation of all green electrodes from panel A, with significant differences (cyan highlighted area) in low (red) vs. high (blue) CP sentences, aligned with blank onset (Time 0). (C)

Averaged cortical activation of all green electrodes from panel A, with significant differences (cyan highlighted area) in low (red) vs. high (blue) CP sentences, aligned with response onset (Time 0).
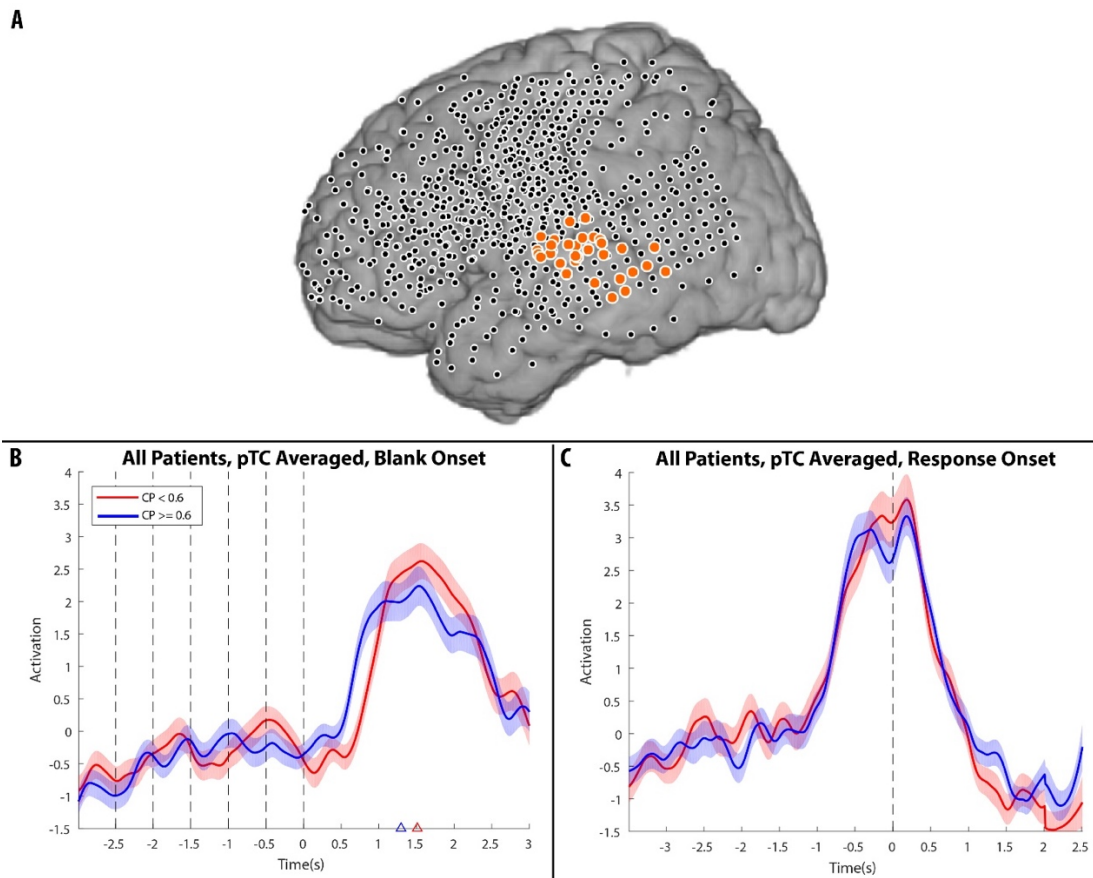
Figure 3.5. Cortical activation averaged across 4 patients with coverage of the posterior temporal cortex.

(A) Standard brain map with normalized electrodes in all patients. Black discs with white strokes represent all implanted electrodes. Electrodes in orange (shown here with larger diameters for illustration purpose) were used to generate the averaged neural activity plots in panels B and C. (B)

Averaged cortical activation of all orange electrodes from panel A, low (red) vs. high (blue) CP groups, aligned with blank onset (Time 0). (C) Averaged cortical activation of all orange electrodes from panel A, low (red) vs. high (blue) CP groups, aligned with response onset (Time 0).

We then sub-divided all trials into 8 finer CP bins, evenly distributed from 0.2 to 1 (Materials and Methods). Across all 45 electrodes showing differences in low vs. high CP sentences, cortical activation was averaged over the time duration of these differences aligned with blank onset as well as response onset (i.e. 0.52 – 1.99s after blank onset and -1.12 – 0.4s after response onset, illustrated in Figure 3.4) across the 8 CP bins. Figure 3.6 shows the result of a linear regression analysis using the averaged cortical activation of the 8 CP bins. Green dots represent the averaged cortical activation across all 45 electrodes with CP bins ranging from 0.2 to 1. Error bars show standard error of the mean. The black dotted lines illustrate the linear fit for the averaged cortical activation, with $R^2 = 0.95$ for blank onset alignment and $R^2 = 0.92$ for response onset alignment. From these results, it appears that neural activity over Broca's area gradually decreased as CP increased from 0.2 to 1.
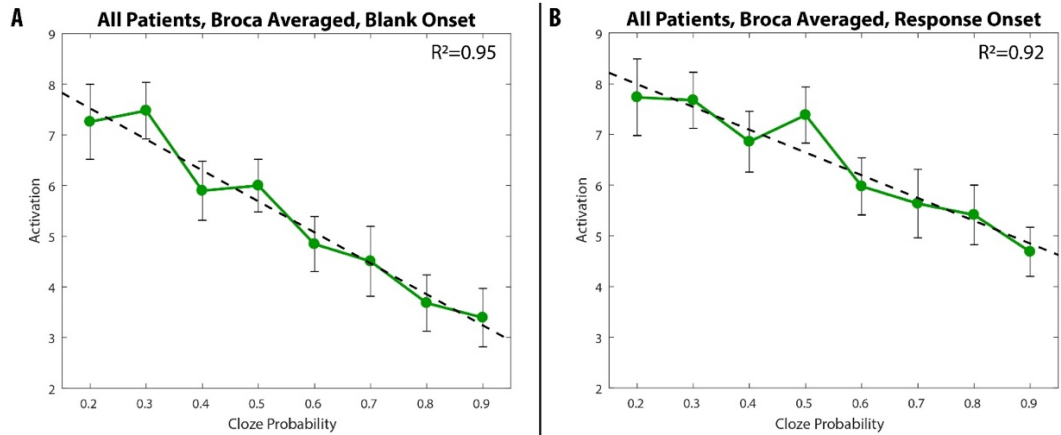
Figure 3.6. Cortical activation averaged by time interval (A) 0.52 – 1.99s post blank onset and (B) -1.12 – 0.4s post response onset, across 45 electrodes over Broca's Area in all patients, for each bin of CP.

Error bars represent standard error of the mean. Dashed lines show linear fits for the averaged cortical activation, with R2 = 0.95 for blank onset alignment and R2 = 0.92 for response onset alignment.

Because previous models of speech production have assigned an important role for syllabification to Broca's area (31), we grouped the trials according to the syllable numbers of our subjects' verbal responses (one vs multiple syllables), and we calculated cortical activation under these two conditions with both blank and response onset alignments (Figure 3.7). There were no significant differences between one vs. multiple syllable responses for blank onset alignment, and only a brief interval of 100ms during which the difference between the two conditions was significant but

contrary to expectations (one-syllable higher than multiple-syllable). Although this analysis alone cannot be considered conclusive, we found no evidence, based on the degree of activation in Broca's area, to support its role in syllabification.
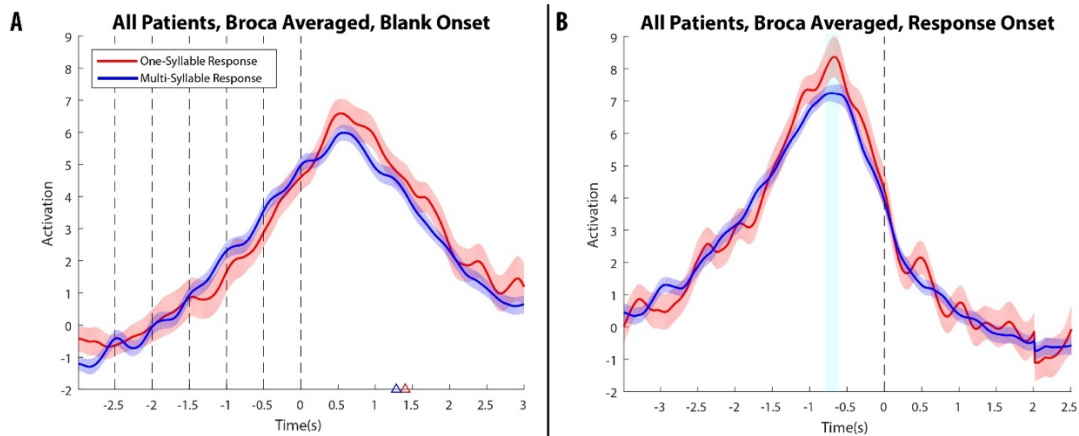
Figure 3.7. Averaged cortical activation across all electrodes showing one (red) vs. multiple (blue) syllable response words across all patients.

(A) Averaged cortical activation of all green electrodes from Figure 3.4A, aligned with blank onset (Time 0). (B) Averaged cortical activation of all green electrodes from Figure 3.4A, aligned with response onset (Time 0). Cyan highlighted area shows significant differences between the two conditions.

Effective Connectivity Analysis. To further investigate the effective connectivity of neural propagation, we used Event-Related Causality (ERC) (106, 107) to estimate task-related, time-resolved causal influences between neural populations (Material and Methods). Here, to test our hypothesis that the role of Broca's area in lexical selection

64

involves the retrieval of both lexical-semantic and lexical-acoustic representations in posterior temporal cortex (pTC), we focused on two major regions of interest in this analysis, namely Broca's area and pTC, which included posterior superior and middle temporal gyri. Results from four out of the six patients (Patients 1, 4, 5 and 6; Patients 2 and 3 didn't have coverage in both Broca's area and pTC) were grouped according to the anatomy illustrated in Figure 3.8A. As shown in Figure 3.8B, we observed significantly increased neural propagation (ERC flows) in sentences with low CP than those with high CP during the following time durations: 1) from pTC to Broca's area (lower left panel), 0.70 – 0.26s before blank onset; 2) from Broca's area to pTC (upper right panel), 0.20 – 1.10s after blank onset; and 3) within Broca's area (upper left panel), 0.84 – 0.32s before and 0.36 – 1.10s after blank onset. There were no significantly increased ERC flows within pTC itself, as shown in the lower right panel of Figure 3.8B. Cyan highlighted areas in the plots illustrate significant differences between the two conditions. To summarize, neural propagation was significantly larger for sentences with higher lexical selection demands: 1) from pTC to Broca's area immediately before onset of the cue to respond; 2) from Broca's area to pTC in the interval between onset of the cue and onset of the response; and 3) within Broca's area itself, beginning before the cue and continuing until response onset.
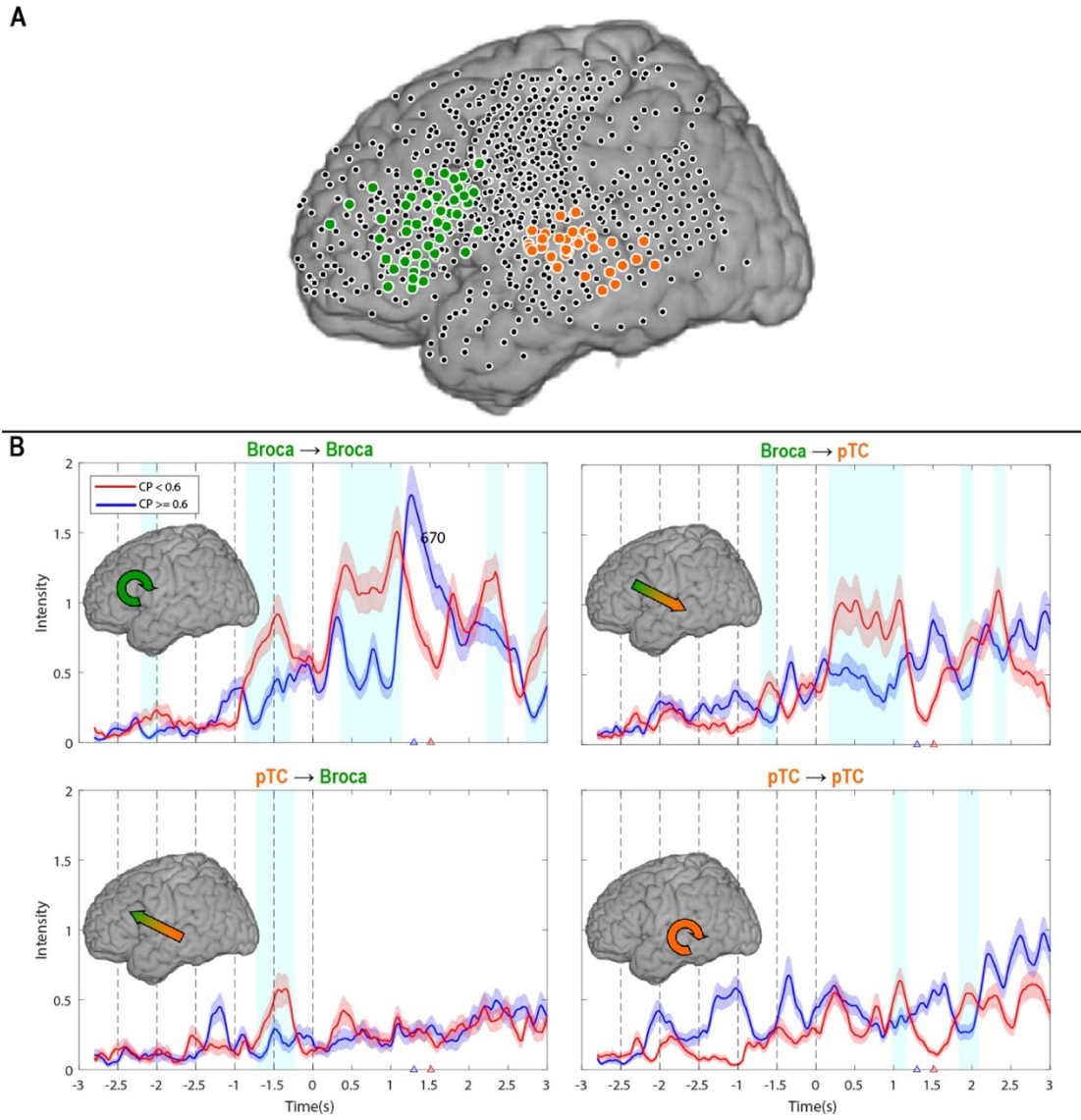
Figure 3.8. Dynamics of effective connectivity between Broca's area and posterior temporal cortex (pTC) for low (red) and high (blue) CP sentences, as revealed by ERC analysis, averaged across 4 patients with coverage for both Broca's area and pTC.

(A) Standard brain map with normalized electrodes in all patients. Black discs with white strokes represent all implanted electrodes. Electrodes in green and orange (shown here with larger diameters for illustration purpose) illustrate selected electrodes over Broca's area and pTC for ERC analysis, respectively. (B) Each plot represents a directed flow of neural activity from one brain region (before the arrow sign) to another (after the arrow sign). The X-axis represents time in seconds, and the Y-axis represents the intensity of the flow. Cyan highlighted areas represent intervals with significant differences by FDR corrected two sample one sided t-test ($p < 0.05$). The arrows on the brains illustrate the direction of the neural propagation for each plot. Cyclic arrows show interactions within a particular brain area, while straight arrows show interactions from one brain area to another.

3.5 Discussion

In this study, we examined cortical activation and neural propagation as six patients performed a sentence completion task in which the difficulty of lexical selection (indexed by sentence cloze probability) was systematically varied. As in previous studies (110), we found that response latencies were greater during completion of sentences with low cloze probability (more difficult lexical selection). However, our ECoG recordings also allowed us to show that during a time interval consistent with lexical selection, Broca's area activation was greater during completion of sentences with higher lexical selection demands. Moreover, during completion of sentences with higher lexical selection demands, neural propagation was greater within Broca's area,

as well as between Broca's area and regions in posterior temporal cortex (pTC) known to store lexical-acoustic and lexical-semantic representations.

Previous studies have demonstrated that sentence cloze probability (CP) is a reliable index of lexical predictability. Readers are usually faster and more accurate during completion of high CP sentences (110). By recording eye movements during sentence reading, fixation and gaze durations are usually shorter for high CP target words (111). In event-related potential (ERP) studies of sentence reading, the amplitude of the N400 component, modulated by a word's predictability, shows a greater negativity upon seeing a low CP target word (112). In the current study, we used direct intracranial cortical recordings to study the neural dynamics of lexical selection processes with an unprecedented combination of temporal and spatial resolution. In the time interval between the last word of the sentence and the onset of the subjects' responses, Broca's area activation was greater during completion of sentences with higher lexical selection demands. When we divided the sentences into finer CP bins, we found a near linear relationship between cortical activation in Broca's area and CP, providing even stronger evidence for its key role in lexical selection.

Prior lesion studies have demonstrated that patients with chronic left prefrontal cortex (PFC) damage often have impaired lexical selection (113, 114). A "race evidence accumulation" model has been proposed to explain these impairments (115, 116). In

this model, the activations of each viable lexical target in a single trial accumulate in parallel and independently, albeit at varying rates. The first target to pass a threshold is selected for response processing. Their findings indicate that left PFC patients have an impaired ability to adjust this threshold. This appears to provide a reasonable explanation for our cortical activation results, where Broca's area is more active with higher lexical selection demands. During completion of low CP sentences in which potential lexical targets are likely to have lower accumulation rates, Broca's area may need to adjust the threshold higher to ensure that the most suitable target wins, and to lower the error rate. As a consequence, it takes more time for a lexical target to reach the adjusted threshold, resulting in a longer response time. This is also consistent with our behavioral results in which patients responded faster during completion of high CP sentences. The race evidence accumulation model, however, does not readily account for selection between two or more lexical items sharing similar accumulation rates. In this case, the items are not easily separated by a raised threshold and a longer response time. The leaky competing accumulator model (117), in contrast, incorporates lateral inhibition and decay in the accumulation process. In this model, candidate lexical targets compete with each other, facilitating convergence on a unique target to reach the threshold for selection and subsequent response processing.

A previous study (94) of overt verbal word production using similar methods investigated the dynamics of neural activation in Broca's area and its effective

connectivity with other areas during verbal repetition of single spoken words and pseudowords, as well as reading single words, where there were no significant demands on lexical selection. A key finding of this study was that Broca's area was active before, but not during, articulation of words and pseudowords, suggesting that Broca's area is primarily engaged in articulatory encoding, i.e. preparation of an articulatory code to be implemented in sensorimotor cortex. This interpretation was further supported by the observation of greater activation in Broca's area during repetition of pseudowords than during repetition of real words, even though the words and pseudowords were matched in length and sublexical phonotactic probabilities. Repeating pseudowords required preparation of a novel articulatory code, placing greater processing demands on Broca's area. Using the same methods used herein to study the dynamics of effective connectivity, the study by Flinker et al. also observed cascading, reciprocal neural propagations, first from superior temporal gyrus (STG) to Broca's area, and during subsequent feedback from Broca's area to STG, then from Broca's area to ventral sensorimotor cortex. This occurred before, but not during articulation, with subsequent feedback from ventral sensorimotor cortex to Broca's area. These findings suggested that Broca's area is an important hub in large scale cortical language networks that, among other functions, coordinates the mapping of lexical-acoustic representations in STG to articulatory representations in sensorimotor cortex.

The current study builds on the previous Flinker et al. study by using a sentence completion task that places demands on lexical selection and varies those demands. Neural propagation from pTC to Broca's area immediately before onset of the blank was significantly larger for sentences with higher lexical selection demands, suggesting that Broca's area received more input from lexical-acoustic and lexical-semantic representations in pTC upon seeing the last word, just before making a decision. Subsequently, neural propagation from Broca's area to pTC in the interval between onset of the blank and onset of the response was greater for sentences with higher lexical selection demands, suggesting that Broca's area provides top-down feedback to lexical-acoustic and lexical-semantic representations, perhaps keeping them active (Figure 3.5), until response selection is complete and the articulatory plan is activated in sensorimotor cortex. These top-down cognitive control processes facilitate lexical access and act to reduce interference in lexical selection for appropriate response execution. In the meantime, there is neural propagation within Broca's area itself, beginning before blank onset and continuing until response onset. This could potentially reflect network interactions within Broca's area during the process of lexical selection.

Overall, our results are consistent with a functional neuroanatomic model of lexical access and selection described by Lau et al. (27), based on fMRI, TMS, and lesion studies (118–123). In this model, the pTC (i.e. the posterior middle temporal gyrus and

71

neighboring parts of the inferior temporal cortex and superior temporal sulcus) mediates the long-term storage of and access to lexical representations. The inferior frontal gyrus (IFG), in contrast, is involved in 'the higher-order processes of selection and controlled retrieval of lexical information'. This model also posits that the anterior part of the IFG mediates controlled retrieval of lexical representations based on top-down information, and that the posterior IFG mediates selection between highly activated candidate representations. Although we did not have enough electrodes over the anterior IFG to study its role in our task, our results do support the active involvement of posterior IFG (i.e. pars opercularis and pars triangularis, a.k.a. Broca's area) during the process of lexical selection. In addition, our effective connectivity results suggest that Broca's area receives information from pTC immediately before the subject is cued to complete the sentence, consistent with the model described above.

In Hagoort's memory, unification and control (MUC) model (80), Broca's area and adjacent cortex is posited to play a key role in the integration (or, "unification") of linguistic meaning with world knowledge. This so-called unification component explicitly includes contextual integration of representations during sentence comprehension and production. According to the model, based on a functional MRI meta-analysis, a unification gradient spans Broca's area: semantic unification in BA47 and BA45; syntactic unification in BA45 and BA44; and phonological unification in BA44 and ventral parts of BA6 (124). Our study supports one feature of this model by

demonstrating a semantic unification effect (i.e. more activation during sentences with higher demands on lexical selection) in BA44 and BA45. In the current study we did not control for syntactic or phonological unification, nor did the electrode coverage in our patients allow us to study the anatomical regions assigned to these processes.

Although our findings provide strong evidence for Broca's area playing a pivotal role in lexical selection, they do not rule out the involvement of other areas in this process since our recordings were limited to the cortical networks that were sampled by the electrodes that were implanted in our subjects for purely clinical purposes and that were engaged during our sentence completion task. Furthermore, event-related causality analysis takes into account partial contributions from selected recording sites but cannot elucidate the entire circuit or assess causality in the same sense as lesion studies. Moreover, our results could arise from a mixture of direct cortico-cortical projections as well as indirect projections from other cortical and subcortical sources.

In summary, our neural activation and propagation results reveal that Broca's area is more active and interacts more with posterior temporal cortex during completion of more demanding sentences. These data document a linear relationship between difficulty of lexical selection (indexed by sentence cloze probability) and Broca's area activity during sentence completion, and lend support for the role of Broca's area in the selection of a unique lexical target from multiple representations. These

observations inform models of the neurobiology of lexical access and selection, with

implications of the fine temporal dynamics of lexical selection during speech.

Chapter 4 Spatial-temporal mapping combined with cortico-cortical evoked potentials in predicting cortical stimulation results

4.1 Abstract

Functional human brain mapping is commonly performed during invasive monitoring with intracranial EEG electrodes prior to resective surgery for drug-refractory epilepsy. The current gold standard, electrocortical stimulation mapping (ESM), is time-consuming, sometimes elicits pain, and often induces afterdischarges or seizures. Moreover, there is a risk of overestimating eloquent areas due to propagation of the effects of stimulation to a broader network of language cortex. Spatial-temporal analysis of passive intracranial electroencephalographic (iEEG) signals has recently emerged as a potential alternative to ESM. Many aspects of passive iEEG mapping are attractive in a clinical setting, especially the ability to rapidly evaluate brain function at all recording sites simultaneously. However, investigators have observed less correspondence between ECoG and ESM maps of language than between their maps of motor function. This may be, in part, because even simple language tasks such as object naming or word reading require the recruitment and interaction of widely distributed cortical areas responsible for different stages of cognitive processing, and

because there is no a priori threshold for a magnitude of activation that is critically important for task performance. We hypothesized that incongruities between ESM and ECoG maps of language function may arise due to propagation of the effects of ESM to cortical areas with strong effective connectivity with the site of stimulation, especially if these areas are activated by the task being tested with ESM. Effective connectivity encompasses not only anatomical connectivity but also the propensity of neural activity in one cortical site to be propagated to another cortical site and to have a causal effect on its neural activity. To test our hypothesis, we evaluated four patients who underwent invasive monitoring for seizure localization, whose language and motor areas were identified using ESM. All patients performed a battery of language tasks, including visual object naming, auditory naming, word reading and auditory word repetition during passive iEEG recordings. To estimate the effective connectivity of stimulation sites with a broader network of task-activated cortical sites, we measured cortico-cortical evoked potentials (CCEPs) elicited across all recording sites by single-pulse electrical stimulation at sites where ESM was performed at other times. With the combination of high gamma power as well as CCEPs results, we were able to train a logistic regression model to predict ESM results at individual electrode pairs. The average accuracy of the classifier was 79.5% using STFM results alone, and 86.2% using both STFM and CCEPs results. These findings suggest that the correspondence between passive iEEG maps and ESM results is greater when the effective connectivity

of ESM stimulation sites with a larger network of task-activated sites is taken into consideration. In light of these findings, we believe that both passive iEEG mapping and cortical network mapping together offer a deeper understanding of the relationship between ESM and passive iEEG mapping results, and that more studies are needed to understand the utility of both mapping techniques in clinical practice.

4.2 Introduction

Despite ongoing advances in non-invasive functional neuroimaging, electrocortical stimulation mapping (ESM) remains the gold standard for mapping cortical function at a sufficiently fine spatial scale in individual patients to guide the surgical resection of brain tissue for the treatment of drug-refractory epilepsy (35, 36) and brain tumors (4). The major advantage of this technique is that it allows clinicians to simulate the neurological consequences of lesioning tissue before it is permanently resected (9). However, there are important practical limitations on its clinical application. Chief amongst these is the risk of triggering afterdischarges and clinical seizures (12, 37, 39) that can prevent comprehensive functional mapping without contributing to localization of the patient's ictal onset zone. Additionally, ESM can elicit pain that prevents mapping at individual sites (125). Lastly, because ESM is done sequentially at pairs of electrodes, finding the optimal stimulation current (37, 38) and then testing the effect of stimulation on different language tasks (126), it is time-consuming. This

can force clinicians to map only a subset of sites. This factor may ultimately pose a particularly acute limitation on ESM as the number and density of ECoG electrodes used for long-term monitoring increases (127, 128).

In addition to the practical limitations on ESM's clinical application, there are a number of concerns about its accuracy and predictive value. The neural populations and operations that are interrupted during stimulation are not well controlled, and it is difficult to rule out distant effects through diaschisis or the distant effects of action potentials evoked by stimulation (39–41). Furthermore, the simulated lesion of ESM cannot take into account the reorganization that occurs after real permanent lesions, and if it is done in only a subset of electrodes, it cannot identify other cortical sites that could potentially assume the function of the lesioned site (i.e., assess functional reserve). Finally, when ESM interrupts the performance of a cognitive task such as word production, the effect is usually all-or-none. The same observed effect can potentially result from interruption of different stages of processing or levels of representation that are necessary for successful task completion.

The limitations of ESM have long motivated the investigation of passive iEEG recordings as a tool for mapping cortical function prior to resective surgery (13, 42, 43, 129, 130). iEEG recordings cannot trigger seizures or pain, and they can be used to simultaneously survey task-related cortical activity in the entire set of implanted

electrodes. In addition, iEEG recordings yield a graded measure of task-related neural activity capable of resolving the activation of cortical sites at temporal scales comparable to the stages of processing that comprise language tasks (131). Thus, the relative degree and timing of activation at a given site can be used to estimate its contribution to these processing stages, providing clinicians with more information as they weigh the benefits and risks of removing epileptogenic tissue vs. sparing eloquent cortex.

In spite of its practical and theoretical advantages over ESM, iEEG spatial-temporal functional mapping (STFM) has not been widely used in clinical practice. One reason for this has been a lack of consensus on which signal components are most informative about task-related neural activity. In recent years, high gamma (~60 to 200 Hz) power changes have been increasingly recognized as a robust and reliable index of task-related activation of cortical populations of neurons (16, 17, 22, 132). This index is highly correlated with blood oxygen level-dependent (BOLD) responses in fMRI (24, 133–135) and with single unit activity recorded by microelectrodes (66, 25). Accordingly, it is highly specific with respect to the location and timing of task-related cortical activation, and it has been observed in nearly every cortical functional-anatomical domain in which it has been studied, including sensorimotor, auditory, visual, and language areas (16, 17, 22). Moreover, recent technological developments have allowed STFM to be performed online, providing immediate feedback to clinicians

(105). STFM can also illuminate the temporal sequence of network activation (dynamics) with a time resolution that is far superior to fMRI, allowing greater insights into the functional role of individual sites.

These properties have made STFM an attractive tool for human research in cognitive and systems neuroscience. Indeed, recent studies have demonstrated extraordinary spatial and temporal selectivity in iEEG-recorded population responses (136). In spite of these advances in research, the potential clinical application of STFM for pre-resective functional mapping has not yet been fully realized. To date, efforts to demonstrate the clinical utility of STFM have used ESM for validation, and although several studies have found strong agreement between ECoG high gamma responses and ESM in motor and early sensory cortices (15, 137–139), there has been less agreement in language cortex (13, 48, 50, 140, 141). In a study comparing STFM and ESM for localization of object naming in 13 patients, for example (13), the authors observed a tradeoff between sensitivity and specificity as the threshold for the magnitude of high gamma responses was varied, i.e. low thresholds yielded high sensitivity but low specificity and vice versa. Among the possible explanations for discrepancies between STFM and ESM, the most important would be if changes in local population firing rates alone do not capture important information about an individual site's role in overall task performance.

The reliance of spoken word production on the function of large-scale cortical networks in frontal, parietal, and temporal lobes has long been appreciated by behavioral neurologists and cognitive psychologists studying the effects of lesions on different brain regions. These effects can be exquisitely specific for different aspects of perceptual processing, semantic and phonological representations, and articulatory plans. Psychophysical investigations into the timing of these different cognitive operations have indicated that they occur in quasisequential stages that overlap in time (cascaded) (31). EEG, MEG, and fMRI studies have provisionally localized these operations to different brain regions, but because of variations in functional anatomy, these insights cannot be clinically applied to individual patients (142, 143). In contrast, iEEG high gamma power changes are sufficiently robust to yield statistically significant responses within individuals, revealing the location and timing of cortical processing at clinically useful resolutions. However, processing at a given site may not always be critical to task performance. Furthermore, processing at each stage likely occurs in sub-networks comprised of multiple cortical sites. The opportunity, and challenge, for iEEG STFM is thus to identify which sites in these sub-networks are most important for task performance so that impairments can be avoided.

We evaluated four patients who underwent invasive monitoring for seizure localization whose language and motor areas were identified using ESM. Additionally, all patients performed language tasks including visual object naming, auditory naming, word

reading and auditory word repetition during passive iEEG recordings. We also measured cortico-cortical evoked potentials (CCEPs) elicited by single-pulse electrical stimulation at distant cortical sites when the patients were awake. With the combination of high gamma power as well as CCEPs results, we were able to train a logistic regression model to predict ESM results at individual electrode pairs. Our findings suggest that additional information about effective connectivity in the overall network of cortical regions activated by language tasks enhance the ability of iEEG STFM to predict ESM results.

In this chapter, we will use insights from the network dynamics during language tasks to improve the accuracy of STFM and better understand the strengths and limitations of both STFM and ESM. This study will exert its most profound and long-lasting impact by providing critical evidence for the clinical utility of STFM for both extraoperative and intraoperative functional mapping prior to resective surgery.

4.3 Methods

Patient information. Four English speaking patients (Table 4.1) with intractable epilepsy underwent placement of subdural electrodes in the left (dominant) hemisphere to localize their ictal onset zone and to identify language and motor areas using electrocortical stimulation mapping. The implanted electrodes consisted of arrays (grids and/or strips) of standard electrodes (2.3mm exposed diameter, 1cm center-to-

center spacing, Adtech, Racine, WI or PMT Crop, Chanhassen, MN) as well as high-density electrodes (2mm exposed diameter, 5mm center-to-center spacing, PMT Crop, Chanhassen, MN). In all patients, the anatomical placement of electrodes was dictated solely by clinical considerations for recording seizures or mapping cortical function.

Patient	Age	Gender	Handedness	Hemisphere Dominance	Hemispheric Coverage	Seizure Onset Zone
1	25	Male	Right	Left	Left	Ventral left precentral gyrus and left inferior premotor area
2	32	Male	Right	Left	Left	Left superior parietal lobule
3	26	Female	Both	Left	Left	Left frontal lobe
4	49	Male	Right	Left	Left	Left fronto-central head regions

Table 4.1. Patient Demographic and Clinical Information

Standard protocol approvals, registrations, and patient consents. Patients were admitted to the Johns Hopkins Epilepsy Monitoring Unit after electrode implantation for a period of 6-14 days. All patients gave informed consent to participate in research testing under a protocol approved by the institutional review board of the Johns Hopkins Medical Institutions.

Experimental Paradigm. A battery of language tasks were performed under ESM and/or passive iEEG recordings. In the word reading task (iEEG), subjects were shown a word on a monitor directly in front of them, and were instructed to read it out loud.

In a paragraph reading task (ESM only), subjects read stories aloud as electrocortical stimulation was intermittently given. In the visual object naming task (iEEG and ESM), subjects were shown a picture stimulus on a monitor (iEEG) or a piece of paper (ESM) directly in front of them. Subjects were instructed to speak the name of the object in the picture, or say "pass" if they could not recall the name. In the auditory word repetition task (iEEG only), subjects were played an audio recording of a spoken word through a speaker placed in front of them. Subjects were instructed to verbally repeat the cued word. In the auditory naming task (iEEG and ESM), subjects were played an audio recording of a spoken sentence describing a certain object through a speaker placed in front of them. They were instructed to verbally name the object out loud. Trial numbers of each task for each patient were governed by the time constraints on patient testing and the set of stimuli used.

Electrode Localization. Electrode locations were identified in a high-resolution post-operative brain CT; electrode locations were then transformed onto a high-resolution pre-operative brain MRI by volumetrically co-registering the pre- and post-operative scans in Bioimage Suite (101). Pre-surgical volumetric MRI as well as electrode locations for individual patients were then normalized onto a Montreal Neurological Institute (MNI) brain atlas to show cross patient results. For details on the MNI electrode registration, see (102).

Data Acquisition and Analysis. Recordings of all standard and high-density electrodes were referenced to a single electrode to minimize extracranial sources of artifact. Raw ECoG signals were recorded with a 256-channel recording system (NeuroPort, BlackRock Microsystems, Salt Lake City, UT; or Nihon Kohden America, Irvine, CA, USA), amplified and sampled the data at up to 30 kHz of sampling rate with an analog third-order Butterworth anti-aliasing filter. The anti-aliased 30 kHz recording was decimated to 1 kHz in all patients prior to any subsequent analysis. Channels with excessive amounts of noise were identified by a clinical neurophysiologist and excluded from analysis. The remaining channels were re-referenced using a common average reference (CAR) filter to remove spatial bias in the raw ECoG amplitudes. Separate CAR blocks were used for all the standard electrodes and all the high-density electrodes in each patient.

ESM Analysis. All patients underwent functional mapping with electrocortical stimulation of motor and language cortex following routine clinical procedures (Lesser et al., 1987; Sinai et al., 2005a). ESM was performed in 2- to 3-h blocks over 1–2 days. Electrode pairs were stimulated using a GRASS S-12 Biphasic Stimulator (Grass-Telefactor/Astro-Med, Inc., West Warwick, RI, USA). Intracranial EEG was continuously monitored for after-discharges and seizures. Two- to 5-s trains of 50 Hz, 0.3 ms, alternating polarity square-wave pulses were delivered in 0.5-mA increments from 1 mA up to a maximum of 12 mA (typically between 7 and 12 mA), or the highest

amperage that did not produce after-discharges at a given electrode pair, maximizing currents at each cortical site regardless of adjacent after-discharge thresholds (Lesser et al., 1984; Pouratian et al., 2004).

Language location was determined as follows: electrode pairs were considered ESM positive for language if stimulation resulted in absent or delayed responses, paraphasic errors, and/or incorrect responses not followed by after-discharges during at least two trials at the same electrode pair, if these errors were not also present during baseline testing (Sinai et al., 2005a). Otherwise, electrode pairs were defined as ESM negative for language, including if there were after-discharges as a result of stimulation, but no hesitation, interruption or incorrect response. If ESM at an electrode pair produced or interfered with involuntary movement, it was considered ESM positive for motor function.

High Gamma Response Analysis. The CAR-filtered ECoG signal was analyzed for the duration of the task in 128ms epochs of data with 112ms overlap. The Fast Fourier transform (FFT) was computed on each window, and the resulting coefficients were then multiplied by a modified flat-top Gaussian window with cutoff between 70-150 Hz, with notch filters applied to 60 Hz and 120 Hz for line noise elimination. The bandpass-filtered spectrum was converted to high gamma amplitude by zeroing the negative frequency components, doubling the positive frequency components,

computing the inverse FFT, and taking the magnitude of the result (i.e. the Hilbert transform) (103, 104). The resulting high gamma amplitude was then log transformed to approximate a normal distribution and decimated to a temporal resolution of 16 ms using a moving average filter. More details of spectral feature extraction methods can be found in (105).

Cortico-cortical Evoked Potentials. The CCEP methodology is described in detail elsewhere (Matsumoto et al. 2004, 2007). Direct electrical stimulation was applied in a bipolar manner to a pair of adjacently placed subdural electrodes using a constant-current stimulator (Grass S12 stimulator, AstroMed, Inc., West Warwick, RI, USA). Single-pulse electrical stimuli (biphasic wave pulse: 0.3-ms duration) were delivered at jittered interstimulus intervals of 3.0–3.6s. Stimulation was monitored by a physician experienced in iEEG interpretation and electrocortical stimulation mapping. One set of trials for each stimulation site comprised 70–200 stimuli, depending on clinical circumstances and the time available for testing. During the recording, we asked the patients to recline comfortably awake on the bed and to continue their usual activities. We titrated stimulation intensity in increments of 0.5–1 mA, making sure that no afterdischarges were induced, up to a maximum of 5 mA for electrode arrays with 0.5 cm spacing or 10 mA for arrays with 1.0 cm spacing. More current was used for electrodes with larger surface area and interelectrode distances to achieve similar current densities. Because stimulation of sensorimotor or visual cortices can sometimes

evoke symptoms at low intensities (i.e., movement or subjective sensory sensation of a part of the body, and phosphenes), which could cause patients to attend to the stimulus and modify their low-frequency oscillations, we sometimes used 5 mA even for arrays with 1.0 cm spacing and confirmed that stimulation produced no symptom.

Accuracy calculation algorithm. To investigate the degree of correspondence between STFM, CCEPs and ESM, we constructed a logistic regression model to predict ESM results using STFM and CCEPs results:

$$ESM = \beta_1 \frac{\sum_{Stim}(STFM_{zscore})}{2} + \beta_2 \frac{\sum_{grid}(CCEPs_{zscore} \times STFM_{zscore})}{\#Electrodes} + \beta_3 \qquad (*)$$

where β_1, β_2 and β_3 are constants.

Training Logistic Regression Classifiers. We trained the data using a generalized linear model regression tool from Matlab to receive values of β_1, β_2 and β_3 in formula (*). The Classification Learner App was also used in Matlab to calculate accuracy and area under curve (AUC) of the ROC curve of the logistic regression model for each task in each patient.

4.4 Results

Electrocortical stimulation mapping (ESM) results for Patient 2 is illustrated as an example in Figure 4.1. Electrode pairs positive for motor, sensory, language and pain

are shown in respective colors in the legend. Electrode pairs clear for the above

functions are shown in green. ESM positive pairs are entered as value 1, and negative

pairs entered as value 0 as the observed responses in the prediction model.
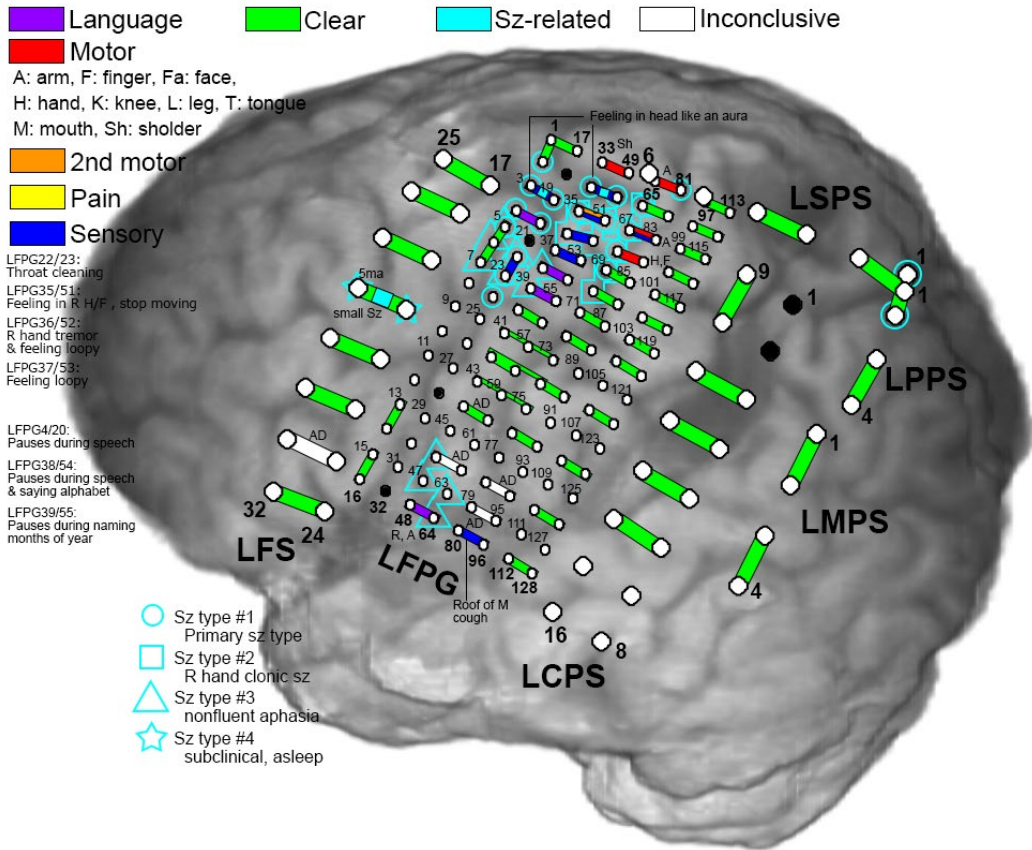
Figure 4.1. ESM results for Patient 2.

Green bars indicate electrode pairs that were negative during stimulation. Purple, red, orange and

blue bars indicate electrode pair(s) that were positive during language, motor, 2nd motor and sensory

89

tasks, respectively. Seizure onset zone are outlined with cyan shapes and more information of a specific pair is noted nearby.

Figure 4.2 shows spatial-temporal function mapping (STFM) results for Patient 2 during a word reading task as an example. A raster plot on the left displays the magnitude of event-related changes in the high gamma amplitude at each time point after stimulus onset, as compared to the baseline. The magnitudes are thresholded for significance ($p < 0.05$) using False Discovery Rate (FDR) correction in the channel raster and are uncorrected in the trial raster. A brain map was displayed on the right to show the locations and relative magnitudes of activations either integrated over the entire post-stimulus interval or at any user-selectable time point in the channel raster. The magnitude of the high gamma power at a particular electrode and time is represented by the size and color of disks overlaid on ECoG electrode locations in a two dimensional snapshot of the three dimensional brain reconstruction. STFM results for all patients in this chapter are available at http://cerebro.neuro.jhu.edu:8080. In the prediction model, an averaged value across time is used for each channel, and the values are normalized between 0 and 1 under the same task for all channels.
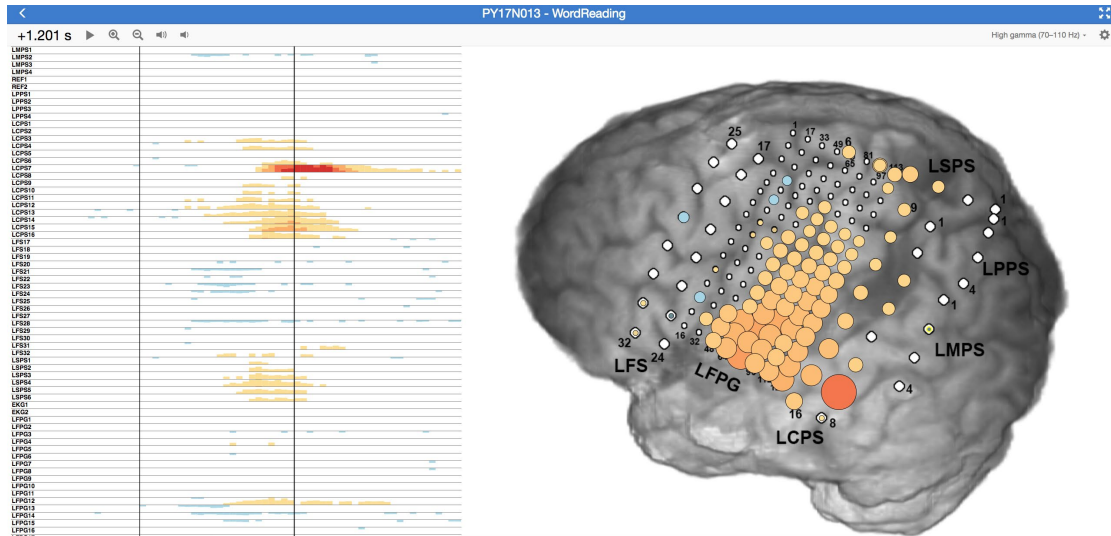
Figure 4.2. STFM results for Patient 2 during a word reading task.

The raster plot on the left shows trial-averaged STFM results in a time by channels manner, and the brain map on the right shows STFM results on an anatomical illustration at a specific time stamp. More details can be found at (105).

Cortico-cortical evoked potentials (CCEPs) results for one stimulation pair (LFS20-LFS28) in Patient 2 are shown in Figure 4.3. We can see CCEPs waves in a time by amplitude manner in each electrode not stimulated, with graded z-score values of different colors shown in the legend. The z-score values for the CCEPs results are normalized between 0 and 1 as one of the input matrices for the prediction model.
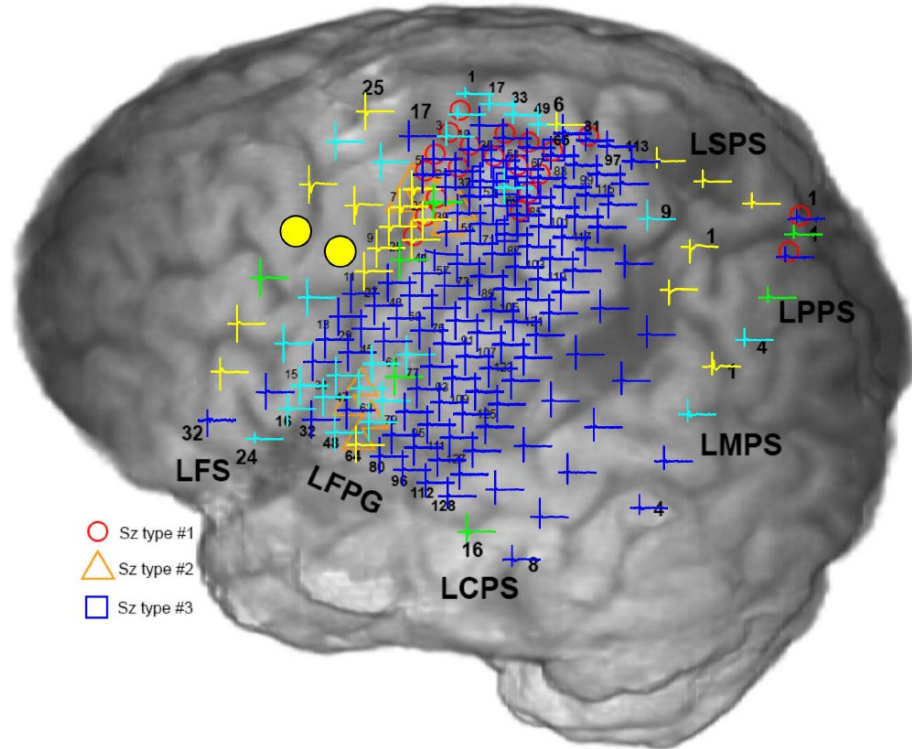
Figure 4.3. CCEPs results for Patient 2 when stimulating electrode pair LFS20-LFS28.

A time by amplitude evoked potential plot is shown in each of the channel without stimulation. Color of the plots indicate z-score categories for that particular channel: blue, cyan, green and yellow means z-score =0, >6, >8 and =10, respectively.

Using formula (*) from Methods, we trained the data using generalized linear model regression to get values of β_1, β_2 and β_3 (Table 4.2).

Patient	Task	β_1	β_2	β_3
1	Word Reading	-713.102	4905.375	-708.415
1	Picture Naming	-496.492	1549.125	-274.776
2	Word Repetition	-0.9827	-4.92218	107.8485
2	Word Reading	-0.98867	-3.86413	91.18006
3	Auditory Naming	-2.55035	1.478216	-61.796
3	Picture Naming	32.09862	-1286.66	-4456.09
3	Word Reading	-95.2168	803.845	-28996.5
4	Auditory Naming	-4.74861	136.977	-27.0329
4	Picture Naming	-258.971	760.3992	1246.639
4	Word Repetition	-288.188	1535.857	1329.284

Table 4.2. Logistic regression parameters using a generalized linear model regression.

The accuracy and arear under the ROC curve (AUC) were calculated with the above logistic regression models (Table 4.3). In order to compare accuracy in predicting ESM results, we first eliminated the second constant β_2 which contains CCEPs analysis results to get the accuracy and AUC when only using STFM results. The averaged accuracy was 79.5% and AUC 0.51. Then, we added β_2 back in and used the formula (*) to predict ESM results with STFM and CCEPs results combined. The average accuracy was 86.2% and AUC 0.67. We then performed a two-sample t-test between STFM only and STFM+CCEPs results, and the p-values for the accuracies and AUCs to be significantly different from each other were 0.26 and 0.23, respectively.

Patient	Task	Accuracy% STFM	AUC STFM	Accuracy% STFM+CCEPs	AUC STFM+CCEPs
1	Word Reading	85.7	0.42	85.7	0.42
1	Picture Naming	85.7	0.5	85.7	0.42

2	Word Repetition	52.4	0.54	71.4	0.63
2	Word Reading	52.4	0.46	71.4	0.53
3	Auditory Naming	92.9	0.08	100	1
3	Picture Naming	71.4	0.79	85.7	0.56
3	Word Reading	85.7	0.15	92.9	1
4	Auditory Naming	84.6	0.14	84.6	0.59
4	Picture Naming	92.3	1	92.3	0.75
4	Word Repetition	92.3	1	92.3	0.75
Averaged Accuracy/AUC		79.5	0.51	86.2	0.67

Table 4.3. Classification accuracy and area under curve using different classification models.

4.5 Discussion

Results from four patients performing a variety of language tasks demonstrated that combining the results of iEEG STFM and CCEPs improved the accuracy of predicting ESM results for language functional mapping of epilepsy patients prior to surgical resections.

There is growing clinical evidence in support of using passive iEEG for functional mapping. Brunner et al. (15) performed a side-by-side comparison of ESM and STFM in motor cortex with favorable results (i.e. no false negatives, ~1% false positives). Mapping language cortex presents additional challenges, however, since multiple sites over large-scale cortical networks are involved. The temporal profile of activation at a given site and its timing relative to other sites could therefore provide insight into its

function and contribution to a given task. For example, semantic knowledge is likely distributed broadly over temporal and frontal cortices (144) . Although some studies have indicated poor sensitivity and specificity of STFM in relation to ESM (e.g. specificity of 78% and sensitivity of 38% during visual object naming (13), a recent report has suggested that in some instances it can be more predictive of post-operative language impairments than ESM (21, 42). More work will be required to correlate surgical outcomes with the location of resected and preserved sites identified by ESM and STFM.

ESM is still the gold-standard for localizing eloquent cortex, but when compared to ground-truth patient outcomes, unpredicted resective deficits can and do still occur.(13, 21, 39, 102, 145) Passive iEEG mapping has been investigated as a replacement for ESM, but to date, its combined sensitivity and specificity relative to ESM have been suboptimal, especially for language mapping.(48) Both methods have potential strengths and limitations. ESM reversibly simulates the behavioral effect of a lesion, but its effects, particularly for long trains, may not be confined to the stimulation site, potentially eliciting action potentials in fibers of passage and interfering with function at distant sites. Passive iEEG provides a temporally specific, graded measure of task-related activation at all recorded sites, but it has been difficult to define a threshold for the magnitude of activation that denotes the importance of a site to task performance.

Current models of word production (31) suggest that cortical language networks are broadly distributed, multi-nodal, and sometimes redundant. However, the behavioral effects of ESM are usually interpreted in a strictly localizationist framework that doesn't consider its impact on network dynamics. iEEG studies of these dynamics provide an unprecedented opportunity to understand ESM within this emerging framework and to develop more accurate predictions of the effects of surgical lesions on behavior. We hypothesized that discrepancies between iEEG high gamma and ESM maps of word production can be accounted for by iEEG models of network dynamics. For example, ECoG(+)/ESM(-) sites may be accounted for by parallel, redundant high efficiency pathways (Fig 4.4). Conversely, ESM(+)/ECoG(-) sites may be accounted for by interference with processing at distant ECoG(+) sites (Fig 4.5). This interference could occur by enhancing or inhibiting population firing at distant, connected sites. We directly tested this possibility by measuring the effect of single pulse electrical stimulation (SPES) in distant ECoG sites (cortical-cortical evoked potentials, CCEPs).
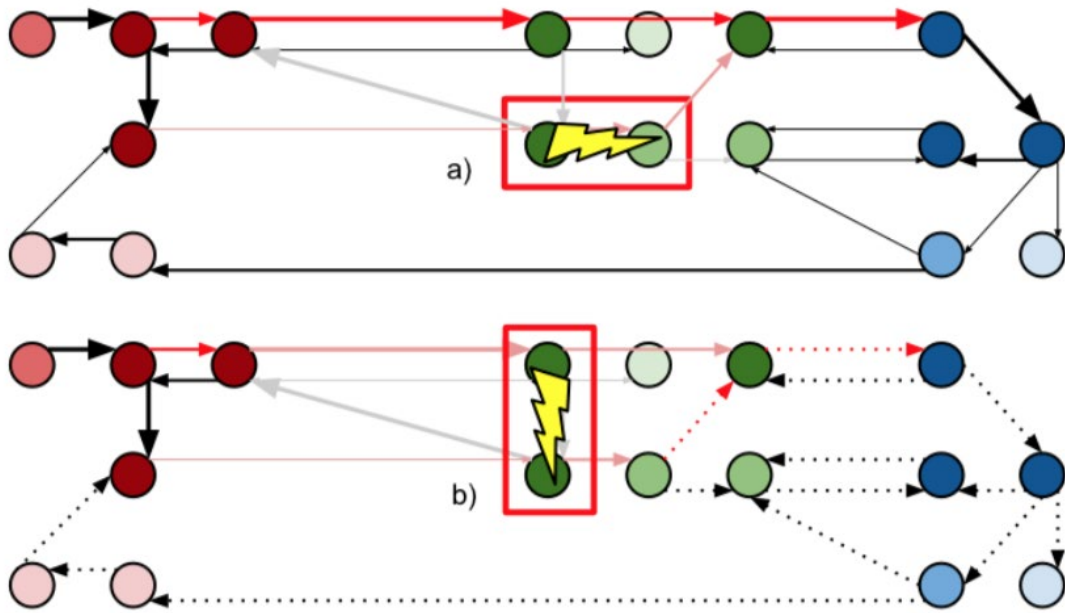
Figure 4.4. Network effects of ESM on multiple high efficiency paths.

Cortical stimulation (boxed in red) is indicated with a lightning bolt. High efficiency paths are indicated with red arrows. Connections disrupted by stimulation are lighter. Dotted arrows denote connections predicted to be disrupted by upstream stimulation. a) ESM only affects one high efficiency path, and may not interfere with task performance. b) ESM induces depolarization blockade of both high efficiency network paths and interferes with task performance.
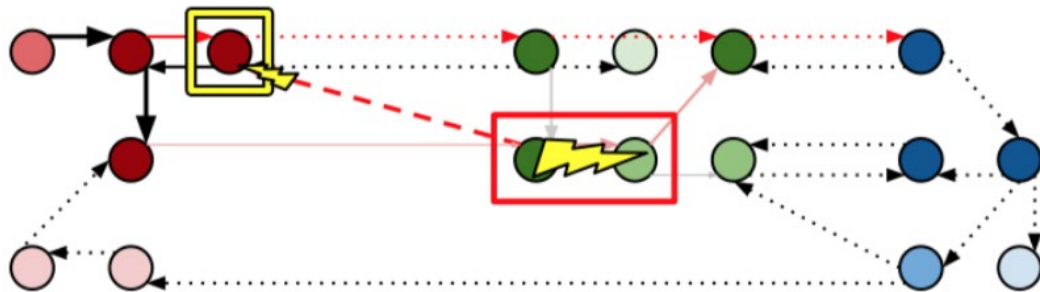
Figure 4.5. Distant effects of cortical stimulation.

Connections coded as in Fig 4.4. Cortical stimulation across two sites (boxed in red) interferes with a distant, strongly connected network hub (boxed in yellow). High efficiency paths from cue- to response-related subnets are thereby disrupted. This results in decreased network efficiency and task performance which wrongly implicates the stimulated site.

In conclusion, this chapter sought to reconcile inconsistencies between the results of STFM and ESM. Agreement between these methods has not been as good for language mapping as it has been for motor mapping. We hypothesized that some of these discrepancies may be due to propagation of ESM effects to cortical areas connected to the site of stimulation. To test this hypothesis, we used cortico-cortical evoked potentials to estimate the effective connectivity of stimulation sites to other sites in the language network. We found that this method improved the accuracy of STFM in predicting ESM results and helped explain similarities and differences between STFM and ESM language maps. We believe that this information will help clinicians better understand the contributions that tested sites make to task performance.

Chapter 5 Conclusions

5.1 Summary of findings

The work presented here has demonstrated the utility of passive iEEG recordings, particularly in high gamma frequencies (70-120Hz), for passive online mapping of human language function at the bedside, probing the role of Broca's area during speech production combined with neural propagation, and improving the accuracy of language mapping combined with effective connectivity analysis. We first showed the feasibility and clinical utility of online spatial-temporal functional mapping (STFM) for mapping human language function, particularly under clinical circumstances in which time is limited and comprehensive ESM is impractical. Next, we demonstrated that Broca's area plays a key role in lexical selection during a sentence completion task by investigating the spatial-temporal dynamics of neural activity combined with analyses of effective connectivity. This study also demonstrated the utility of STFM for identifying the functional role of a given cortical area in a complex language task. Finally, we combined the results of STFM and cortico-cortical evoked potentials (CCEPs) to build and test a model for predicting ESM results. This method improved the accuracy of STFM with respect to ESM and better described the relationship between STFM and ESM language maps. These results suggest that STFM is a

promising tool for testing both research and clinical hypotheses if combined with cortical network dynamics.

5.2 Future directions

5.2.1 Temporally restricted electrocortical stimulation mapping (trESM)

During clinical ESM, long stimulation trains (2-5 seconds) are employed because the timing of targeted neural processing is not known in advance. One way to overcome these limitations is by 1) using STFM to derive time windows of functionally critical activation at individual cortical sites, 2) using the resulting time windows to tailor the duration and onset of cortical stimulation trains, and 3) systematically analyzing the impact of stimulation on response accuracy and latency.

The feasibility of tailoring the timing of ESM was demonstrated in a previous study of the temporal dynamics of lexical semantic processing for visual objects in fusiform gyrus (146). In this study, the onset of stimulation trains was varied with respect to the onset of visual stimuli (400 to 900-ms in 50-ms increments) during visual object naming (Figure 5.1). The latency at which stimulation interfered with naming varied according to subjective object familiarity, but it was possible to infer that critical task-related processing at this site was completed between 450 and 750-ms after stimulus onset.
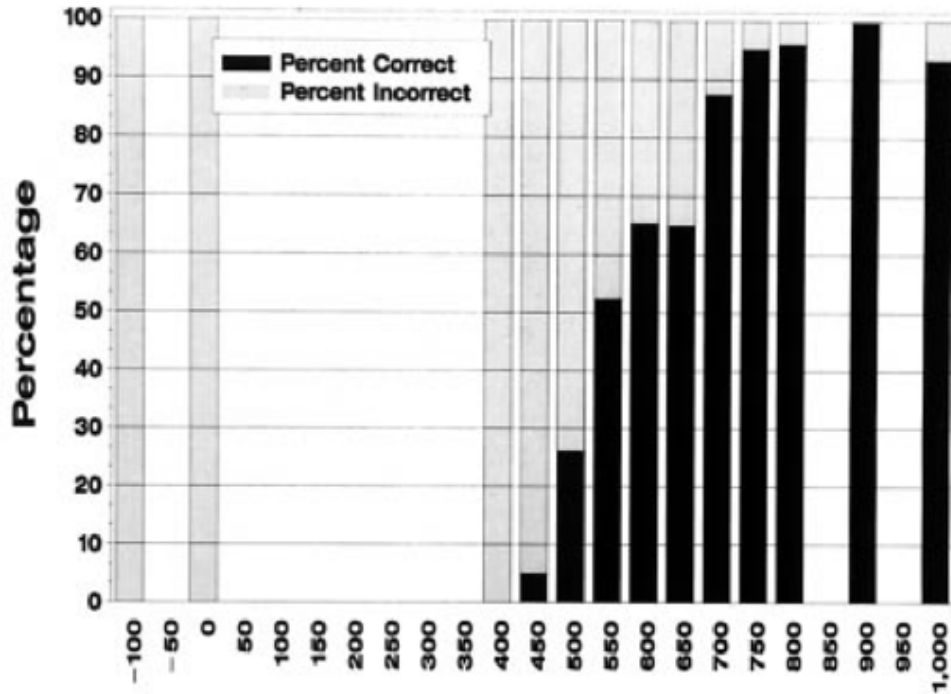
Figure 5.1. Visual object (picture) naming performance as a function of the onset of electrocortical stimulation relative to onset of the picture.

Horizontal axis = time (in msec) between onset of electrical and visual stimuli. Vertical axis =% of objects named correctly and incorrectly at each temporal offset. Adapted from Hart J Jr, et al. (1998) (146)

An important limitation of this study was that when it was done, the lab did not yet have a reliable method for deriving the spatial-temporal correlates of cortical processing from passive ECoG recordings. Thus, the completion of processing could only be inferred from the results of cortical stimulation. Also, visual stimuli were

101

visible until the patient spoke, and 5-s stimulus trains were used to prevent the patient from simply delaying their responses until after stimulation. I will present the visual stimulus for 50-ms to prevent this strategy while still allowing interruption or slowing of the patient's responses by time-restricted stimulation trains.

I predict that temporally specific stimulation of target electrodes over Broca's area will a) increase the number of task performance errors (unable to read/repeat words, semantic or phonemic paraphasias, absent responses), and/or b) increase the latency of (correct and incorrect) verbal responses.

The former will be interpreted as an interruption or perturbation of cortical processing that is critical for accurate responses. This may occur at different processing stages. More likely, however, I predict that stimulation will significantly delay verbal response latencies by temporarily blocking Broca's area function. I predict that stimulation at the onset of Broca's area activation will produce the greatest increase in latency, with decreasing effects as the activation is allowed to proceed for longer periods before stimulation. Consequently, stimulation that begins after the offset of propagation will have little or no effect on response latency. I predict that longer stimulation trains will delay responses more than shorter ones. I also expect that stimulations of higher intensity will delay responses more than lower intensity ones.

5.2.2 Predicting post-operative language outcomes

Our team has begun an admittedly coarse approach to finding an independent identification of functional cortex via identification of regions of interest (ROIs), which conservatively demarcate functional anatomy. Using this technique, we were able to make a preliminary case that iEEG functional mapping outperforms stimulation mapping. Ultimately, however, STFM will need to show superior performance in predicting post-operative deficits to truly replace ESM. In addition to being an independent standard, predicting post-operative deficits is the ultimate goal of epilepsy surgery planning.

The use of post-operative deficits as a gold standard is certainly not without its own challenges. Aggregating databases of post-operative deficits and their relationships with functional mapping results is difficult since putative eloquent cortex as identified is preferentially spared. This means that there would be an underrepresentation of ESM-positive sites in such a database. The net effect of such a sampling bias would be an overestimation of STFM's relative sensitivity and an overestimation of ESM's relative specificity (see Table 5.1). This could, of course, be overcome by simply including enough patients in the database that these factors could be balanced appropriately. Beyond the issue of sampling bias is the complication that deficits are not truly binary: they may be incomplete or vary in duration (e.g., deficits may be

chronic or resolve several months after surgery). Segmenting the database into sub-categories provides opportunities to highlight a role for STFM but further increases the size requirements of the cohort.

Deficit?	Truth	ESM	STFM	Information Gained
Yes	+	+	+	None
Yes	+	+	-	STFM sensitivity decrease
Yes	+	-	+	ESM sensitivity decrease
Yes	+	-	-	None
Yes	-	+	+	None
Yes	-	+	-	ESM Sensitivity Increase (incorrect)
Yes	-	-	+	STFM Sensitivity Increase (incorrect)
Yes	-	-	-	None
No	-	+	+	None
No	-	+	-	ESM Specificity Decrease
No	-	-	+	STFM Specificity Decrease
No	-	-	-	None

Table 5.1. Information gained from resections, ESM, and STFM results for resected sites.

Grayed out rows are ESM-positive and would thus be underrepresented in a database of resected sites. Each row corresponds to a specific set of attributes of a single resected site: (1) Did the resection cause a deficit in the task of interest? (2) Is this site truly functionally related to the task of interest? (3) Did ESM identify this site as task-related? and (4) Did STFM identify this site as task-related? The last column highlights information gained (sometimes incorrectly) about a site with the specified set of attributes. Note: this table assumes that a lesion could result from the resection of another site, which is why the first and second columns are different.

Appendices

Appendix 1. Sentence stems used in the described sentence completion task, with responses and cloze probabilities (CPs) for each sentence stem. Sentences were selected from the Bloom and Fischler 1980 library.

Training Set			
No	**Sentence**	**Response**	**CP**
1	'They took short trips during the'	'SUMMER'	0.51
2	'The hunter shot and killed a large '	'DEER'	0.43
3	'He was afraid to work the night'	'SHIFT'	0.89
4	'The old house was built entirely of'	'WOOD'	0.63
5	'Bill jumped in the lake and made a big'	'SPLASH'	0.99
6	'The man was caught selling an illegal'	'DRUG'	0.77
7	'His ring fell into a hole in the '	'SINK'	0.23
8	'We used to get company every'	'NIGHT'	0.37
Block 1			
No	**Sentence**	**Response**	**CP**
1	'Jim hit his horse with a'	'WHIP'	0.49
2	'It was important to be on'	'TIME'	0.77
3	'Surgery was needed to repair his failing'	'HEART'	0.53
4	'What you find depends on where you'	'LOOK'	0.49
5	'Matt was wild when he was'	'YOUNG'	0.49
6	'Larry chose not to join the '	'CLUB'	0.34
7	'To tune your car you need a special '	'TOOL'	0.55
8	'The death of his dog was a great '	'SHOCK'	0.29
9	'Scotty licked the bottom of the'	'BOWL'	0.53
10	'A future energy source is the'	'SUN'	0.78
11	'He disliked having to commute to the'	'CITY'	0.27
12	'Motorcycles can create a lot of'	'NOISE'	0.77
13	'The loaf was eaten except for a small '	'PIECE'	0.49
14	'The lawyer feared that his client was '	'GUILTY'	0.73

105

15	'They sat together without speaking a single'	'WORD'	0.98
16	'The ruby was so big, it looked like a'	'ROCK'	0.33
17	'Dan caught the ball with his '	'HAND(S)'	0.49
18	'A direct attack failed, so they changed the'	'STRATEGY'	0.37
19	'Rushing out he forgot to take his '	'COAT'	0.24
20	'They were startled by the sudden '	'NOISE'	0.59
21	'He was miles off the main'	'ROAD'	0.48
22	'The surface of the water was nice and '	'SMOOTH'	0.26
23	'George must keep his pet on a'	'LEASH'	0.89
24	'His boss refused to give him a'	'RAISE'	0.96
25	'He disappeared last year, and has not been'	'SEEN'	0.68
26	'Her new shoes were the wrong '	'SIZE'	0.78
27	'The young boy was granted a small '	'ALLOWANCE'	0.3
28	'She went to the salon to color her'	'HAIR'	0.99
29	'She tied up her hair with a yellow'	'RIBBON'	0.88
30	'He scraped the cold food from his '	'PLATE'	0.87
31	'The boat passed easily under the'	'BRIDGE'	0.95
32	'His view was blocked by the music '	'STAND'	0.25
33	'Bob would often sleep during his lunch '	'HOUR'	0.54
34	'Fred sat in his chair on the back '	'PORCH'	0.69
35	'She cleaned the dirt from her '	'SHOE(S)'	0.33
36	'It was clear that the leg was '	'BROKEN'	0.64
37	'You can''t take the test without a '	'PENCIL'	0.61
38	'The child was born with a rare'	'DEISEASE'	0.88
39	'You can''t buy anything for a'	'DIME'	0.33
40	'The dough was put in the hot '	'OVEN'	0.85
41	'Ray fell down and skinned his'	'KNEE(S)'	0.91
42	'There are times when life seems '	'DULL'	0.27
43	'When you go to bed turn off the'	'LIGHT(S)'	0.89
44	'You''ll never achieve anything if you don''t'	'TRY'	0.63
45	'The old house will be torn '	'DOWN'	0.93
46	'Most students prefer to work during the '	'DAY'	0.51
47	'Cathy is liked by all her'	'FRIENDS'	0.77
48	'The surgeon tried vainly to save his '	'PATIENT'	0.61
Block 2			

No	Sentence	Response	CP
1	'Jan tried to squeeze in, but there was no'	'ROOM'	0.89
2	'Hank reached into his pocket to get the '	'MONEY'	0.41
3	'Her job was easy most of the '	'TIME'	0.91
4	'During class Jack had to borrow some'	'PAPER'	0.61
5	'He crept into the room without a '	'SOUND'	0.7
6	'Harriet sang while my brother played the '	'PIANO'	0.48
7	'The wooded lake made a pretty '	'SCENE'	0.41
8	'The baby cried and upset her '	'MOTHER'	0.75
9	'Jill looked back through the open '	'DOOR'	0.53
10	'The mole lived in a hole in the'	'GROUND'	0.74
11	'Success is often just a matter of hard'	'WORK'	0.9
12	'The actor was praised for being very '	'GOOD'	0.24
13	'He liked lemon and sugar in his'	'TEA'	0.94
14	'New York is a very busy '	'CITY'	0.78
15	'Their picnic was ruined by the'	'RAIN'	0.76
16	'The person who caught the thief deserves our '	'THANKS'	0.34
17	'Mary couldn''t leave the parlor until her hair was'	'DRY'	0.55
18	'He was knocked off his board by the first'	'WAVE'	0.68
19	'Coming in he took off his '	'COAT'	0.31
20	'Jack bet all he had on the last '	'RACE'	0.65
21	'Most cats see very well at '	'NIGHT'	0.92
22	'The rabbit hid in the tall'	'GRASS'	0.63
23	'I thought the sermon was very'	'GOOD'	0.33
24	'The cigar burned a hole in the'	'COUCH'	0.2
25	'Joan showed her friend a new card '	'TRICK'	0.41
26	'The thick mud stuck to her'	'SHOES'	0.59
27	'You can''t open the door with the wrong'	'KEY'	0.81
28	'The children held their hands and formed a'	'CIRCLE'	0.89
29	'The child went ever higher on the'	'SWING'	0.28
30	'Bob thought she had such a friendly'	'SMILE'	0.54
31	'Before jogging, it''s a good idea to'	'STRETCH'	0.47
32	'The dog chased our cat up the '	'TREE'	0.68
33	'The pain she felt was all in her '	'HEAD'	0.48

No	Sentence	Response	CP
34	'Paul has always wanted to be a '	'DOCTOR'	0.54
35	'He loosened the tie around his'	'NECK'	0.96
36	'The bad boy was sent to his'	'ROOM'	0.78
37	'At night they often took a short '	'WALK'	0.68
38	'At first the woman refused, but she changed her'	'MIND'	0.99
39	'Abby brushed her teeth after every'	'MEAL'	0.88
40	'The girl knew a lot for her'	'AGE'	0.88
41	'Sometimes success is simply a matter of'	'LUCK'	0.26
42	'They rested under a tree in the '	'SHADE'	0.38
43	'Even for an amateur, he was pretty'	'GOOD'	0.8
44	'The difficult concept was beyond his'	'COMPREHENSION'	0.22
45	'Helen reached up to dust the '	'SHELF(VES)'	0.37
46	'My uncle gave my mother a big '	'KISS'	0.5
47	'The truck that Bill drove crashed into the '	'TREE'	0.25
48	'Rita slowly walked down the shaky'	'LADDER'	0.39

Block 3			
No	**Sentence**	**Response**	**CP**
1	'Tim threw a rock and broke the'	'WINDOW'	0.81
2	'They wanted their parents to come '	'HOME'	0.62
3	'In the morning Jake took out the'	'GARBAGE'	0.48
4	'Joan fed her baby some warm'	'MILK'	0.96
5	'He was soothed by the gentle '	'MUSIC'	0.23
6	'The final score of the game was '	'TIED'	0.37
7	'She dropped a glass and woke up the'	'BABY'	0.39
8	'He bought them in the candy '	'STORE'	0.74
9	'They went to the rear of the long '	'LINE'	0.22
10	'A large stone blocked the entrance to the '	'CAVE'	0.58
11	'Did you want to go to the'	'MOVIES'	0.47
12	'One of the scout troops got'	'LOST'	0.6
13	'For a runner Ted is rather '	'SLOW'	0.67
14	'Barry wisely chose to pay the '	'BILL'	0.36
15	'All the guests had a very good '	'TIME'	0.83
16	'When the power went out, the house became'	'DARK'	0.9
17	'The pizza was too hot to'	'EAT'	0.89

No	Sentence	Response	CP
18	'Next year my little son will be going to'	'SCHOOL'	0.79
19	'My aunt likes to read the daily '	'PAPER'	0.47
20	'John poured himself a glass of '	'MILK'	0.46
21	'The girl was advanced for her'	'AGE'	0.53
22	'The long test left the class '	'EXHAUSTED'	0.26
23	'Jim had learned the special passage by '	'HEART'	0.33
24	'The crime rate has gone up this '	'YEAR'	0.79
25	'The wealthy child attended a private '	'SCHOOL'	0.82
26	'No one wanted to accuse him of'	'STEALING'	0.29
27	'The Smiths had never visited that'	'PLACE'	0.25
28	'The child learned to count to'	'TEN'	0.77
29	'The cup of tea felt very'	'WARM'	0.51
30	'The gas station is about two miles down the'	'ROAD'	0.96
31	'Without food a man would die in several '	'DAYS'	0.56
32	'The lecture should last about one'	'HOUR'	0.96
33	'The better students thought the test was too'	'EASY'	0.8
34	'Ellen liked to season her food with'	'SALT'	0.62
35	'You could count on Dale on being late for '	'CLASS'	0.28
36	'Even their friends were left in the '	'DARK'	0.37
37	'He put his feet up on the'	'TABLE'	0.5
38	'Dean''s leg was broken, so Ed went to get'	'HELP'	0.64
39	'George could not believe his son stole a '	'CAR'	0.71
40	'He smiled and sat down at the '	'TABLE'	0.57
41	'Brian poured some sauce on his rare'	'STEAK'	0.73
42	'He hung her coat in the'	'CLOSET'	0.87
43	'Their money was divided by the'	'BANK(ER)'	0.34
44	'Vic asked her to repeat what she had'	'SAID'	0.92
45	'John swept the floor with a'	'BROOM'	0.96
46	'To find the body, they had to drain the'	'LAKE'	0.4
47	'Stan slowed down going around the'	'CORNER'	0.49
48	'The student went home during the'	'BREAK'	0.62
Block 4			
No	Sentence	Response	CP
1	'The earth is shaped like a '	'BALL'	0.44
2	'Three people were killed in a major highway '	'ACCIDENT'	0.84

3	'On their visit to England, they took a formal'	'TOUR'	0.47
4	'Plants will not grow in dry '	'SOIL'	0.42
5	'None of his books made any '	'SENSE'	0.88
6	'Starting a business takes a lot of'	'MONEY'	0.6
7	'It"s easy to get lost without a'	'MAP'	0.7
8	'Sam could not believe her story was'	TRUE	0.84
9	'Too many men are out of '	'WORK'	0.68
10	'They left the dirty dishes in the'	'SINK'	0.93
11	'The little girl was afraid of the'	'DARK'	0.52
12	'He drove the nail into the '	'WOOD'	0.32
13	'Father carved the turkey with a'	'KNIFE'	0.99
14	'The ship disappeared into the thick'	'FOG'	0.88
15	'The kind old man asked us to '	'STAY'	0.26
16	'The sandwich wasn"t very good without a slice of'	'CHEESE'	0.45
17	'Every spring they held the annual '	'BALL'	0.23
18	'They liked to sleep out under the'	'STARS'	0.61
19	'Bob proposed, but she turned him'	'DOWN'	0.97
20	'The apple pie had a delicious'	'TASTE'	0.54
21	'Ken built his new house on a quiet '	'LAKE'	0.32
22	'Phil put some drops in his'	'EYES'	0.8
23	'Every month Rick had to clean his '	'ROOM'	0.32
24	'The storm made the air damp and '	'COLD'	0.25
25	Ample food was made for the'	'PARTY'	0.22
26	'It was a long class and everyone was getting'	'BORED'	0.5
27	'She locked the valuables in the'	'SAFE'	0.53
28	'He lay down and went to'	'SLEEP'	0.92
29	'The sail got loose, so they tightened the'	'ROPES'	0.44
30	'My father and mother are getting'	'DIVORCED'	0.54
31	'Autumn is a good time to buy some new'	'CLOTHES'	0.71
32	'He wondered if the storm would be'	'OVER'	0.32
33	'Ira turned on the radio and listened to the'	'MUSIC'	0.56
34	'On his vacation he got some needed'	'REST'	0.71
35	'A dog has a good sense of'	'SMELL'	0.78
36	'The front was clearly marked on the weather'	'MAP'	0.66
37	'George had been fired, but he couldn"t tell his'	'WIFE'	0.72

38	'He had to fill his truck with'	'GAS'	0.33
39	'Dick wrote a chapter in the'	'BOOK'	0.86
40	'Suzy liked to play with her toy '	'DOLL(S)'	0.41
41	'He wondered if the storm had done much'	'DAMAGE'	0.97
42	'The car stalled because the engine failed to '	'START'	0.32
43	'The boys were given hamburgers for'	'LUNCH'	0.63
44	'My sister bought tickets for the opening '	'GAME'	0.27
45	'Billy hit his sister on the '	'HEAD'	0.69
46	'He went to the factory where the toys were'	'MADE'	0.77
47	'The paper was too thick to'	'CUT'	0.2
48	'He mailed the letter without a '	'STAMP'	0.99

Bibliography

1. Organization WH (2006) *Neurological Disorders: Public Health Challenges* (World Health Organization).

2. Engel AK, Moll CKE, Fried I, Ojemann GA (2005) Invasive recordings from the human brain: Clinical insights and beyond. *Nat Rev Neurosci* 6(1):35–47.

3. Berger MS, Kincaid J, Ojemann GA, Lettich E (1989) Brain mapping techniques to maximize resection, safety, and seizure control in children with brain tumors. *Neurosurgery* 25:786–792.

4. Sanai N, Mirzadeh Z, Berger MS (2008) Functional outcome after language mapping for glioma resection. *N Engl J Med* 358(1):18–27.

5. Lachaux JP, Rudrauf D, Kahane P (2003) Intracranial EEG and human brain mapping. *J Physiol-Paris* 97(4–6):613–628.

6. Podkorytova I, Hoes K, Lega B (2016) Stereo-Encephalography Versus Subdural Electrodes for Seizure Localization. *Neurosurg Clin N Am* 27(1):97–109.

7. Wyllie E, et al. (1988) Subdural electrodes in the evaluation for epilepsy surgery in children and adults. *Neuropediatrics* 19(2):80–86.

8. Goldring S, Gregorie EM (1984) Surgical management of epilepsy using epidural recordings to localize the seizure focus. Review of 100 cases. *J Neurosurg* 60(3):457–466.

9. Ojemann G, Ojemann J, Lettich E, Berger M (1989) Cortical language localization in left, dominant hemisphere. An electrical stimulation mapping investigation in 117 patients. *J Neurosurg* 71(3):316–26.

10. Bookheimer SY, et al. (1997) A direct comparison of PET activation and electrocortical stimulation mapping for language localization. *Neurology* 48(4):1056–65.

11. FitzGerald DB, et al. (1997) Location of language in the cortex: a comparison between functional MR imaging and electrocortical stimulation. *Am J Neuroradiol* 18(8):1529–39.

12. Blume WT, Jones DC, Pathak P (2004) Properties of after-discharges from cortical electrical stimulation in focal epilepsies. *Clin Neurophysiol Off J Int Fed Clin Neurophysiol* 115(4):982–989.

13. Sinai A, et al. (2005) Electrocorticographic high gamma activity versus electrical cortical stimulation mapping of naming. *Brain* 128(Pt 7):1556–70.

14. Sabsevitz DS, et al. (2003) Use of preoperative functional neuroimaging to predict language deficits from epilepsy surgery. *Neurology* 60(11):1788–92.

15. Brunner P, et al. (2009) A practical procedure for real-time functional mapping of eloquent cortex using electrocorticographic signals in humans. *Epilepsy Behav* 15(3):278–86.

16. Crone NE, Korzeniewska A, Franaszczuk PJ (2011) Cortical gamma responses: searching high and low. *Int J Psychophysiol* 79(1):9–15.

17. Lachaux JP, Axmacher N, Mormann F, Halgren E, Crone NE (2012) High-frequency neural activity and human cognition: past, present and possible future of intracranial EEG research. *Prog Neurobiol* 98(3):279–301.

18. Berger H (1929) Über das Elektrenkephalogramm des Menschen. *Arch Für Psychiatr Nervenkrankh* 87(1):527–570.

19. Jasper HH, Carmichael L (1935) Electrical Potentials from the Intact Human Brain. *Science* 81(2089):51–3.

20. Crone NE, Miglioretti DL, Gordon B, Lesser RP (1998) Functional mapping of human sensorimotor cortex with electrocorticographic spectral analysis. II. Event-related synchronization in the gamma band. *Brain J Neurol* 121 (Pt 12):2301–2315.

21. Cervenka MC, Boatman-Reich DF, Ward J, Franaszczuk PJ, Crone NE (2011) Language mapping in multilingual patients: electrocorticography and cortical stimulation during naming. *Front Hum Neurosci* 5:13.

22. Jerbi K, et al. (2009) Task-related gamma-band dynamics from an intracerebral perspective: review and implications for surface EEG and MEG. *Hum Brain Mapp* 30(6):1758–71.

23. Logothetis NK, Pauls J, Augath M, Trinath T, Oeltermann A (2001) Neurophysiological investigation of the basis of the fMRI signal. *Nature* 412(6843):150–7.

24. Khursheed F, et al. (2011) Frequency-specific electrocorticographic correlates of working memory delay period fMRI activity. *Neuroimage* 56(3):1773–82.

25. Manning JR, Jacobs J, Fried I, Kahana MJ (2009) Broadband shifts in local field potential power spectra are correlated with single-neuron spiking in humans. *J Neurosci* 29(43):13613–20.

26. Miller KJ, et al. (2010) Cortical activity during motor execution, motor imagery, and imagery-based online feedback. *Proc Natl Acad Sci*:200913697.

27. Lau EF, Phillips C, Poeppel D (2008) A cortical network for semantics: (de)constructing the N400. *Nat Rev Neurosci* 9(12):920–933.

28. Cohen L, et al. (2002) Language-specific tuning of visual cortex? Functional properties of the Visual Word Form Area. *Brain* 125(Pt 5):1054–69.

29. Howard D, et al. (1992) The cortical localizations of the lexicons: Positron Emission Tomography evidence. *Brain* 115:1769–1782.

30. Tan LH, Laird AR, Li K, Fox PT (2005) Neuroanatomical correlates of phonological processing of Chinese characters and alphabetic words: a meta-analysis. *Hum Brain Mapp* 25(1):83–91.

31. Indefrey P, Levelt WJ (2004) The spatial and temporal signatures of word production components. *Cognition* 92(1–2):101–44.

32. Wildgruber D, Ackermann H, Klose U, Kardatzki B, Grodd W (1996) Functional lateralization of speech production at primary motor cortex: a fMRI study. *Neuroreport* 7(15–17):2791–2795.

33. Postma A (2000) Detection of errors during speech production: a review of speech monitoring models. *Cognition* 77(2):97–132.

34. Hashimoto Y, Sakai KL (2003) Brain activations during conscious self-monitoring of speech production with delayed auditory feedback: an fMRI study. *Hum Brain Mapp* 20(1):22–28.

35. Lesser R, Gordon B, Uematsu S (1994) Electrical stimulation and language. *J Clin Neurophysiol* 11:191–204.

36. Penfield W, Jasper H (1954) *Epilepsy and the functional anatomy of the human brain* (Little, Brown, and Company, Boston). 1st Ed.

37. Lesser RP, et al. (1984) Cortical afterdischarge and functional response thresholds: results of extraoperative testing. *Epilepsia* 25(5):615–621.

38. Pouratian N, Cannestra AF, Bookheimer SY, Martin NA, Toga AW (2004) Variability of intraoperative electrocortical stimulation mapping parameters across and within individuals. *J Neurosurg* 101(3):458–466.

39. Hamberger MJ (2007) Cortical language mapping in epilepsy: a critical review. *Neuropsychol Rev* 17(4):477–89.

40. Ishitobi M, et al. (2000) Remote discharges in the posterior language area during basal temporal stimulation. *Neuroreport* 11(13):2997–3000.

41. Karakis I, et al. (2015) Intra-stimulation discharges: An overlooked cortical electrographic entity triggered by direct electrical stimulation. *Clin Neurophysiol* 126(5):882–888.

42. Cervenka MC, et al. (2013) Electrocorticographic functional mapping identifies human cortex critical for auditory and visual naming. *Neuroimage* 69:267–76.

43. Crone NE, et al. (2001) Electrocorticographic gamma activity during word production in spoken and sign language. *Neurology* 57(11):2045–53.

44. Lachaux JP, et al. (2007) A Blueprint for Real-Time Functional Mapping via Human Intracranial Recordings. *PLoS ONE* 2(10):e1094.

45. Miller KJ, et al. (2007) Real-time functional brain mapping using electrocorticography. *Neuroimage* 37(2):504–7.

46. Schalk G, et al. (2008) Real-time detection of event-related brain activity. *Neuroimage* 43(2):245–9.

47. Cheung C, Chang EF (2012) Real-time, time-frequency mapping of event-related cortical activation. *J Neural Eng* 9(4):046018.

48. Bauer PR, et al. (2013) Mismatch between electrocortical stimulation and electrocorticography frequency mapping of language. *Brain Stimul* 6(4):524–31.

49. Ruescher J, et al. (2013) Somatotopic mapping of natural upper- and lower-extremity movements and speech production with high gamma electrocorticography. *NeuroImage* 81:164–177.

50. Wu M, et al. (2010) Electrocorticographic frequency alteration mapping for extraoperative localization of speech cortex. *Neurosurgery* 66(2):E407-9.

51. Davis AE, Wada JA (1978) Speech dominance and handedness in the normal human. *Brain Lang* 5(1):42–55.

52. Duncan JS, et al. (2004) Geometric strategies for neuroanatomic analysis from MRI. *NeuroImage* 23 Suppl 1:S34-45.

53. Canolty RT, et al. (2007) Spatiotemporal dynamics of word processing in the human brain. *Front Neurosci* 1(1):185–96.

54. Bruns A (2004) Fourier-, Hilbert- and wavelet-based signal analysis: are they really different approaches? *J Neurosci Methods* 137(2):321–332.

55. Benjamini Y, Hochberg Y (1995) Controlling the False Discovery Rate: A Practical and Powerful Approach to Multiple Testing. *J R Stat Soc Ser B Methodol* 57(1):289–300.

56. Nobre AC, Allison T, McCarthy G (1994) Word recognition in the human inferior temporal lobe. *Nature* 372:260–263.

57. Tanji K, Suzuki K, Delorme A, Shamoto H, Nakasato N (2005) High-frequency gamma-band activity in the basal temporal cortex during picture-naming and lexical-decision tasks. *J Neurosci* 25(13):3287–93.

58. McNemar Q (1947) Note on the sampling error of the difference between correlated proportions or percentages. *Psychometrika* 12(2):153–157.

59. Kojima K, et al. (2013) Gamma activity modulated by picture and auditory naming tasks: Intracranial recording in patients with focal epilepsy. *Clin Neurophysiol* 124(9):1737–1744.

60. Cushing H (1908) A NOTE UPON THE FARADIC STIMULATION OF THE POSTCENTRAL GYRUS IN CONSCIOUS PATIENTS. Available at: http://brain.oxfordjournals.org/content/brain/33/3/204.full.pdf.

61. Penfield W, Boldrey E (1937) Somatic Motor and Sensory Representation in the Cerebral Cortex of Man as Studied by Electrical Stimulation. *Brain* 60(4):389–443.

62. Krauss GL, et al. (1996) Cognitive effects of resecting basal temporal language areas. *Epilepsia* 37(5):476–83.

63. Nii Y, Uematsu S, Lesser RP, Gordon B (1996) Does the central sulcus divide motor and sensory functions? Cortical mapping of human hand areas as revealed by electrical stimulation through subdural grid electrodes. *Neurology* 46:360–367.

64. Matsumoto R, et al. (2004) Functional connectivity in the human language system: a cortico-cortical evoked potential study. *Brain* 127(Pt 10):2316–30.

65. Matsuzaki N, Juhász C, Asano E (2013) Cortico-cortical evoked potentials and stimulation-elicited gamma activity preferentially propagate from lower- to higher-order visual areas. *Clin Neurophysiol* 124(7):1290–1296.

66. Ray S, Crone NE, Niebur E, Franaszczuk PJ, Hsiao SS (2008) Neural correlates of high-gamma oscillations (60-200 Hz) in macaque local field potentials and their potential implications in electrocorticography. *J Neurosci* 28(45):11526–11536.

67. Hickok G, Poeppel D (2007) The cortical organization of speech processing. *Nat Rev Neurosci* 8(5):393–402.

68. Damasio AR, Geschwind N (1984) The neural basis of language. *Annu Rev Neurosci* 7:127–47.

69. Buchsbaum BR, Hickok G, Humphries C (2001) Role of left posterior superior temporal gyrus in phonological processing for speech perception and production. *Cogn Sci* 25(5):663–678.

70. Price CJ (2000) The anatomy of language: contributions from functional neuroimaging. *J Anat* 197 Pt 3:335–59.

71. Broca P (1861) Remarques sur le siège de la faculté du langage articulé, suivies d'une observation d'aphémie (perte de la parole). *Bull Memoires Soc Anat Paris* 6:330–357.

72. Broca P (1865) Sur le siège de la faculté du langage articulé (15 juin). *Bull Société Anthropol Paris* 6:377–393.

73. Wernicke C (1874) *Der aphasische Symptomencomplex: Eine psychologische Studie auf anatomischer Basis* (Cohn.).

74. Lichtheim L (1885) On aphasia. *Brain* 7:433–484.

75. Geschwind N (1965) DISCONNEXION SYNDROMES IN ANIMALS AND MAN. *Brain* 88(3):585–585.

76. Indefrey P (2011) The spatial and temporal signatures of word production components: a critical update. *Lang Sci* 2:255.

77. Hickok G, Poeppel D (2004) Dorsal and ventral streams: a framework for understanding aspects of the functional anatomy of language. *Cognition* 92(1–2):67–99.

78. Hickok G, Poeppel D (2007) The cortical organization of speech processing. *Nat Rev Neurosci* 8(5):393–402.

79. Hagoort P (2005) On Broca, brain, and binding: a new framework. *Trends Cogn Sci* 9(9):416–423.

80. Hagoort P (2013) MUC (Memory, Unification, Control) and beyond. *Front Psychol* 4. doi:10.3389/fpsyg.2013.00416.

81. Thompson-Schill SL, et al. (1998) Verb generation in patients with focal frontal lesions: A neuropsychological test of neuroimaging findings. *Proc Natl Acad Sci* 95(26):15855–15860.

82. Snijders TM, et al. (2009) Retrieval and Unification of Syntactic Structure in Sentence Comprehension: an fMRI Study Using Word-Category Ambiguity. *Cereb Cortex* 19(7):1493–1503.

83. Berry I, et al. (1995) Activation of Association Auditory Cortex Demonstrated with Functional MRI. *NeuroImage* 2(3):215–219.

84. Crone NE, Boatman D, Gordon B, Hao L (2001) Induced electrocorticographic gamma activity during auditory perception. *Clin Neurophysiol* 112(4):565–82.

85. Crone NE, et al. (2001) Electrocorticographic gamma activity during word production in spoken and sign language. *Neurology* 57(11):2045–2053.

86. Edwards E, et al. (2010) Spatiotemporal imaging of cortical activation during verb generation and picture naming. *Neuroimage* 50(1):291–301.

87. Fifer MS, et al. (2014) Simultaneous Neural Control of Simple Reaching and Grasping With the Modular Prosthetic Limb Using Intracranial EEG. *IEEE Trans Neural Syst Rehabil Eng* 22(3):695–705.

88. Gonzalez A, et al. (2015) Electrocorticography reveals the temporal dynamics of posterior parietal cortical activity during recognition memory decisions. *Proc Natl Acad Sci* 112(35):11066–11071.

89. Lachaux J-P, et al. (2007) Relationship between task-related gamma oscillations and BOLD signal: New insights from combined fMRI and intracranial EEG. *Hum Brain Mapp* 28(12):1368–1375.

90. Siero JCW, et al. (2014) BOLD matches neuronal activity at the mm scale: A combined 7T fMRI and ECoG study in human sensorimotor cortex. *NeuroImage* 101:177–184.

91. Crone NE, Korzeniewska A, Franaszczuk PJ (2011) Cortical gamma responses: searching high and low. *Int J Psychophysiol* 79(1):9–15.

92. Lachaux JP, Axmacher N, Mormann F, Halgren E, Crone NE (2012) High-frequency neural activity and human cognition: past, present and possible future of intracranial EEG research. *Prog Neurobiol* 98(3):279–301.

93. Sahin NT, Pinker S, Cash SS, Schomer D, Halgren E (2009) Sequential Processing of Lexical, Grammatical, and Phonological Information Within Broca's Area. *Science* 326(5951):445–449.

94. Flinker A, et al. (2015) Redefining the role of Broca's area in speech. *Proc Natl Acad Sci U S A* 112(9):2871–2875.

95. Collard MJ, et al. (2016) Cortical subnetwork dynamics during human language tasks. *NeuroImage* 135:261–272.

96. Taylor WL (1953) "Cloze Procedure": A New Tool for Measuring Readability. *Journal Bull* 30(4):415–433.

97. Bloom PA, Fischler I (1980) Completion norms for 329 sentence contexts. *Mem Cognit* 8(6):631–642.

98. Block CK, Baldwin CL (2010) Cloze probability and completion norms for 498 sentences: Behavioral and neural validation using event-related potentials. *Behav Res Methods* 42(3):665–670.

99. Schalk G, McFarland DJ, Hinterberger T, Birbaumer N, Wolpaw JR (2004) BCI2000: a general-purpose brain-computer interface (BCI) system. *IEEE Trans Biomed Eng* 51(6):1034–1043.

100. Boersma P, Van Heuven V (2001) Speak and unSpeak with PRAAT. *Glot Int* 5(9/10):341–347.

101. Duncan JS, et al. (2004) Geometric strategies for neuroanatomic analysis from MRI. *NeuroImage* 23 Suppl 1:S34-45.

102. Cervenka MC, et al. (2013) Electrocorticographic functional mapping identifies human cortex critical for auditory and visual naming. *Neuroimage* 69:267–76.

103. Canolty RT, et al. (2007) Spatiotemporal dynamics of word processing in the human brain. *Front Neurosci* 1(1):185–96.

104. Bruns A (2004) Fourier-, Hilbert- and wavelet-based signal analysis: are they really different approaches? *J Neurosci Methods* 137(2):321–332.

105. Wang Y, et al. (2016) Spatial-temporal functional mapping of language at the bedside with electrocorticography. *Neurology* 86(13):1181.

106. Korzeniewska A, Crainiceanu CM, Kuś R, Franaszczuk PJ, Crone NE (2008) Dynamics of event-related causality in brain electrical activity. *Hum Brain Mapp* 29(10):1170–1192.

107. Korzeniewska A, Franaszczuk PJ, Crainiceanu CM, Kuś R, Crone NE (2011) Dynamics of large-scale cortical interactions at high gamma frequencies during word production: Event related causality (ERC) analysis of human electrocorticography (ECoG). *NeuroImage* 56(4):2218–2237.

108. Ruppert D, Wand MP, Carroll RJ (2003) Semiparametric Regression. *Camb Core*. doi:10.1017/CBO9780511755453.

109. Ray S, Crone NE, Niebur E, Franaszczuk PJ, Hsiao SS (2008) Neural Correlates of High-Gamma Oscillations (60–200 Hz) in Macaque Local Field Potentials and Their Potential Implications in Electrocorticography. *J Neurosci* 28(45):11526–11536.

110. Staub A, Grant M, Astheimer L, Cohen A (2015) The influence of cloze probability and item constraint on cloze task response time. *J Mem Lang* 82:1–17.

111. Rayner K, Well AD (1996) Effects of contextual constraint on eye movements in reading: A further examination. *Psychon Bull Rev* 3(4):504–509.

112. Kutas M, Hillyard SA (1984) Brain potentials during reading reflect word expectancy and semantic association. *Nature* 307(5947):161–163.

113. Ries SK, Greenhouse I, Dronkers NF, Haaland KY, Knight RT (2014) Double dissociation of the roles of the left and right prefrontal cortices in anticipatory regulation of action. *Neuropsychologia* 63:215–225.

114. Schnur TT, Schwartz MF, Brecher A, Hodgson C (2006) Semantic interference during blocked-cyclic naming: Evidence from aphasia. *J Mem Lang* 54(2):199–227.

115. Anders R, Riès S, van Maanen L, Alario FX (2015) Evidence accumulation as a model for lexical selection. *Cognit Psychol* 82:57–73.

116. Anders R, Riès S, Van Maanen L, Alario F-X (2017) Lesions to the left lateral prefrontal cortex impair decision threshold adjustment for lexical selection. *Cogn Neuropsychol* 34(1–2):1–20.

117. Usher M, McClelland JL (2001) The time course of perceptual choice: the leaky, competing accumulator model. *Psychol Rev* 108(3):550–592.

118. Poldrack RA, et al. (1999) Functional Specialization for Semantic and Phonological Processing in the Left Inferior Prefrontal Cortex. *NeuroImage* 10(1):15–35.

121

119. Dapretto M, Bookheimer SY (1999) Form and Content: Dissociating Syntax and Semantics in Sentence Comprehension. *Neuron* 24(2):427–432.

120. Rodd JM, Davis MH, Johnsrude IS (2005) The Neural Mechanisms of Speech Comprehension: fMRI studies of Semantic Ambiguity. *Cereb Cortex* 15(8):1261–1269.

121. Gough PM, Nobre AC, Devlin JT (2005) Dissociating Linguistic Processes in the Left Inferior Frontal Cortex with Transcranial Magnetic Stimulation. *J Neurosci* 25(35):8010–8016.

122. Thompson-Schill SL, D'Esposito M, Aguirre GK, Farah MJ (1997) Role of left inferior prefrontal cortex in retrieval of semantic knowledge: A reevaluation. *Proc Natl Acad Sci* 94(26):14792–14797.

123. Thompson-Schill SL, D'Esposito M, Kan IP (1999) Effects of Repetition and Competition on Activity in Left Prefrontal Cortex during Word Generation. *Neuron* 23(3):513–522.

124. Hagoort P, Indefrey P (2014) The Neurobiology of Language Beyond Single Words. *Annu Rev Neurosci* 37(1):347–362.

125. Lesser RP, et al. (1985) Ipsilateral trigeminal sensory responses to cortical stimulation by subdural electrodes. *Neurology* 35:1760–1763.

126. Schäffler L, Lüders HO, Dinner DS, Lesser RP, Chelune GJ (1993) Comprehension deficits elicited by electrical stimulation of Broca's area. *Brain J Neurol* 116 (Pt 3):695–715.

127. Viventi J, et al. (2011) Flexible, foldable, actively multiplexed, high-density electrode array for mapping brain activity in vivo. *Nat Neurosci* 14(12):1599–605.

128. Bouchard KE, Chang EF (2014) Neural decoding of spoken vowels from human sensory-motor cortex with high-density electrocorticography. *Conf Proc Annu Int Conf IEEE Eng Med Biol Soc IEEE Eng Med Biol Soc Annu Conf* 2014:6782–6785.

129. Crone NE, Miglioretti DL, Gordon B, Lesser RP (1998) Functional mapping of human sensorimotor cortex with electrocorticographic spectral analysis. II. Event-related synchronization in the gamma band. *Brain* 121(Pt 12):2301–15.

130. Grossman M, Gotman J (2001) As time goes by: high temporal and spatial resolution in cognitively related cortical function. *Neurology* 57(11):1947–8.

131. Edwards E, et al. (2010) Spatiotemporal imaging of cortical activation during verb generation and picture naming. *Neuroimage* 50(1):291–301.

132. Crone NE, Sinai AS, Korzeniewska A (2006) High-frequency gamma oscillations and human brain mapping with electrocorticography. *Prog Brain Res* 159:279–302.

133. Genetti M, et al. (2014) Comparison of high gamma electrocorticography and fMRI with electrocortical stimulation for localization of somatosensory and language cortex. *Clin Neurophysiol Off J Int Fed Clin Neurophysiol.* doi:10.1016/j.clinph.2014.04.007.

134. Lachaux JP, et al. (2007) Relationship between task-related gamma oscillations and BOLD signal: New insights from combined fMRI and intracranial EEG. *Hum Brain Mapp.* doi:10.1002/hbm.20352.

135. Siero JCW, et al. (2014) BOLD matches neuronal activity at the mm scale: A combined 7 T fMRI and ECoG study in human sensorimotor cortex. *NeuroImage* 101:177–184.

136. Flinker A, et al. (2010) Single-trial speech suppression of auditory cortex activity in humans. *J Neurosci* 30(49):16643–50.

137. Crone NE, et al. (1998) Functional mapping of human sensorimotor cortex with electrocorticographic spectral analysis. I. Alpha and beta event-related desynchronization. *Brain* 121(12):2271–2299.

138. Miller KJ, et al. (2007) Spectral changes in cortical surface potentials during motor movement. *J Neurosci* 27(9):2424–32.

139. Sinai A, et al. (2009) Intracranial mapping of auditory perception: event-related responses and electrocortical stimulation. *Clin Neurophysiol* 120(1):140–9.

140. Towle VL, et al. (2008) ECoG gamma activity during a language task: differentiating expressive and receptive speech areas. *Brain* 131(Pt 8):2013–27.

141. Miller KJ, Abel TJ, Hebb AO, Ojemann JG (2011) Rapid online language mapping with electrocorticography. *J Neurosurg Pediatr* 7(5):482–90.

142. Rademacher J, Caviness VS Jr, Steinmetz H, Galaburda AM (1993) Topographical variation of the human primary cortices: implications for neuroimaging, brain mapping, and neurobiology. *Cereb Cortex N Y N 1991* 3(4):313–329.

143. Ojemann GA (1979) Individual variability in cortical localization of language. *J Neurosurg* 50(2):164–169.

144. Mesulam MM (1990) Large-scale neurocognitive networks and distributed processing for attention, language, and memory. *Ann Neurol* 28:597–613.

145. Kojima K, et al. (2012) Multimodality language mapping in patients with left-hemispheric language dominance on Wada test. *Clin Neurophysiol* 123(10):1917–24.

146. Hart J Jr, et al. (1998) Temporal dynamics of verbal object comprehension. *Proc Natl Acad Sci U A* 95(11):6498–503.

Yujing Wang

5979 Cypress Springs Rd, Elkridge, M.D. 21075

Phone: +1 (410) 868-9239   **Email**: wangyujing07@gmail.com

Education

08/2013 **–** 10/2018   **University of Maryland College Park,** College Park, MD, U.S.A
Ph.D. in Bioengineering, A. James Clark School of Engineering

08/2011 **–** 05/2013   **Johns Hopkins University,** Baltimore, MD, U.S.A.
Master of Science in Biomedical Engineering, Whiting School of Engineering

08/2007 **–** 07/2011   **Tsinghua University,** Beijing, China
Bachelor of Science in Biomedical Engineering, School of Medicine

Experience

RESEARCH EXPERIENCE

Research Trainee, Johns Hopkins University
05/2014 **–** Present
Affiliation: Cognitive Neurophysiology and BMI Lab, Department of Neurology
Advisor: Dr. Nathan Crone

Project (major): Mapping Human Auditory and Language Function using Electrocorticography (ECoG) Recordings
As a Masters' student in Biomedical Engineering at Hopkins I built a trial-based online spatial-temporal functional mapping system that complements electrocortical stimulation mapping in patients undergoing neurosurgical resections for epilepsy or tumors. As a PhD student, I will continue to develop this system and use it to collect and analyze ECoG data from auditory and language experiments under the supervision of Dr. Nathan Crone. I will conduct experiments aimed at understanding the neural mechanisms underlying speech perception and production in the human brain. This will include studying the dynamics of brain networks perceiving and producing speech and using these dynamics in a brain-computer interface designed to produce speech from ECoG. In the course of this work I will be responsible for researching the literature on my topic, designing experiments, conducting experiments and collecting all data necessary for their interpretation, data archival, analysis, and interpretation and publication of my results. I will finish publishing a peer-reviewed paper started during my master's degree work, and then I will publish at least the minimum number of papers, including first author papers, to satisfy the requirements for completion of my Ph.D. at University of Maryland.

Research Assistant, Johns Hopkins University & University of Maryland College Park
02/2014 **–** 04/2014
Affiliation: Cognitive Neurophysiology Lab, Department of Neurology
Co-advisors: Dr. Nathan Crone, Dr. Yu Chen

Project: Reconstructing Speech from Human Auditory Cortex Using Electrocorticography

Lab Rotation, University of Maryland College Park
        10/2013 **–** 12/2013
Affiliation: Bio-photonic Imaging Laboratory, Department of Bioengineering
Advisor: Dr. Yu Chen

Project: Angled Fluorescence Laminar Optical Tomography (aFLOT) Based Voltage-Sensitive Dye Imaging System for Sub-cortex 3-D Neuronal Function Imaging

Lab Rotation, University of Maryland College Park
        08/2013 **–** 10/2013
Affiliation: Neural Systems Laboratory, Institute for System Research
Advisors: Dr. Shihab Shamma, Dr. Jonathan Fritz

Project: Click Discrimination Phase-Lock Analysis Using Single Neuron Recordings on the Ferret Auditory Cortex

Research Assistant, Johns Hopkins University
        08/2011 **–** 05/2013
Affiliation: Neuroengineering & Biomedical Instrumentation Lab, Department of Biomedical Engineering
Advisors: Dr. Nitish Thakor, Dr. Nathan Crone

> *Project (major): Trial-based Online Spatial-temporal Electrocorticographic Functional Mapping System*
> - Implemented Hilbert transform and flat-Gaussian frequency windowing as the most suitable feature extraction approach for the system.
> - Discovered sufficiently fast and robust statistical analysis method for the system.
> - Built up a MATLAB Graphical User Interface (GUI) that visualizes mapping results with both raster plots and brain maps, for maximum observation convenience for clinicians and researchers.
> - Assisted with data collection, built up communications with patients and clinicians.
> - The system has become a routine analysis procedure, used with 8 patients to date across a variety of tasks.
>
> *Project: How Micro-ECoG Shows Robustness and Higher Spatial Resolution than Standard ECoG*
> - Statistically significant and stable high gamma responses emerged with fewer trials in activated microelectrodes than in neighboring activated macroelectrodes.
> - Observed spatial heterogeneity of the microelectrode responses.
> - Compared the difference amongst using results from Electrocortical Stimulation Mapping (ESM), offline matching-pursuit analysis and online functional mapping.
>
> *Project: ECoG Brain-Computer Interface (BCI) for Controlling an Advanced Prosthetic Limb*
> - Implemented the online functional mapping system as an electrode pre-selection tool for decoding.

Project (ongoing): Event-Related Causality (ERC) Analysis within Micro-ECoG and Standard ECoG

- Compared silent-distant reference with common average reference to determine the better referencing approach in terms of performing ERC within micro-ECoG and standard ECoG.
- Interested in how flows of ERC may occur between micro- and standard electrodes in terms of communication in different time stages (e.g. stimulus perception and speech production).

Research Assistant, Tsinghua University
08/2008 – 07/2011
Affiliation: Neural Engineering Lab, Department of Biomedical Engineering
Advisors: Dr. Shangkai Gao, Dr. Bo Hong

Project (graduate thesis): Semantic-Related ECoG Language Tasks Analysis

- Part of the WUSTL-Tsinghua Joint *Big-Brain Project*.
- Designed to demonstrate the feasibility of a BCI based on ECoG to control external devices and utilize them to better understand the electrophysiology of cortical function
- Contributed to the signal analysis on how cortex gets different information presented by visual symbolic, visual lexical and auditory lexical.

Project (Student Research Training Problem): A BCI System Based on Mobile Phone Using C#

- Developed a Windows Mobile phone-based portable BCI system, using C# and Visual Studio
- Applied as one of the *National Innovation Research Programs*
- Won silver medal in the 28Th Tsinghua Challenge Cup Competition

Research Technician (Internship), Tsinghua University Affiliated Yuquan Hospital
06/2010 – 07/2010
Affiliation: Epilepsy Center
Advisor: Dr. Wenjing Zhou, director of the epilepsy center

- Designed various language tasks and successfully determined language functional areas for epilepsy patients using ECoG high gamma responses.
- Developed a MATLAB Graphic User Interface automatically generating a standard diagnostic report for functional mapping results with visualization for clinicians.
- Observed surgeries, learned about MRI vs. CT co-registration techniques during internship.

TEACHING EXPERIENCE

Teaching Assistant	Biocomputational Methods / BIOE241, University of Maryland	Spring, 2015
Teaching Assistant	Biocomputational Methods / BIOE241, University of Maryland	Fall, 2014
Teaching Assistant	Systems Bioengineering Lab I / EN.580.424,	

	Johns Hopkins University	Spring, 2013
Teaching Assistant	Systems Bioengineering Lab I / EN.580.423,	
	Johns Hopkins University	Fall, 2012
Grader	Systems and Controls / EN.580.222,	
	Johns Hopkins University	Spring, 2012
Grader	Statistical Mechanics and Thermodynamics / EN.580.321,	
	Johns Hopkins University	Fall, 2011

Memberships

Student member, *Society for Neuroscience*.
Member, *American Epilepsy Society*.
Student member, *American Academy of Neurology*

Publications

Published Manuscripts

- Usami K, Milsap GW, Korzeniewska A, Collard MJ, **Wang Y**, Lesser RP, Crone NE. Cortical responses to input from distant areas are modulated by local spontaneous alpha/beta oscillations. *Cerebral Cortex*. 2018 Jan 24. doi: 10.1093/cercor/bhx361. [Epub ahead of print] PubMed PMID: 29373641.
- Collard MJ, Fifer MS, Benz HL, McMullen DP, **Wang Y**, Milsap GW, Korzeniewska A, Crone NE. Cortical subnetwork dynamics during human language tasks. *NeuroImage*. 2016 Jul 15;135:261-72. doi: 0.1016/j.neuroimage.2016.03.072. Epub 2016 Apr 2. PubMed PMID: 27046113; PubMed Central PMCID: PMC4985237.
- **Wang Y**, Fifer MS, Flinker A, Korzeniewska A, Cervenka MC, Anderson WS, Boatman-Reich DF, Crone NE. Spatial-temporal functional mapping of language at the bedside with electrocorticography. *Neurology*. 2016 Mar 29;86(13):1181-9. doi: 10.1212/WNL.0000000000002525. Epub 2016 Mar 2. PubMed PMID: 26935890; PubMed Central PMCID: PMC4818563.
- Guo MM, **Wang Y**, Xu GZ, Milsap G, Thakor Nitish V, Crone N. Time-varying dynamic Bayesian network model and its application to brain connectivity using electrocorticograph. *Wuli Xuebao/Acta Physica Sinica*. 2016 Feb 5;65(3). 038702.
- Fifer MS, Hotson G, Wester BA, McMullen DP, **Wang Y**, Johannes MS, Katyal KD, Helder JB, Para MP, Vogelstein RJ, Anderson WS. Simultaneous neural control of simple reaching and grasping with the modular prosthetic limb using intracranial EEG. *IEEE transactions on neural systems and rehabilitation engineering*. 2014 May;22(3):695-705. doi: 10.1109/TNSRE.2013.2286955. Epub 2013 Oct 24. PubMed PMID: 24235276; PubMed Central PMCID: PMC4030429.
- Qian T, **Wang Y**, Zhou W, Gao S, Hong B. Speech function mapping of human brain based on electrocorticography. *J Tsinghua Univ (Sci & Technol).* 2013;53(09):116-20.

Manuscripts in Preparation

- **Yujing Wang**, Anna Korzeniewska, Kiyohide Usami, Alyssandra Valenzuela, Nathan E. Crone. Spatial-temporal dynamics of neural activity in Broca's area during lexical selection: an intracranial EEG study. In preparation. Submitted to *PNAS*, under review.

- Anna Korzeniewska, **Yujing Wang**, Nathan E. Crone et al. Increased long-range top-down network interactions at high gamma frequencies underlie human behavioral priming and repetition suppression. Submitted to *Brain*, under review.
- Griffin Milsap, Maxwell Collard, Christopher Coogan, Qinwan Rabbani, **Yujing Wang**, Nathan E. Crone. Keyword Spotting using Human Electrocorticographic Recordings. Submitted to *Frontiers in Neuroscience*, under review.
- **Yujing Wang**, Miaomiao Guo, Anna Korzeniewska, Nathan Crone et al. Decoding Human Speech with Multi-scale ECoG Connectivity Dynamics. In preparation.
- Geoffrey Newman, **Yujing Wang**, Nitish Thakor, Nathan Crone. Brain State Detection in Human ECoG Using Stability Clustering. In preparation.

Presentations at National Conferences
- **Y. Wang**, A. Korzeniewska, K. Usami, A. Valenzuela, N. E. Crone, Spatial-temporal dynamics of neural activity in Broca's area during lexical selection: an intracranial EEG study, *Society for Neuroscience*, San Diego, 2018 (upcoming). Poster Presentation.
- **Y. Wang**, A. Valenzuela, N. E. Crone et al., Spatial-temporal dynamics of neural activity in Broca's area during sentence completion measured with intracranial EEG, *Society for Neuroscience*, Washington, D.C., 2017. Platform talk.
- **Y. Wang**, M. S. Fifer, N. E. Crone et al., A region of interest approach to comparing electrocorticography and electrocortical stimulation for clinical language mapping, *American Epilepsy Society*, Philadelphia, PA, 2015. Poster Presentation.
- **Y. Wang**, M. S. Fifer, N. E. Crone et al., Comparison of electrocorticography and electrocortical stimulation in mapping classical language areas: A region of interest approach, *Society for Neuroscience Annual Meeting*, Chicago, IL, 2015. Poster Presentation.
- A. Korzeniewska , S.Dalvin, **Y. Wang**, G. Milsap, A. Flinker, N.E. Crone, The impact of lexical retrieval on high-gamma effective connectivity in human language networks, *Society for Neuroscience Annual Meeting*, Washington, DC, 2014. Poster
- **Y. Wang**, A. Korzeniewska, F. L. Higgen, N. E. Crone, Effective Connectivity Mapping in Humans Using Hybrid Electrocorticography, *Society for Neuroscience Annual Meeting*, San Diego, CA, 2013. Poster Presentation.
- M. S. Fifer, G. Hotson, B. A. Wester, **Y. Wang**, M. S. Johannes et al., Continuous Actuation of The Modular Prosthetic Limb Using Electrocorticographic Signals During Overt Reaching and Grasping Movements, *Society for Neuroscience Annual Meeting*, San Diego, CA, 2013. Poster Presentation.
- M. Cervenka, A. Korzeniewska, J. Yoke, M. Fifer, **Y. Wang**, N. Crone et al., Electrocorticographic Mapping Of Self And Object Mental Rotations, *American Epilepsy Society*, Washington, DC, 2013. Poster Presentation.
- **Y. Wang**, M. S. Fifer, N. E. Crone et al., Microelectrodes Record Electrocorticographic High Gamma Responses With Increased Sensitivity and Spatial Resolution During Human Language Tasks, *Society for Neuroscience Annual Meeting*, New Orleans, LA, 2012. Poster Presentation.